TA7
.C6
CER94-95-3

Colorado State University

ESSAYS ON RIVER MECHANICS

Presented by the Graduate Students
in CE 717 - River Mechanics (Spring, 1995)

Instructor: P.Y. Julien

April, 1995

LIBRARIES
MAY 19 1995
COLORADO STATE UNIVERSITY

CER94-95-PYJ-3

BARCODE INSIDE

Colorado State University

ESSAYS ON RIVER MECHANICS

Presented by the Graduate Students
in CE 717 - River Mechanics (Spring, 1995)

Instructor: P.Y. Julien

April, 1995

U18401 0457233

CER94-95-PYJ-3

FOREWORD

I am very pleased to honor the work of the graduate students in the class CE-717 River Mechanics with this report of their technical papers. Each student worked on a particular aspect of river engineering in order to meet the following objectives:

1) familiarize with the recent literature and new methodologies not available in textbooks;
2) compare various methods (new versus old) and discuss the advancement of engineering technology on a given topic;
3) develop skills to point out the key elements of recent technological developments;
4) share interesting findings with the other students through an oral presentation and a written paper.

The requirements for this project were:

1) select a topic relevant to river mechanics and sediment transport;
2) conduct a literature review including papers published in the past five years;
3) compare new methods with those detailed in textbooks on either a theoretical basis or through comparison with an appropriate data set;
4) write a 12 page paper following the ASCE editorial standards (these papers are included herein);
5) summarize the analysis and discuss the major findings in a 20 minute oral presentation.

The reader will certainly agree with me that the objectives were met with great success. I am personally impressed with the overall quality of the reports presented and I can only compliment them all on their effort.

Pierre Y. Julien
Associate Professor
Civil Engineering Department

TABLE OF CONTENTS

Rock DurabilityAssessment
(A Comparison of Acceptance Criteria)

By Gregory V. Wilkerson

Introduction

Evaluation of rock quality/durability is a required task in determining the suitability of rock for use as a construction material. In construction, rocks are used as aggregate in concrete mixtures; as base material in road construction and the construction of structures; and to protect river banks, highway embankments and coastal shorelines from the erosive forces in their respective environments. Criteria for accepting or rejecting rock vary primarily as a function of the intended use. Other reasons include the ability to excavate sufficient quantities of the material; the ability of the quarry to produce material of the required size (Bureau of Reclamation, 1987); and the production and hauling cost of the material.

This report will examine rock suitability criteria established by several federal and state agencies. In particular, this report will consider applicability of the criteria to evaluating marginal quality sandstone rock. In a study performed by Abt et al. (1994a), eighteen sandstone rock samples and one basalt, one tuff, and one limestone rock sample were submitted to several standardized laboratory tests. The results of these tests will be reviewed considering acceptability criteria established by six agencies: the U.S. Bureau of Reclamation; the U.S. Army Corps of Engineers; the U.S. Department of Agriculture, Soil Conservation Service; the California Department of Transportation; the United States Nuclear Regulatory Commission; and the Construction Industry Research and Information Association / Center for Civil Engineering Research, Codes, and Specifications.

Background

Field Assessment of Rock Quality

Assessment of a potential quarry site requires field and laboratory analysis of the physical quality of the rock (Koopmans and Watts, 1992). Guidelines regarding information to be gathered from field investigations vary among authors. One reason for the variation is that the general stone size required for a project affects which aspects of a quarry and its operations are most important. For example, Lienhart and Stransky (1981) emphasize the need to consider the

spacing and orientation of faults and joints at a quarry being considered for the production of armor stone since they can limit the size of stone produced or, possibly, be used to advantage in a carefully designed blasting program. The production of aggregate for concrete and riprap, being smaller in size, is less effected by the structural features of a rock mass. Regardless of the stone sized required, the site investigation requires observation of landform characteristics (i.e., ridges, benches, or rock-cored terraces), identification of rock type and rock mass conditions, and in-service performance of rock units exposed to the environment (Summer and Johnson, 1982).

Koopmans and Watts (1992) discuss armor stone suitability assessment methods used by Ontario Hydro. Physical suitability is determined by considering previous armor stone use, visual comparison with suitable rocks, and laboratory testing. Considering that the most reliable method for determining the weathering resistance of armor stone is to subject it to natural climatic conditions for an extended period of time, they recommend, where possible, that inspections be performed at locations where the questionable rock has experienced years of natural weathering. When no previous use of a certain material is adequately known, Koopmans and Watts suggest visually examining and comparing rock at the proposed quarry site to suitable rock from other quarries.

Petrographic Examination

Petrography is the field and laboratory investigation of rocks which yields data that leads to their description and classification. Petrology is the scientific study of the origin, structure, constitution and characteristics of rocks. In practice, one seldom distinguishes between petrography and petrology, as in this writing (Krumbein and Pettijohn, 1938). In evaluating rock for use as riprap, petrographic examinations provide detection of weaknesses and defects in the rock mass, such as clay seams, rock alterations, unsound portions, etc., which may affect the rock's durability (DePuy and Ensign, 1965). American Society of Testing and Materials (ASTM) standard C 295 (1993) provides guidance for petrographic examinations leading to the description and classification of rock and its constituents. The purpose of the examination, as described therein, is:----

- to determine the physical and chemical characteristics of the material;
- to describe and classify the constituents of the sample;
- to determine the relative amounts of the constituents of the sample; and
- to compare samples of aggregate from new sources with samples of aggregate from one or more sources, for which test data or performance records are available.

Identification of the constituents of a sample is usually a necessary step toward recognition of the properties that may be expected to influence the behavior of the material in its intended use (ASTM, 1993). A study of six different sandstones performed by Shakoor and Bonelli (1991) attempted to relate the relationships between the mechanical properties (compressive strength, tensile strength, Young's modulus, and Poisson's ratio), petrographic characteristics, and engineering index properties (percent absorption, density, slake durability, and pore size distribution). Similarly, Vernik et al. (1993) determined empirical relationships between compressive strength and porosity of siliciclastic rocks.

Data derived from petrographic analysis can potentially be used to help predict the quality/durability of a rock. Studies indicate that porosity is the best single-variate predictor of strength in sedimentary rocks (Rzhevsky and Novik 1971, Deere and Miller 1969, Dunn et al. 1973).

Laboratory Assessment of Rock Quality

There are many laboratory tests available to assist in the assessment of a rocks suitability. Generally, the tests are indicators of different rock qualities although some test similar properties. Measurable properties include density and unit weight; relative density (specific gravity); porosity and effective porosity (the pore space that is interconnected and connected to the outside surface); water absorption; and resistance to degradation by abrasion, freezing and thawing, and erosion.

The evaluation procedures reviewed herein generally require laboratory tests that have been standardized by the American Society for Testing and Materials (ASTM) and/or the International Society for Rock Mechanics (ISRM) (i.e., specific gravity, absorption, sodium sulfate, Los Angeles abrasion). Other, non-standardized, rock evaluation procedures have been developed and are presented in the literature. Among these procedures are acoustic emissions monitoring (Hardy, 1981), ultrasonic cavitation testing (DePuy and Ensign 1965), mill abrasion (Latham 1991, CIRIA/CUR 1991, and Latham 1993), and point load index (Brown 1981).

Physical/Mechanical Properties and Engineering Index Tests

No single rock test is considered completely indicative of the properties required for its success as a construction material (i.e., as embankment material; as foundation material in the construction of roads and other structures; as aggregate in concrete mixtures; or as a protective cover for river banks and coastal shorelines). In addition, requirements for rock quality and

durability are dependent on a number of factors (i.e., the proposed application, the environment to which the rock will be exposed, the design life of the project, the ability to quarry the material, and the degree of risk deemed acceptable). Consequently, numerous procedures have been developed for quantitatively assessing rock quality and durability.

Typically, criteria for determining rock suitability require a suite of tests to be performed on any rock sample being considered for use. Presented below are descriptions of rock tests frequently required in evaluation procedures established by federal and state agencies in the United States.

Direct Tensile Strength

The direct tensile strength test, as its name implies, is used to determine the tensile strength of rock. The test consists of cementing metal caps to the ends of a cored cylindrical rock specimen and applying a tensile load to the specimen via linkages to the metal caps. ASTM standard D 2936 provides criteria for measuring the direct tensile strength of rock core specimens.

Indirect Tensile Strength

The direct tensile strength test is difficult and expensive for routine use in contrast to the splitting tensile strength (Brazilian strength) test -- an "indirect" tensile strength test that is simpler and less expensive (ASTM, 1993). The splitting tensile strength test is performed by applying "diametral line compression" to a circular disk shaped specimen. Splitting tensile strength is then calculated as a function of the applied compressive load and the dimensions of the specimen. ASTM standard D 3967 provides criteria for measuring the indirect tensile strength of rock core specimens.

Unconfined Compressive Strength

A cylindrical rock specimen is laid between two steel bearing plates through which a gradually increasing compressive load is applied to the specimen until it fails. The maximum load carried by the specimen during the test, divided by the cross sectional area of the specimen is its unconfined compressive strength. ASTM standard D 2938 provides criteria for measuring the unconfined compressive strength of intact rock core specimens.

Specific Gravity and Absorption

The specific gravity of a rock is the ratio of the weight (or mass) of a unit volume of the rock to a unit volume of water. Absorption is the percent increase in weight due to water in the pores of the rock. The specific gravity and absorption capability of a rock is an indicator of its quality. Among other reasons, a rock's specific gravity is an important design consideration because it describes how easily the rock will be displace due to buoyancy (DePuy and Ensign, 1965).

ASTM standards C 127 and C 128 specify methods for determining the specific gravity and absorption of aggregates.

Los Angeles Abrasion

The Los Angeles abrasion test is a measure of degradation of mineral aggregates of standard grading resulting from a combination of actions including abrasion or attrition, impact, and grinding in a rotating steel drum (ASTM, 1993). According to DePuy and Ensign (1965), the test is generally related to rock quality, but is not necessarily a measure of durability, especially as related to deterioration from frost action or wetting and drying. However, Depuy and Ensign also state that the test provides a basis for estimating resistance to abrasive forces in handling and erosive forces in service. ASTM standards C 131 and C 535 provide criteria for measuring resistance to degradation using the Los Angeles testing machine.

Sulfate Soundness

The sulfate soundness test is used to estimate the soundness of aggregates when subjected to weathering. The test consists of repeatedly immersing a graded aggregate sample in saturated solutions of sodium or magnesium sulfate followed by oven drying to dehydrate the salt precipitated in permeable pore spaces (ASTM, 1993). After undergoing the specified number of cycles, the weighted percentage loss of the sample is reported. ASTM standard C 88 provides criteria for sulfate soundness testing.

Slake Durability

The slake durability test is used to qualitatively estimate the durability of weak rocks in the service environment and to assign quantitative durability values. The test is performed in a cylindrical drum (formed with square mesh, woven-wire cloth) with rigid plates on the ends. After being placed in the drum the rock sample is oven-dried and weighed. Next, the drum is placed horizontally in a trough filled with distilled water. (The drum is supported by the trough in a manner such that it is free to rotate.) The drum is then rotated at a specified speed for a specified time period. After being rotated, the sample is dried and weighed. A second rotation cycle is performed and again the sample is dried and weighed. The slake durability index is calculated as the ratio of (a) the mass of the sample after the second cycle and (b) the mass of the sample before the first cycle -- multiplied by one-hundred. ASTM standard D 4644 provides criteria for determining the slake durability of shales and weak rocks.

Schmidt Hammer Test

The Schmidt hammer test is performed with a Rebound Hammer - a spring loaded steel hammer that when released strikes a plunger in contact with the surface of the material being tested (ASTM, 1993). The rebound distance of the steel hammer from the steel plunger is

measured on a scale attached to the frame of the instrument and recorded as the rebound number. This test is primarily used to test the strength and other properties of concrete in-situ but can be used to test cylindrical cores of rock by bracing the sample in a "core cradle." ASTM standard C 805 provides criteria for determining rebound numbers.

Freeze-Thaw Cycling

The purpose of freeze-thaw cycling test is to determine the effects of freezing and thawing on rock specimens and the resistance of the rock to deterioration (ASTM, 1993). It is an accelerated weathering test designed to simulate wintertime conditions and the freezing and thawing affects on rock deterioration. The results of the test provide an indication of the durability of a rock specimen in similar conditions. ASTM standard D 5312 provides criteria for a freeze-thaw cycling test.

Wet-Dry Cycling

The purpose of wet-dry cycling tests is to determine the effects of wetting and drying on rock specimens and the resistance of the rock to deterioration (ASTM, 1993). It is an accelerated weathering test designed to simulate wetting and drying conditions. The results of the test indicate the durability of a rock specimen in similar conditions. ASTM standard D 5313 presents criteria for a wet-dry cycling test.

Sonic Velocity

The sonic velocity test measures the velocity of sound through rock. The velocity is influenced by the rock's porosity, pore-size distribution, mineralogical composition, crystal size and orientation as well as discontinuities (i.e., bedding planes, joints and fractures) (Sengupta, 1975). Velocity measurements taken before, during and after freeze-thaw testing provide an indication of potential rock breakdown (Koopmans and Watts, 1992). Additional information regarding sonicscope measurements has been published by Leslie et al. (1950), the Highway Research Board (1963), and Sengupta (1975).

NRC Rock Evaluation Procedure

The United States Nuclear Regulatory Commission (NRC) rock evaluation procedure (Johnson et al., 1993) uses the results of six laboratory tests to formulate a quantitative measure of rock quality/durability (i.e., a rock score). The NRC rock evaluation procedure was used by Abt et al. (1994a) to evaluate twenty-one rock samples (18-sandstone, 1-basalt, 1-limestone, and 1-tuff). The test results and NRC rock scores for the samples tested by Abt et al. will serve

herein as a baseline for comparison of criteria established by other agencies. Following is a description of the NRC rock evaluation procedure.

The NRC rock evaluation procedure was developed as part of an investigation of engineering techniques and methodologies for the evaluation of plans for reclaiming unprotected uranium mill tailings impoundments (Johnson et al., 1993). Low-level waste and uranium mill tailings waste disposal sites normally employ protective cover systems to limit radioactive releases and to prevent erosion and dispersion of contaminated material. Reclamation of uranium mill tailings sites are particularly challenging for the NRC because federal regulations impose criteria for long-term reclamation; protective cover systems must be designed to be effective for time periods ranging from two hundred to one thousand years (40 CFR Part 192, 10 CFR Part 61, and 10 CFR Part 40, Appendix A), and require that proposed designs should provide overall site stability with no routine maintenance (10 CFR Part 40, Appendix A).

In 1990, the NRC developed a quantitative procedure for assessing the quality and durability of rock for use as erosion protection at waste disposal sites (NRC, 1990 and Johnson et al., 1993). Development of the procedure was based on experience with various reclamation designs and on published rock quality procedures (i.e., Lindsey et al., 1982 and DuPuy, 1965).

The procedure developed by the NRC uses the results of six standardized tests: specific gravity, absorption, sodium sulfate, Los Angeles abrasion, Schmidt hammer, and tensile strength. For each test result, a score between zero and ten is assigned based on the result of the test. Each score is then multiplied by a weighting factor based on the "applicability of the test" to the rock type being tested. The final, the rock quality rating is reported as a percentage and is calculated by dividing the sum of the weighted scores by the total possible score.

The NRC uses petrographic analysis to obtain qualitative information on the rock being evaluated. To be acceptable for long-term use the rock must qualitatively be rated as "fair," and must not contain substantial amounts of smectites and expanding clay-lattice materials (Johnson et al., 1993).

Comparison of Rock Quality/Durability Criteria

A comparison of criteria for riprap quality/durability was performed by Lienhart (1992) and Abt et al. (1994a). Table 1 summarizes riprap quality standards established by the U.S. Bureau of Reclamation; the U.S. Army Corps of Engineers; the U.S. Department of Agriculture, Soil Conservation Service; the California Department of Transportation; the United States Nuclear Regulatory Commission (NRC); and the Construction Industry Research and Information Association / Center for Civil Engineering Research, Codes, and Specifications. The U.S.

Nuclear Regulatory Commission regulations are the most stringent because designs must meet two hundred to one thousand year performance criteria, whereas other agency designs have a fifty to one hundred year performance criteria (Abt et al., 1994a).

Given the criteria established by agencies included in Table 1, rock test results from a study performed by Abt et al. (1994a) will be evaluated. Abt et al. submitted eighteen sandstone rock samples and one basalt, one tuff, and one limestone rock sample to six ASTM standardized tests. The tests that were performed are sodium sulfate, Los Angeles (LA) abrasion, specific gravity, absorption, Schmidt hammer, and tensile strength. The results of the tests are presented in Table 2.

NRC rock scores are also presented in Table 2. The rock scores were determined using NRC rock scoring criteria developed by Johnson et al. (1993). Table 3 shows the ranking of the rock samples based on their NRC rock score. The data in Table 2 was similarly ranked according to the results of each test to facilitate analysis of the test results considering the criteria presented in Table 1. Following are general comments regarding the observed trends.

Analysis

Based on their NRC rock score, the two highest quality rock samples in Table 3 are the Kain, NV and Kaibab, NV samples, a basalt and limestone rock, respectively. They were included in the in study performed by Abt et al. (1994a) as control rocks. The Kain, NV sample was known to be of high quality and the Kaibab, NV sample was known to be of moderate quality. The North Canyon, NV sample, a tuff rock, was also included in the study as a control rock. It was known to be of poor quality. Sandstone rock, in general, is considered to be of marginal quality. It is appropriate that all of the sandstone rock samples scored below the Kain, NV and Kaibab, NV samples and above the North Canyon, NV sample.

It is noted that the Kain, NV sample (high quality) meets the acceptance criteria of all of the agencies represented in Table 1 except NRC absorption criteria. Likewise, the Kaibab, NV sample (moderate quality) meets only some of the criteria in Table 1. More specifically, its specific gravity (2.73) and absorption (1.0%) meet all of the presented criteria except the NRC absorption criteria. The reported Los Angeles (LA) abrasion loss for the sample is 17%. This value is for 100 revolutions, though, and would be much higher if the test had been performed using 500 revolutions as required by the USBR, USACE, and CALTRANS -- probably about 65%. Regarding the absorption and sodium sulfate tests, the Kaibab, NV sample did not meet any of the criteria presented in Table 1.

Table 1 - Criteria for Stone Quality/Durability Acceptance (modified from Abt et al., 1994)

Test	ASTM Standard	USBR	USACE	USDA-SCS	CIRCA/CUR	CALTRANS	NRC
Specific Gravity	C 127	> 2.5	> 2.6	> 2.5	> 2.3	> 2.5	> 2.65
Absorption	C 127	< 1%	< 1%	< 2%	< 6%	< 2%	< 0.5%
Sodium Sulfate Loss	C 88	< 10%	< 5%	< 10%	< 30%	< 5%	< 5%
Freeze Thaw Loss	D 5312	< 5% (12 cycles)	< 10% (12 cycles)		< 2% (25 cycles)		
LA Abrasion Loss	C 131 & C 535	< 40% (500 revs)	< 20% (500 revs)			< 40% (500 revs)	< 5% (100 revs)

ASTM - American Society for Testing and Materials, 1993 (the standards are shown for reference only and may or may not be employed by the respective agencies).

USBR - U.S. Bureau of Reclamation

USACE - U.S. Army Corps of Engineers

USDA-SCS - U.S. Department of Agriculture, Soil Conservation Service

CIRCA/CUR - Construction Industry Research and Information Association in the UK and the Center for Civil Engineering Research, Codes and Specifications in the Netherlands

CALTRANS - California Department of Transportation

NRC - U.S. Nuclear Regulatory Commission

Table 2 - Physical Test Results (Modified from Abt et al., 1994)

Site No.	Sitename	Rock Type	Formation	Sodium Sulfate [% Loss]	L.A. Abrasion [% Loss]	Apparant Specific Gravity	Absorption [%]	Schmidt Hammer [Rebound No.]	Tensile Strength [p.s.i.]	NRC Rock Score
1	Kain, NV	Basalt	NA	0.3	3.4	2.76	0.7	30.0	2020	93
2	North Canyon, NV	Tuff	NA	39.2	17.0	2.30	10.8	10.0	290	11
3	Kaibab, NV	Limestone	NA	3.8	6.5	2.73	1.0	19.0	711	61
4	Cedar Fort., UT	Sandstone	Diamond Creek	4.4	15.4	2.48	2.5	32.0	1633	46
5	Sand Island, UT	Sandstone	Buff	100.0	27.3	2.41	10.5	10.0	250	12
6	Sego Canyon, UT	Sandstone	Sego	72.4	22.0	2.52	6.7	14.0	250	19
7	Chaco Canyon, NM	Sandstone	Cliff	23.4	9.2	2.67	1.6	27.0	990	50
8	Escalante Canyon, CO	Sandstone	Morris	4.2	7.6	2.52	2.3	25.0	1450	52
9	Shavano V., CO	Sandstone	Morris	34.1	18.5	2.47	5.1	26.0	937	30
10	Hogback Ridge, SD	Sandstone	Dakota	99.0	27.0	2.43	7.3	12.0	253	14
11	Hunter Canyon, CO	Sandstone	Mesa Verde	61.2	18.6	2.44	6.2	11.0	420	20
12	Wallace Ruin, CO	Sandstone	Mancos Stringer	19.5	13.8	2.60	3.3	27.0	695	38
13	Cave Towers, UT	Sandstone	Morris	50.3	24.7	2.50	6.7	13.0	439	20
14	Ruin Springs, UT	Sandstone	Dakota	82.3	22.3	2.51	6.0	18.0	822	26
15	Santa Clara, UT	Sandstone	Shinarp	18.0	22.1	2.48	4.4	28.3	534	29
16	Mitchell Ruin, CO	Sandstone	Dakota	47.6	24.8	2.49	4.1	25.4	562	26
17	Pig Ruin, CO	Sandstone	Dakota	64.0	24.2	2.47	5.1	10.0	331	17
18	Hovenweep, UT	Sandstone	Dakota	97.2	27.0	2.47	6.4	10.0	203	15
19	Little Creek, UT	Sandstone	Shinarp	76.2	24.3	2.56	4.2	12.0	251	19
20	Green River, UT	Sandstone	Unknown	10.6	12.8	2.52	2.4	30.0	1200	46
21	Falls City, TX	Sandstone	Unknown	1.0	21.0	2.09	9.0	55.0	1040	45

10

Table 3

Rank	Site Name	NRC Rock Score	Rank	Site Name	NRC Rock Score
1	Kain, NV	93	12	Ruin Springs, UT	26
2	Kaibab, NV	61	13	Cave Towers, UT	20
3	Escalante Canyon, CO	52	14	Hunter Canyon, CO	20
4	Chaco Canyon, NM	50	15	Little Creek, UT	19
5	Cedar Fort., UT	46	16	Sego Canyon, UT	19
6	Green River, UT	46	17	Pig Ruin, CO	17
7	Falls City, TX	45	18	Hovenweep, UT	15
8	Wallace Ruin, CO	38	19	Hogback Ridge, SD	14
9	Shavano V., CO	30	20	Sand Island, UT	12
10	Santa Clara, UT	29	21	North Canyon, NV	11
11	Mitchell Ruin, CO	26			

Regarding the specific gravity of the sandstone rocks, only the Chaco Canyon, NM sample (specific gravity = 2.67) meets all of the criteria presented in Table 1. One sample, Wallace Ruin, CO has a specific gravity of 2.6 and a total of eight of the sandstone samples (44%) have specific gravities of 2.5 or higher.

The absorption test results for the sandstone rock samples fared poorly in comparison to the criteria presented in Table 1. All of the agencies, except CIRCA/CUR, require absorption percentages to be less than 2%. The Chaco Canyon, CO sample, with a reported absorption of 1.6%, meets the USDA-SCS, CIRCA/CUR, and CALTRANS criteria but not the USBR, USACE, or NRC criteria. Eleven of the sandstone samples (61%) meet the CIRCA/CUR criteria, that is, their reported absorption is less then or equal to 6%.

The sodium sulfate test results for the sandstone rock samples were poor for all but two of the samples. The Escalante Canyon, CO and Cedar Fort, UT, samples meet the sodium sulfate criteria of all the agencies and a total of six sandstone samples (33%) meet the lowest established criteria (CIRIA/CUR requires sodium sulfate loss less then 30%). It is noted that the Chaco Canyon, NM sample, the highest ranking sandstone sample regarding specific gravity and absorption test results, ranked sixth regarding sodium sulfate test results.

It is noted that the Los Angeles abrasion (LAA) test results presented in Table 1 are for 100 revolutions whereas most of the agencies using the LAA test require it to be performed with 500 revolutions. An approximate relation developed by Abt (1994b) for 100 revolution and 500 revolution LAA test results is

$$\mathbf{LAA_{100} = 0.286 * (LAA_{500} - 5.0)} \qquad \text{Eq. (1)}$$

where $\mathbf{LAA_{100}}$ and $\mathbf{LAA_{500}}$ are the percent losses for 100 and 500 revolution LAA tests, respectively. Applying Eq. (1) to the LAA criteria presented in Table 1, the 40% and 20% maximum loss for 500 revolutions become 10.0% and 4.3%, respectively, for 100 revolutions.

Using the equivalent 100 revolution LAA test results, all of the sandstone samples, except the Escalante Canyon, CO, and Chaco Canyon, CO samples, tested poorly. The LAA test results for Escalante Canyon, CO, and Chaco Canyon, CO, are 7.6% and 9.2%, respectively.

Conclusion

The criteria presented in Table 1 suggests that most sandstone rock is not suitable for construction applications. Some sandstone rocks, though, are marginally acceptable for use (i.e., the Chaco Canyon, NM, and Escalante Canyon, CO samples). Where the cost of using lower quality rock, such as sandstone, is significantly less then the cost of acquiring higher quality rock it is reasonable to consider its use (Bureau of Reclamation, 1987). Also, oversizing of inferior quality rock has been recommend by Nelson et al. (1986) as a method of making up for the structural deficiencies of a proposed rock source.

The evaluation criteria used by most agencies is similar. As demonstrated in this report, the criteria presented in Table 1 would select a high quality rock (like the Kain, NV, basalt rock) and reject intermediate quality rock (like the Kaibab, NV, limestone rock), marginal quality rock (i.e., sandstone) and poor quality rock (like the North Canyon, NV, tuff rock).

REFERENCES

Abt, S. R., Peters, M. R., Thornton, C. I., Hogan, S. A., Wilkerson, G. V. (1994a). "Methodologies for Design of Soil Covers, Interim Report III, Gully Intrusion into Reclaimed Slopes, Rock Durability Assessment," U.S. Nuclear Regulatory Commission, Contract No.: NRC-02-91-007, Washington, D.C.

Abt, S. R. (1994b). Personal communication. Colorado State University, Fort Collins, CO.

Ang, A. H-S., Tang, W. H. (1975). **Probability Concepts in Engineering Planning and Design** John Wiley & Sons, New York, Vol. 1.

ASTM (1993). **Annual Book of ASTM Standards**, American Society for Testing and Materials, Phildelphia, PA, Vol. 04.02.

Bradley, B. A. (1988). "Wallace Ruin Interim Report," Southwestern Lore, Vol. 54, No. 2, pp. 8-33, June.

Brown E. T. (Ed.)(1981). **Rock Characterization Testing and Monitoring: ISRM Suggested Methods**, Pergamon Press, Oxford, pp. 71-121.

Bureau of Reclamation (1987). **Design of Small Dams**, U.S. Department of the Interior, Bureau of Reclamation, Denver, CO.

Chow, V. T., Maidment D. R., Mays, L. W. (1988). **Applied Hydrology**, McGraw-Hill, New York.

CIRIA/CUR (1991). **Manual for the Use of Rock in Coastal and Shoreline Engineering**. Published jointly by the Construction Industry Research and Information Association in the UK, (Special Publication 83) and the Centre for Civil Engineering Research, Codes and Specifications (Report 154) in the Netherlands.

Deere, D. U. and Miller, R. P. (1969). "Engineering Classification and Index Properties for Intact Rock," Technical Report AFWL-TR-65-116.

DePuy, G. W., and Ensign, T. F. (1965). "Riprap Testing Research Comparison of an Ultrasonic Cavitation Test with Petrographic and Physical Tests to Evaluate Rock Durability," U.S. Bureau of Reclamation Report No. ChE-23, U.S. Department of the Interior, Denver, CO.

Highway Research Board Bibliography 33 (1963). "Non-Destructive Testing of Concrete," Publication 1070.

Johnson, T. L., Abt, S. R. and Fliegel, M. H. (1993). "Verification of Rock Durability Evaluation Procedures Using Petroglyphs and Indian Rock Art," **Rock for Erosion Control, ASTM STP 1177**, American Society for Testing and Materials, Philadelphia, PA, pp. 29-37.

Kindsvater, C. E., and Carter, R. W. C (1957). Discharge Characteristics of Rectangular thin Plate Weirs," Proceedings of the Amercian Society of Civil Engineers, Journal of the Hydraulics Division, Vol. 83, No. HY6, pp 1453/1-1453/36, December.

Krumbein, W. C., and Pettijohn, F. J. (1938). "Manual of Sedimentary Petrography." Appleton-Century-Crofts, NewYork.

Koopmans, R., and Watts, R. B. (1992). "The Assessment of Armourstone for Shoreline Protection," **Durability of Stone for Rubble Mound Breakwaters**, American Society of Civil Engineers, New York, NY, pp. 82-94.

Latham, J-P. (1993). "A Mill Abrasion Test for Wear Resistance of Armour Stone," **Rock for Erosion Control, ASTM STP 1177**, American Society for Testing and Materials, Philadelphia, PA, pp. 46-61.

Leslie, J. R. and Cheeseman, W. J. (1950). "An Ultrasonic Method of Studying Deterioration and Cracking in Concrete Structures," Proceedings, American Concrete Institute, Vol 46, p. 17.

Lienhart, D.A. (1992). "Laboratory Testing of Stone for Rubble Mound Breakwaters: An Evaluation," **Durability of Stone for Rubble Mound Breakwaters**, American Society of Civil Engineers, New York, NY, pp. 19-33.

Lienhart, D. A., and Stransky, T. E. (1981). "Evaluation of Potential Sources of Riprap and Armor Stone - Methods and Considerations," Bulletin of the Association of Engineering Geologists, 18, No. 3, pp. 323-332.

Lindsey, C. G., L. W. Long, and C. W. Gegej (1982). "Long-term Survivability of Riprap for Armoring Uranium Mill Tailings and Covers: A Literature Review," NUREG/CR-2642 (PNL-4225), U. S. Nuclear Regulatory Commission, Washington, D.C.

Nelson, J. D., Abt, S. R., Volpe, R. L., van Zyl, D., Hinkle, N. E., and Staub, W. P. (1986). "Methodologies for Evaluating Long-Term Stabilization Designs of Uranium Mill Tailings Impoundments," NUREG/CR-4620; U.S. Nuclear Regulatory Commission, Washington, DC.

Rzhevsky V. and Novik G. (1971). **The Physics of Rocks**, MIR Publishers, Moscow, p. 370.

Sengupta, M. (1975). "A New Method of Evaluation for Dimension Stone from Diamond-Drill Core." **CIM Bulletin**, pp. 65 - 70.

Runyon, R. P., and Haber, A. (1980). **Fundamentals of Behavioral Statistics**, Addison-Wesley Publishing Co., Inc., Reading, MA.

Shakoor, A., and Bonelli, R. E. (1991). "Relationship between Petrographic Characteristics, Engineering Index Properties, and Mechanical Properties of Selected Sandstones," Bulletin of the Association of Engineering Geologists, 28, No. 1, pp. 55-71

Summer, R. M., Johnson, R. E. (1982). "Rock Durability Evaluation Procedure for Riprap and Diversion Channel Construction in Coal Mining Areas," **1982 Symposium on Surface Mining, Hydrology, Sedimentology and Reclamation**; December 5-10, 1982 (Lexington, Ky.: University of Kentucky), pp. 433-437.

Taylor, J. K. (1990). **Statistical Techniques for Data Analysis**, Lewis Publishers, Inc., Chelsea, MI.

Vernik, L., Bruno, M., Bovberg, C. (1993). "Empirical Relations between Compressive Strength and Porosity of Siliciclastic Rocks," Int. J. Rock Mech. Min. Sci. & Geomech. Abstr., 30, No. 7, pp. 677-680.

Estimating Upland Erosion Using the Universal Soil Loss Equation Application to Goodwin Creek, Panola County, MS

By Darcy K. Noss

April 1995

INTRODUCTION

The amount of sediment in fluvial systems is usually governed by the availability of upstream supply rather than by the sediment transport capacity of the rivers. Soil erosion from upland areas is the source of most sediment transported in rivers. Thus an understanding of the processes governing upland erosion provides insight into the conditions for sediment transport in rivers.

The extent of erosion, specific degradation, and sediment yield in a river basin is primarily a function of topography, soil, vegetation, landuse, geology, and climate. Erosion rates in upland areas are determined by the erosive forces of rainfall and runoff, and by soil resistance to detachment and transport. The major components of erosion losses and sediment yield are attributed to sheet and rill erosion (Julien & Gonzalez, 1991). Human activity is responsible for increased rates of erosion over the normal (or geological) erosion rate. The erodibility of natural soils is increased when soils are plowed and tilled, with resulting accelerated erosion rates up to 10 tons/acre-year, which is 100 times the normal erosion rate. Erosion rates of grazed areas can exceed 5 tons/acre-year. Average values of 40 to 50 tons/acre-year can be expected when there is urban development in areas without vegetation. The total volume of soil eroded during a year, in a given watershed, is capable of creating a great deal of damage downstream.

The ability to predict and control soil erosion rates in upland areas of watershed basins is clearly a priority. Unfortunately, due to the number of factors involved, soil erosion is not easily predicted. In the 1960's the Universal Soil Loss Equation (USLE) was empirically derived to predict average annual soil loss due to sheet and rill erosion. The USLE has been widely used, yet applications have been limited by the fact that the equation was developed for plots not exceeding 1 hectare. In the 1980's, Julien and Frenette performed studies on the Chaudiere Basin in Canada, in order to determine the applicability of the USLE at larger scales. Their analysis included subdividing the basin into grid cells and determining a correction factor for the evaluation of actual losses as a function of basin-averaged losses. Today the use of Geographic Information Systems (GIS) allows for a quick replication of Julien & Frenette's work, based on the GIS's capability to represent characteristics of watershed basins within a grid cell environment. The focus of this paper is to test the method developed by Julien & Frenette, using the GIS program GRASS, and to draw conclusions regarding the applicability of the correction factor within a GIS environment.

PROCESSES -- UPLAND EROSION

A major source of sediment transported by rivers is soil erosion from upland areas. Upland erosion is defined as the detachment and entrainment of solid particles from the land surface. Erosion can be caused by water, gravity, wind, and ice, of which water is the most widespread cause. Soil erosion by water is a complex process governed by raindrop impact and runoff, involving the detachment of soil particles and their transport downstream (see Fig. 1).

The erosive potential of rainfall depends on raindrop fall velocity, size distribution, and total mass at impact. Raindrops may transport detached soil downstream by the splash process, but more often eroded soil is moved downstream by surface runoff. For a given storm, once the infiltration capacity of the soil has been exceeded, the rate of soil erosion will depend on runoff flow velocity and the susceptibility of the soil to the forces of flowing water. Properties of the soil such as particle size, shape, density, cohesiveness, and aggregate strength determine the resistance of the soil to erosive forces.

Water erosion is classified as sheet erosion and rill erosion. Thin overland flow, otherwise known as sheet erosion, is defined as the detachment of land surface material by raindrop impact. The transport capacity of sheet flow increases with field slope and flow discharge per unit width. As sheet flow concentrates and the unit discharge increases, the increased sediment transport capacity scours microchannels. These microchannels are called rills. Rill erosion occurs as a result of the removal of soil by concentrated sheet flow.

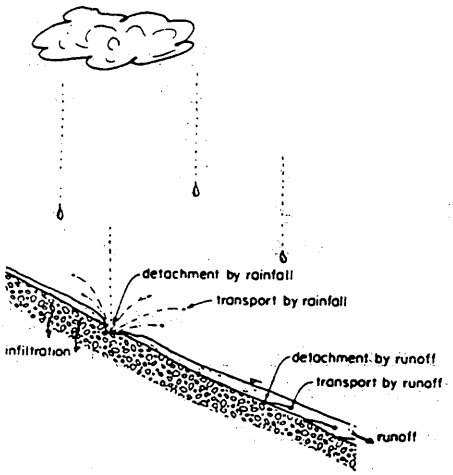

Figure 1: Soil erosion processes during rainfall

Overland flow is capable of detaching and transporting large amounts of sediment from upland areas. In terms of watershed characteristics, sheet and rill erosion are primarily controlled by landform geometry, surface slope, overland runoff length, rainfall intensity, ground cover, canopy cover, land use and conservation practices. The Universal Soil Loss Equation was developed to estimate soil losses, based on the main processes governing soil erosion.

METHODS TO EVALUATE UPLAND EROSION

A. Microscale

1. The Universal Soil Loss Equation (USLE)

Surface erosion begins when raindrops impact the ground and detach soil particles by splash. Kinetic energy released when the raindrop hits the soil surface is sufficient to break the bonds between soil particles. Yet if there is no surface runoff, soil erosion losses will be small. Musgrave performed a study of 40,000 storms on experimental plots in the United States, and

determined that soil erosion loss is a function of soil erodibility, runoff length and slope, maximum 30-min amount of rainfall, and a cover factor. This study eventually led to the development of the USLE, which is used to predict long-term average soil losses in runoff from field areas under specific cropping and management systems. The USLE has been found to be applicable for areas up to 1 hectare (0.1 km^2). Soil loss, in annual tons/acre, is calculated as:

$$A = R*K*L*S*C*P \quad (1)$$

where A = soil loss per unit area [tons/acre]

R = rainfall erosivity factor

K = soil erodibility factor [tons/acre]

L = field length factor, normalized to a plot length of 72.6 ft

S = field slope factor, normalized to a field slope of 0.09

C = cropping-management factor, normalized to a tilled area with continuous fallow

P = conservation practice factor, normalized to a straight-row farming up and down slope

The rainfall factor R accounts for geographic differences in rainfall intensity-duration-frequency. Figure 1 shows a map of the R values which have been determined for Eastern United States.

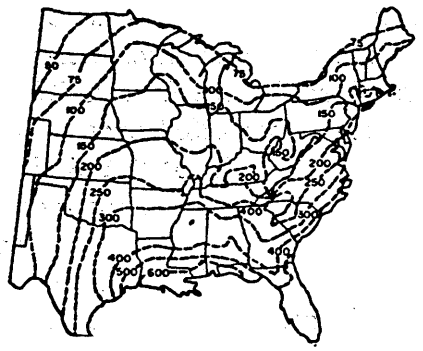

Figure 1: Rainfall index R

The soil-erodibility factor K is a measure of the intrinsic susceptibility of a given soil to soil erosion. Table 1 shows estimated values for K, as a function of soil type.

Textural class	Organic matter content, % 0.5	2
Fine sand	0.16	0.14
Very fine sand	0.42	0.36
Loamy sand	0.12	0.10
Loamy very fine sand	0.44	0.38
Sandy loam	0.27	0.24
Very fine sandy loam	0.47	0.41
Silt loam	0.48	0.42
Clay loam	0.28	0.25
Silty clay loam	0.37	0.32
Silty clay	0.25	0.23

Source: From Schwab et al.[10]

Table 1: Soil erodibility factor K

The slope-length factor L accounts for the increased quantity of runoff that occurs as distance from the top of the slope increases. The length factor L is standardized to a plot length of 76 ft. The slope-steepness factor S accounts for the increased velocity of runoff as slope steepens, and is standardized to a slope of 0.09. The LS factor can be calculated as (Meyer, 1971):

$$LS = L^{0.5}(0.0076 + 0.0053*S + 0.00076*S^2)$$

where L is in feet and S is in percent.

The factor C accounts for different cropping and management combinations. Estimated values of C are shown in Table 2.

Undisturbed forest land						
Percent of area covered by canopy of trees and undergrowth		Percent of area covered by duff at least 2 in deep		Factor C		
100–75		100–90		0.0001–0.001		
70–45		85–75		0.002–0.004		
40–20		70–40		0.003–0.009		
Permanent pasture, range, and idle land[a]						
	Cover that contacts the soil surface					
Vegetative canopy	Percent ground cover					
Type and height[b]	Type[c]	0	20	40	60	80	95+
No appreciable canopy	G	0.45	0.20	0.10	0.042	0.013	0.003
	W	0.45	0.24	0.15	0.091	0.043	0.011
Tall weeds or short brush with average drop fall height of 20 in	G	0.17–0.36	0.10–0.17	0.06–0.09	0.032–0.038	0.011–0.013	0.003
	W	0.17–0.36	0.12–0.20	0.09–0.13	0.068–0.083	0.038–0.041	0.011
Appreciable brush or bushes, with average drop fall height of 6 1/2 ft	G	0.28–0.40	0.14–0.18	0.08–0.09	0.036–0.040	0.012–0.013	0.003
	W	0.28–0.40	0.17–0.22	0.12–0.14	0.078–0.087	0.040–0.042	0.011
Trees, but no appreciable low brush. Average drop fall height of 13 ft	G	0.36–0.42	0.17–0.19	0.09–0.10	0.039–0.041	0.012–0.013	0.003
	W	0.36–0.42	0.20–0.23	0.13–0.14	0.084–0.089	0.041–0.042	0.011

Table 2: Crop management factor C

The conservation practice P is determined by the extent of strip cropping, contouring, and terracing practices in the basin. Such practices tend to reduce the erosive potential of water in upland areas. Typical P values are shown in Table 3.

Land slope, %	Farming on contour	Contour strip crop	Terracing *	Terracing †
2–7	0.50	0.25	0.50	0.10
8–12	0.60	0.30	0.60	0.12
13–18	0.80	0.40	0.80	0.16
19–24	0.90	0.45	0.90	0.18

Source: From Wischmeier.[141]
* For erosion-control planning on farmland.
† For prediction of contribution to off-field sediment load.

Table 3: Conservation practice P

2. Simplified USLE

A simplified version of the USLE was developed by Julien (1982). After examining the relative magnitudes of the components in the USLE, Julien concluded that for a given watershed the rainfall index ***R***, soil erodibility *K*, conservation practice ***P***, and slope length ***L*** can be considered relatively constant. Therefore the determining factors are slope **S** and conservation practice **C**. The simplified equation is based on the USLE and on the Kilinc sediment discharge equation (Kilinc, 1972). According to Kilinc, sediment discharge is calculated as $q_s \sim S^{\beta} \cdot q^{\gamma}$, where $\gamma = 2.05$ and $\beta = 1.46$. The simplified USLE resulted from the incorporation of this slope dependency into the soil loss equation $A = R*K*P*L^{0.5}(0.0076 + 0.0053*S + 0.00076*S^2)*C$. The erosion rate is calculated as:

$$e = B*S^{1.46}*C \qquad (2)$$

where $B = 4.696*R*K*P*L^{0.5}$.

B. Macroscale

Technically the USLE and the simplified USLE should only be applied to small watersheds. In their paper titled "Macroscale Analysis of Upland Erosion" Julien & Frenette (1987) examine scale effects in using the USLE to calculate erosion losses from large basins. They applied the simplified USLE to the Chaudiere Basin in Canada, which is 3000 km^2. The objective of the study was to determine if grid sizes beyond the applicability of soil-loss equations would provide sufficient accuracy for the prediction of upland erosion losses. Based on physical characteristics of the Chaudiere Basin, the simplified USLE used in the study was determined as:

$$e = 226*S^{1.46}*C$$

where e = soil erosion loss per unit area [kt/km^2]

S = slope [m/m]

C = crop-management factor

An *estimated* value of soil loss for the entire basin was calculated, taking average watershed values of slope and crop management factor. The equation was applied to grid sizes ranging from 0.03 to 4 km^2 in order to calculate *actual* soil loss per cell, for comparison with the *estimated* soil loss for the entire basin. From their study Julien & Frenette concluded that mean characteristics of a basin can be used to calculate *actual* upland erosion losses, with the introduction of a correction factor.

The correction factor is defined as $Q_e = e/e_o$, where e is the *estimated* soil loss using average basin characteristics and e_o is the *actual* soil loss. The correction factor varies as a function of watershed size, and can be calculated as (Julien & Frenette, 1987):

$$Q_e = 0.75\, Q_{es}\, A^{-0.137} \quad \text{for } A > 0.125 \text{ km}^2 \qquad (3)$$

$$Q_e = Q_{es} \quad \text{for } A < 0.125 \text{ km}^2 \qquad (4)$$

where $Q_{es} = 1.13$

A = total watershed area

Thus, knowing the *estimated* soil loss and Q_e, the *actual* soil loss is evaluated as: $e_o = e/Q_e$.

The correction factor method proposed by Julien & Frenette should be applicable in any river basin. The method is also applicable for the USLE, with *actual* soil loss A_o calculated as $A_o = A/Q_e$. *A* is the *estimated* soil loss using mean characteristics. The objective of this study was to evaluate the correction factor method on a watershed located in northern Mississippi.

LOCATION PARAMETERS

A. Site

The site chosen for this study was Goodwin Creek, located in Panola County, Mississippi (Fig. 3). The watershed drains an area of 21.6 km^2, and is characterized as having excessive upland erosion. Landuse and management practices ranging from timbered areas to row crops influence the rate and amount of sediment delivered to the streams as a result of upland erosion. Land management activities are limited in the watershed, with only 13% of the total area under cultivation. The rest of the area is idle pasture and forest land.

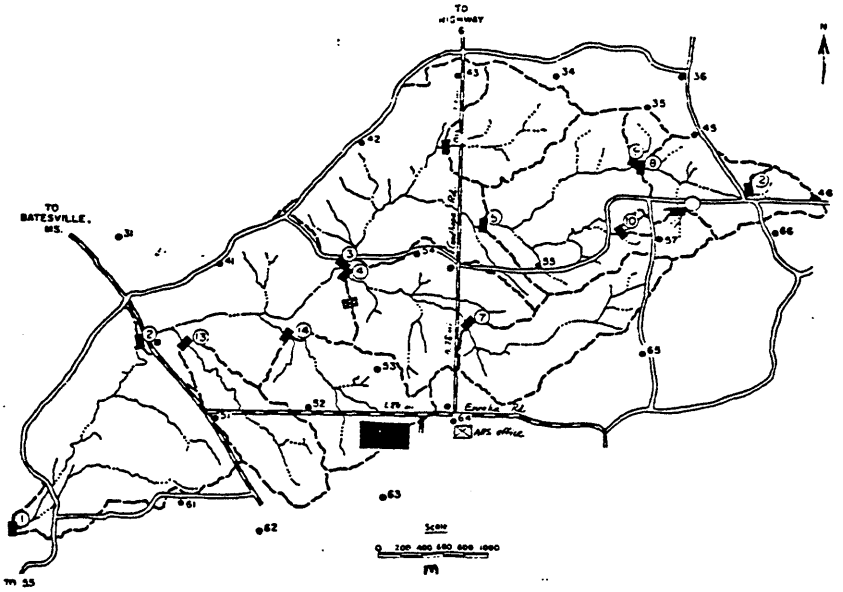

Figure 3: Goodwin Creek

The GIS GRASS environment allows for the display and manipulation of raster maps which define characteristics of the watershed. Raster representation assumes that geographical space can be treated as a flat Cartesian surface, and each grid cell is associated with a square parcel of land. Input data available for Goodwin Creek consisted of the following raster maps:

1. A USGS DEM - digital elevation map (Fig. 4)
2. A soil map generated by the Soil Conservation Service (Fig. 5), and
3. A landuse map (Fig. 6)

All the input data were in a 30x30 m grid format.

B. Location Parameters

1. Microscale

The USLE parameters used in evaluating erosion rates on a microscale level included ***R***, ***K***, ***L***, ***S***, ***C***, and ***P***. Parameter values were evaluated on a grid cell by grid cell basis. Figure 1 was used to specify a rainfall index ***R*** of 330 for Panola County, MS. Although the soil map contained 10 different soil types, the soils could be reclassified into two general categories, based on an analysis of soil characteristics done by the Soil Conservation Service (Galberry, 1960). Fine

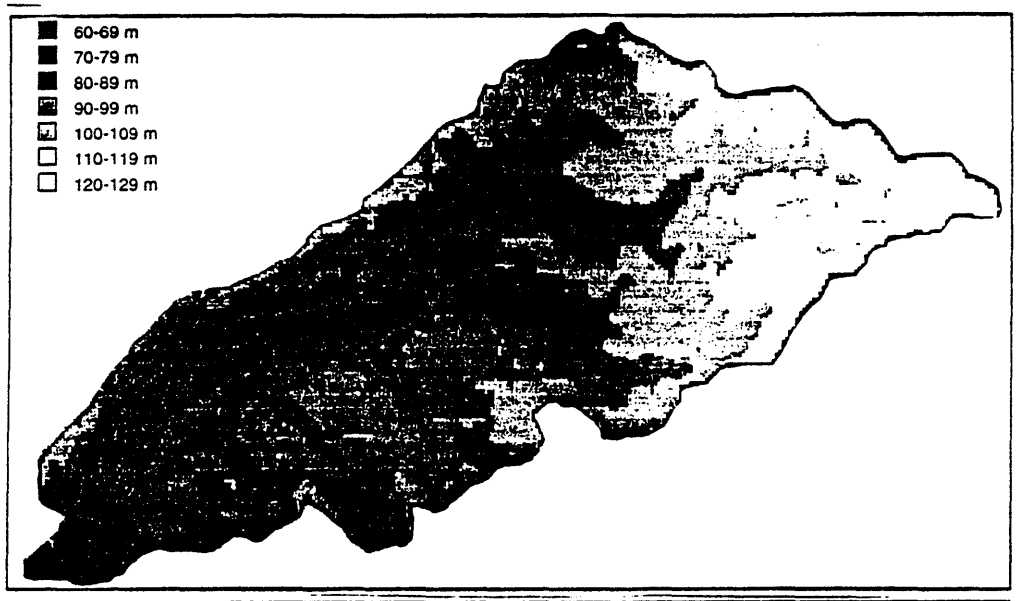

Figure 4:
Elevation map

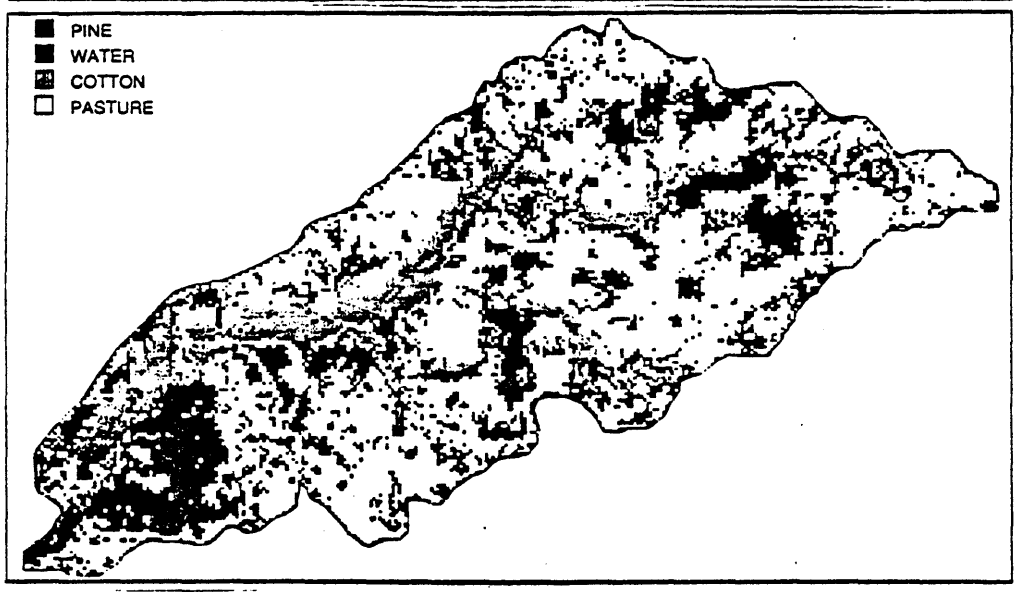

Figure 5:
Soil map

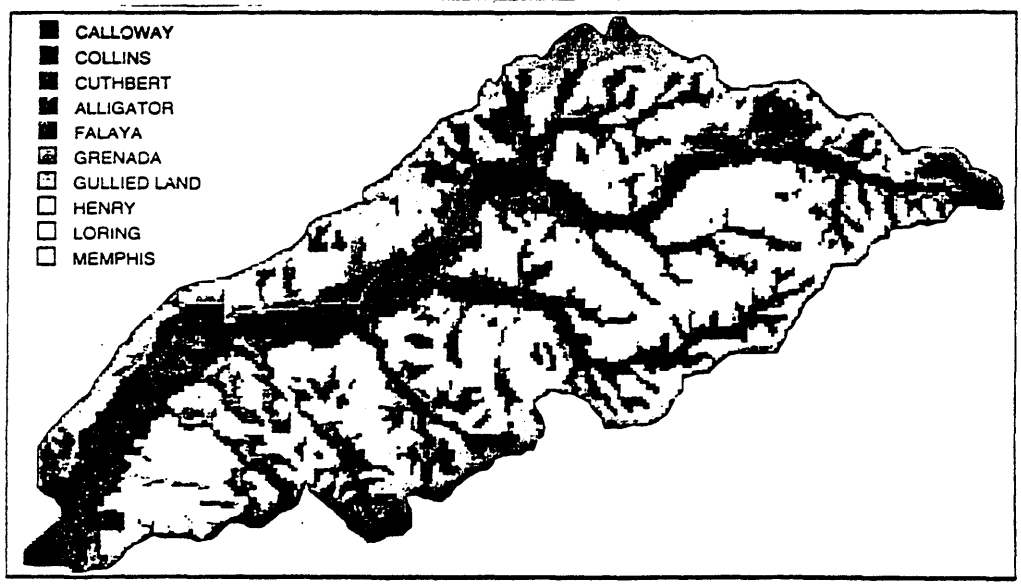

Figure 6:
Landuse map

sandy loam was assigned a K value of 0.47 tons/acre and silt loam was assigned a value of 0.48 tons/acre (Table 1). The runoff length L was determined as 150 meters (495 ft), based on the drainage density of the basin. Individual cell slopes were calculated from the Goodwin Creek digital elevation model. The slopes ranged from 0-24%. Crop management values were estimated as a function of landuse categories. From Table 2, C_{pine}=0.02, $C_{pasture}$ = 0.013, and C_{cotton}=0.65. These values were verified with information from Meyer's chapter on "Soil erosion by water in upland areas" (Meyer, 1971). The conservation practice P value was taken equal to 1, as contouring, strip cropping, and terracing are not typically practiced in this region.

Using the USLE equation, a microscale value of the erosion rate was calculated for each grid point, with $A = R*K*L*S*C*P$. Using the simplified USLE, erosion rates on the microscale level were calculated as $e = B*S^{1.46}*C$, with $B = 4.696*330*K_{avg}*1*495^{0.5} = 34{,}478*K_{avg}$. K_{ave} was calculated to be 0.478, as a weighted average of the parameters $K_{sandy\ loam} = 0.47$ covering an area of 3.4 km^2 and $K_{silt\ loam} = 0.48$ covering an area of 18.2 km^2. Incorporating K_{avg} into the above equation, the simplified version of the USLE used to calculate losses at the grid scale became: $e = 16{,}478*S^{1.46}*C$.

2. Macroscale

On the macroscale level, mean values were used in *estimating* average soil losses for the basin. The correction factor was then applied to the *estimated* value in order to calculate *actual* soil losses. Mean values for Goodwin Creek, as determined above, were $R = 330$, $L = 150$ m (495 ft), $P = 1$, and $K = 0.478$. The average slope S was calculated from the approximation given by Julien & Frenette (1987):

$$S = \frac{elevation_{max} - elevation_{min}}{A^{0.5}} = \frac{129m - 66m}{(21{,}607{,}000m^2)^{0.5}} = 0.014$$

An average C value of 0.098 was calculated according to landuse distribution: for C_{pine} = 0.002, A = 5.608 km^2; for C_{water}=0, A=0.093 km^2; for C_{cotton}=0.65, A=2.969 km^2; and for $C_{pasture}$ = 0.013, A = 12.938 km^2.

The *estimated* soil loss, using the USLE, was calculated as:

$$A = R*K*P*L*S*C, \text{ where } LS = L^{0.5}(0.0076 + 0.0053*S + 0.00076*S^2)$$

The *estimated* soil loss, using the simplified USLE, was calculated as:

$$e = 16{,}478*S^{1.46}*C$$

The correction factor was then applied to the *estimated* values of soil loss in order to determine *actual* values of soil loss. Q_e corresponding to the size of the Goodwin Creek basin (21.6 km^2) was determined as:

$$Q_e = 0.75\ Q_{es}\ A^{-0.137} \qquad \text{for } A > 0.125 \text{ km}^2$$

$$Q_e = 0.556$$

Using the USLE, the *actual* soil losses were then calculated to be $A_o = A/Q_e$. Using the simplified USLE, the *actual* soil losses were calculated as $e_o = e/Q_e$.

RESULTS

A. Microscale Results

Figure 7 shows plots of estimated erosion rates at different grid scales, as a function of the area of the watershed associated with each rate. The plots give an indication of the distribution and range of erosion rates calculated on the microscale level, for both the USLE and the simplified USLE. Erosion rates up to 727 tons/acre were calculated on a 30x30 m grid scale.

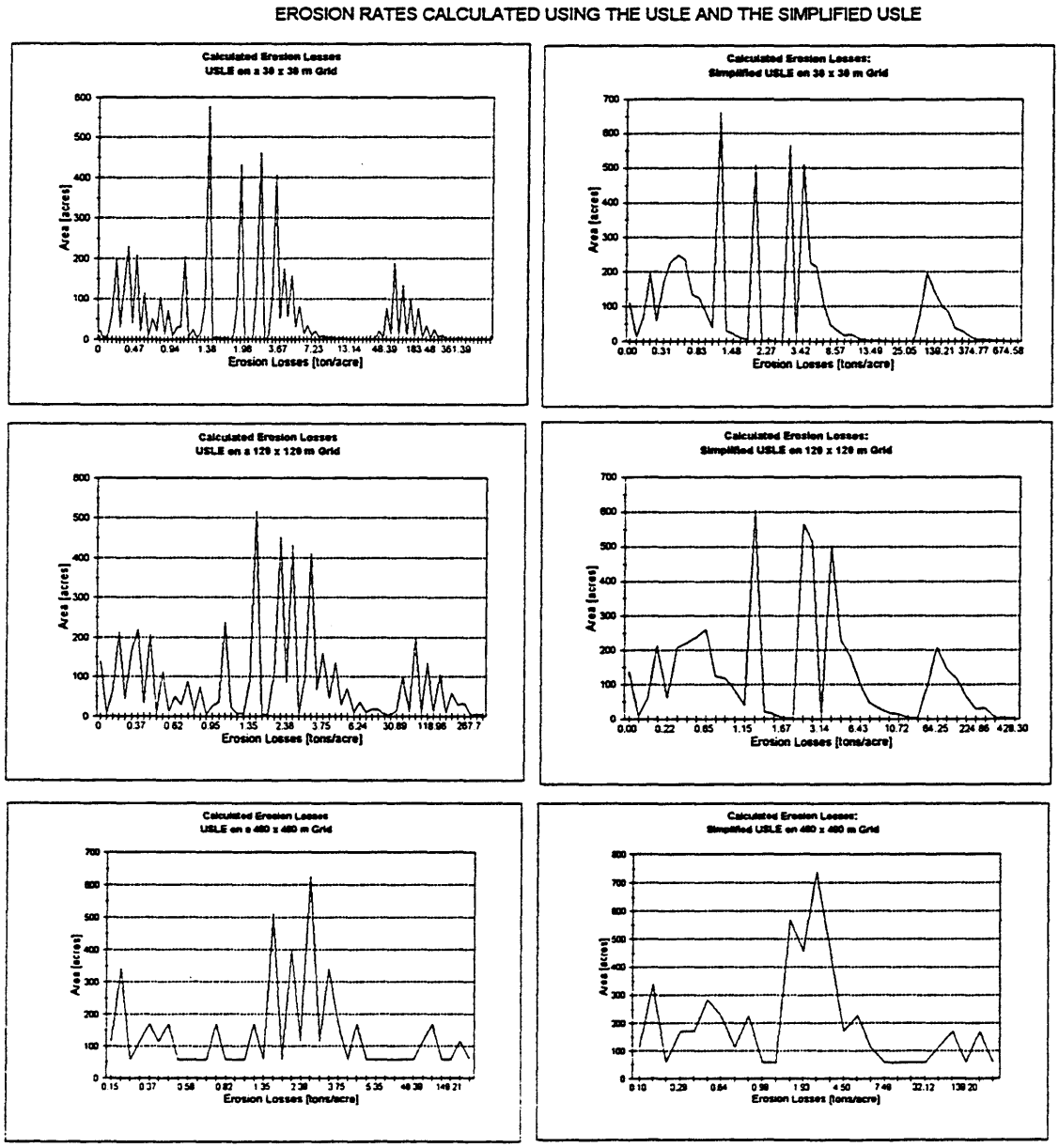

Figure 7: Distribution of microscale erosion rates at different grid scales

Table 4 presents a summary of calculated values of erosion rates at the microscale level:

Grid Size [m]	A_o of max coverage [tons/acre]	Weight AvgA_o [tons/acre]	e_o of max coverage [tons/acre]	Weight Avg e_o tons/acre]
30 x 30	1.38	17.08	1.28	18.12
60 x 60	1.38	16.74	1.28	18.15
120 x 120	1.38	15.37	1.28	16.30
480 x 480	2.43	15.46	2.78	16.52
600 x 600	3.05	28.03	3.43	30.65

Table 4: Microscale values of erosion rates at different scales

As demonstrated in Table 4, the two methods led to a similar erosion rate occurring the most often (1-3 tons/acre), as well as a similar weighted average erosion rate (ranging from 5-30 tons/acre).

Total erosion rates are shown in Table 5, where the average cell loss was determined as the sum of all cell losses divided by the total watershed area of 5339 acres.

Grid Size [m]	Total Calculated Loss A USLE [tons]	Avg Cell Loss A_o [tons/acre]	Total Calculated Loss e Simplified USLE [tons]	Avg Cell Loss e_o [tons/acre]
30 x 30	91207	17.08	98327	18.42
60 x 60	89093	16.69	96593	18.09
120 x 120	82279	15.41	87206	16.33
480 x 480	82717	15.49	88399	16.56
600 x 600	147128	27.56	160836	30.12

Table 5: Calculated losses at the microscale

Once again, the USLE and the simplified USLE produce similar results. Total annual calculated losses range from 90 kt to 160 kt. Average erosion rates of range between 15 and 30 tons/acre.

B. Macroscale Results

On the macroscale level, *actual* erosion rates can be calculated by applying a correction factor to the *estimated* value using average parameters. *Estimated* values of soil loss rates were calculated as: $A = R*K*P*L*S*C$

$A = (330)*(0.478)*(1)*495^{0.5}(0.0076 + 0.0053*1.4 + 0.00076*(1.4)^2)*(0.098)$

$A = 5.679$ tons/acre for the USLE

Using the simplified equation, *estimated* values of soil loss rates were calculated as:

$e = 16{,}478 * S^{1.46} * C$

$e = 16{,}478 * (0.014)^{1.46} * (0.098)$

$e = 3.173$ tons/acre for the simplified USLE

When the correction factor of 0.556, which corresponds to an area of 21.6 km^2, is applied to the *estimated* values, the *actual* soil loss rates were calculated as:

A_o = (5.679 tons/acre)/0.556 = 10.214 tons/acre

e_o = (3.173 tons/acre)/0.556 = 5.707 tons/acre

C. Comparing Microscale and Macroscale

As indicated above, the erosion rates calculated at the microscale level ranged from 15-30 tons/acre, for both methods. Erosion rates calculated at the macroscale level, based on a correction factor of 0.556, were 10.21 tons/acre for the USLE, and 5.71 tons/acre for the simplified USLE. The microscale values are slightly higher than the macroscale values. Yet according to Julien & Frenette's research, the correction factor can vary within a given range. As a comparison, correction factors for Goodwin Creek were determined based on microscale calculations of erosion rates. Thus for grid sizes less than 0.125 km^2, the correction factor was:

Q_e = Macroscale erosion rate /(Microscale erosion rate/1.13)

For grid sizes greater than 0.125 km^2, the correction factor was:

Q_e = Macroscale erosion rate/(Microscale erosion rate/(0.75*1.13*$A^{-0.137}$))

The values of Q_e based on Goodwin Creek results are shown in Figure 8, superimposed on the correction factor plot developed by Julien & Frenette (1987).

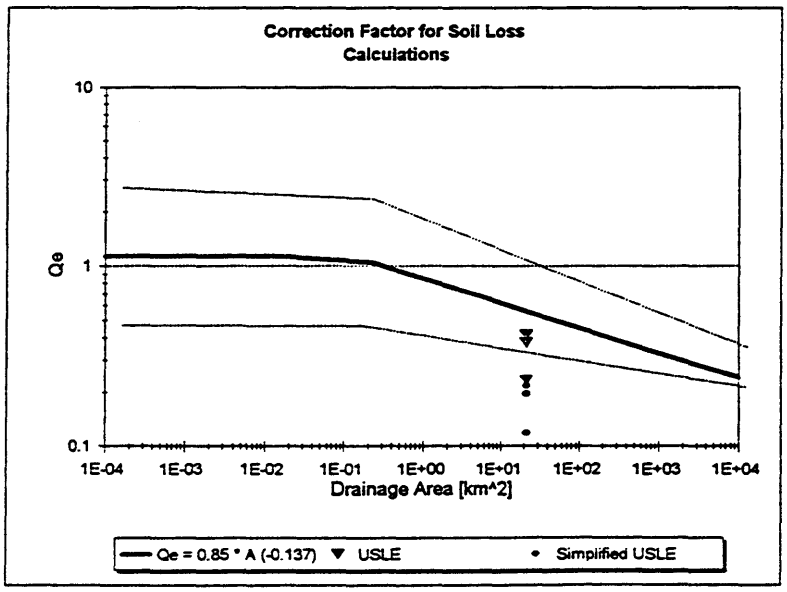

Figure 8: Q_e values using various grid sizes

COMPARISON WITH FIELD DATA

In order to compare results from this study with field data, the sediment delivery ratio was used to calculate sediment yield for Goodwin Creek. The sediment yield is the total amount of sediment which is delivered to the outlet of the watershed. The sediment delivery ratio (SDR) is defined as the percentage of sediment delivered from the erosion source, including gully erosion and streambank erosion, to a specified location such as the outlet of the watershed. SDR is calculated as:

$$SDR = 0.41 * A_t^{-0.3} \qquad (A_t \text{ in } km^2) \qquad (7)$$

According to this equation, for Goodwin Creek,

$$SDR = 0.41*(21.607)^{-0.3} = 0.163$$

Sediment yield can be then be calculated as SDR = Y/S, where Y is sediment yield and S is sediment source. Based on microscale estimates of erosion rates, a value of 15 tons/acre is used as an approximate value for Goodwin Creek. The total volume of eroded sediment available for transport is evaluated as:

$$S = 15 \text{ tons/acre} * 5339 \text{ acres} = 80 \text{ kt}$$

$$Y = 0.163 * 80 \text{ kt} = \underline{13 \text{ kt/yr}}$$

Bingner et al. (1989) provide measured values of sediment yield for the Flannigan Watershed, which is located near Goodwin Creek. The measured values are presented in Table 6, with the total annual yield calculated assuming a SDR of 0.163 for Goodwin Creek.

Year	Sediment Yield [tons/acre]	Number of Events	Sediment Yield Y [kt/year]
1981	10.38	70	9.03
1982	13.34	74	11.61
1983	91.43	65	79.57
1984	24.71	72	21.50
Average value	35.09		30.54

Table 6: Representative measured values of erosion rates

Based on field data reports, the sediment yield would seem to fluctuate within a range of 10-30 kt/year. The sediment yield calculated using the USLE and the simplified USLE was within this range.

Yet when evaluating sediment yield, it is important to consider that the USLE does not account for all the physical processes involved in upland erosion. Sediment losses or gains between the field and the stream are not accounted for, nor are gully erosion or landslides included. Ideally the annual soil loss computed using the USLE should be modified to account for deposition as upland runoff passes through heavy vegetation or where the slope flattens, and for other sources of erosion or sedimentation between the upland region and the point of sediment yield measurement. In addition, the USLE was only developed for material 1 mm or finer. This will particularly lead to inaccuracies in estimations for larger watersheds, where gullies and

channels concentrate flows which can carry sediment greater than 1 mm in diameter. Therefore calculations of sediment yield based on upland erosion rates will always only be approximations.

CONCLUSIONS

The results showed general agreement in the values of soil loss calculated at the microscale, regardless of the data resolution. Both the USLE and the simplified USLE calculated similar values of total annual erosion losses and average erosion rates. The correction factor applicable to Goodwin Creek, based on the relationship between microscale and macroscale results, falls within an acceptable range of that determined by Julien & Frenette (1987). Thus this study verifies the fact that an *actual* erosion rate can be evaluated using a correction factor applied to an *estimated* rate using mean characteristics.

The correction factor method allows one to bypass calculations for individual cells, and still arrive at a fairly accurate value of soil loss resulting from upland erosion. For conditions such as those in the Goodwin Creek watershed, the USLE will give better results than the simplified USLE, due to the distribution of the slope and the crop management factor. When considering watersheds with slopes above 10% and high C values, the USLE should be applied instead of the simplified USLE.

Despite the inaccuracies inherent in estimating sediment yield based on the USLE, the equation can be used calculate fairly accurate upland erosion loss rates, even in large watersheds. Most importantly, linked with GIS the USLE can provide a better understanding of the physical parameters controlling erosion in any given watershed.

REFERENCES

Bingner, R.L., C.E. Murphree, and C.K. Mutchler, 1987, "Comparison of Sediment Yield Models on Watersheds in Mississippi", Trans. of the Society of Agricultural Engineers, Vol 32(2), March-April, pp. 1529-534.

Frenette, M., and P.Y. Julien, 1987, "Computer Modeling of Soil Erosion and Sediment Yield from Large Watersheds", International Journal of Sediment Research, No.1, November 1987, pp. 39-66.

Galberry, H.S., 1960, "Soil Survey of Panola County, Mississippi", Soil Survey Series 1960, No. 10, pp. 1-33.

Julien, P.Y, and M. Gonzalez del Tanago, 1991, "Spatially Varied Soil Erosion under Different Climates", Hydrological Sciences Journal, 36, 6, 12/1991, pp. 511-523.

Julien, P.Y., and M. Frenette, 1987, "Macroscale Analysis of Upland Erosion", Hydrological Sciences Journal, 32, 3, 9/1987, pp. 347-358.

Julien, P.Y., 1982, "Prediction d'apport solide pluvial et nival dans les cours d'eau nordiques a partir du ruissellement surperficiel, " These de doctorat, University Laval, Quebec, 240 pp.

Kilinc, M.Y., 1972, "Mechanics of soil erosion from overland flow generated by simulated rainfall", Ph.D. dissertation, Colorado State University, Fort Collins, 183 pp.

Meyer, C.D., ARS, & Purdue University, 1971, Chapter 27: Soil Erosion by Water on Upland Areas, in River Mechanics Vol.II, H.W. Shen (editor), pp. 27.1-27.5.

Shen, H.W, and P.Y. Julien, 1993, Chapter 12: Erosion and Sediment Transport, in Handbook of Hydrology, D. R.

COMPARISON OF "NEW" AND "OLD" METHODS FOR PREDICTING MANNING'S *n* IN COARSE BED STREAMS

By Syndi J. Dudley

ABSTRACT: The most common means of describing resistance in rivers is Manning's roughness coefficient, *n*. Ten river reaches with pre-determined roughness coefficients were used for the purposes of comparing three quantitative methods for predicting Manning's *n* in coarse bed streams. The methods were selected such that they represent a period of 22 years in this field of research. The most recently developed method was regarded as questionable due to spurious correlation. The other two methods provide reasonable estimates for low values of Manning's *n* but underestimate the *n*-value as roughness increases.

INTRODUCTION

Determination of flow depth and velocity in natural and man-made channels requires an understanding of the resistance to flow caused by boundary roughness. Flow resistance is complicated by the interaction of many factors. Among these factors are stream bed particle size, bank irregularity, vegetation, channel alignment, bed configuration, channel obstructions, converging or diverging streamlines, sediment load, and surface waves (Limerinos, 1970). The most common means for describing resistance to flow is the Manning's roughness coefficient, *n*. The Manning's roughness coefficient appears in the general Manning equation for computing velocity, V, in open channel flow;

$$V = \frac{\Phi}{n} R^{2/3} S_f^{1/2} \qquad (1)$$

where R is the hydraulic radius in feet, S is the energy gradient, and Φ equals 1.0 if SI units are used and 1.49 if English units are used. The Manning's equation is empirical in nature and was developed using a curve-fitting process. Although this equation was developed for conditions of uniform flow in channels where the slope of the water surface and energy gradient are parallel to the bed, it is often applied to unsteady, gradually varied flow.

The Manning's equation can be used in conjunction with the continuity equation to calculate the stream discharge, Q, in cubic feet per second, yielding the following expression:

$$Q = \frac{\Phi}{n} A R^{2/3} S_f^{1/2} \quad (2)$$

where A is the cross-sectional area in square feet.

In general, there are three methods for estimating the Manning's roughness coefficient: 1) the visual comparison approach; 2) quantitative method; and, 3) step-by-step procedure. Chow (1959), Barnes (1967) and Hicks and Mason (1991) provide guidance for estimating roughness coefficients using the "visual comparison" approach. These references present photographs, descriptions, cross-section properties of streams and their respective Manning *n*-values that can be compared with the reach under investigation. The results using the visual comparison method are approximate since the reach under investigation can never have the exact roughness characteristics as the reference stream reach.

Quantitative methods are typically empirically derived predictive equations, such as those developed by Jarrett (1984), Limerinos (1970) and Ugarte and Madrid (1992). These equations are derived from regression analysis using measured discharge and stream properties from limited data sets. No single empirical formula can be applied to any stream or range of roughness because the formulas are developed using local river data.

The step-by-step procedure for selecting Manning's roughness coefficient (Cowan, 1956) involves estimating a base roughness value for a straight, smooth channel of uniform cross-sectional shape with the same bed material as the reach of interest, then adjusting the base-value to account for surface irregularities, variations in channel cross-section, obstructions, vegetation and meandering. The base-value can be estimated using available tabulated values for a given bed material size or by quantitative methods (Arcement and Schneider, 1984).

DATA COLLECTION

Hicks and Mason (1991) presents general information, photographs, descriptions, bed material gradation and tables of the hydraulic properties, including pre-determined Manning's roughness coefficients, for 78 stream reaches representing a broad range of New Zealand Rivers. The criteria used by Hicks and Mason (1991) for selecting the reaches were:

1) it is straight;
2) is length is at least five times its width;
3) it has uniform cross-sections or is converging;
4) its flow is contained without overflow;
5) it has straight entrance and exit conditions, with no backwater effects.

In this study, 10 reaches representing coarse bed streams were selected from the Hicks and Mason (1991) data set for the purpose of comparing *n*-values predicted by empirical equations developed by Jarrett (1984), Limerinos (1970) and Ugarte and Madrid (1992). While there are a numerous empirical equations available for predicting roughness coefficients in coarse bed streams, these references were chosen for a three primary of reasons. First, these references represent a period of 22 years of investigation of flow resistance in coarse bed streams. A primary objective of this paper is to assess the progress made or the lack of progress in this area of research. Second, the data needed to apply the equations are available in Hicks and Mason (1991). Third, Jarrett (1984) and Limerinos (1970) equations are commonly used methods for predicting roughness in coarse bed streams.

Table 1 summarizes the hydraulic properties of the 10 stream reaches used for comparing the prediction equations. In Table 1, Q is the stream discharge; R is the hydraulic radius; V is the mean velocity; Fr is the Froude number; S_f is the friction slope; A is the cross-sectional area; d_{84} is the intermediate particle diameter corresponding the 84 percentile of a cumulative frequency distribution of the diameters of randomly sampled surficial bed material; R/d_{84} is the index of relative smoothness; and, *n* is the Manning's roughness coefficient.

It should be noted that Hicks and Mason (1991) present hydraulic data for a broad range of discharge values for each study reach to show variations in roughness with discharge. For the purposes of the comparison analysis, one discharge value was used from each site. While the sites were selected to represent a variety of flow conditions, the discharge values were deliberately chosen at or near low flow to avoid complicating factors introduced by bank vegetation which was present at all sites. The roughness measured is therefore primarily due to the effects of the coarse bed material. The Hutt at Kaitoke site shown at low flow in Figure 1 is typical of stream reaches used in this study.

PREDICTION EQUATIONS

Limerinos (1970) used fifty current-meter measurements of discharge and field survey data for 11 rivers in California to compute Manning's roughness coefficient by the Manning formula. The criteria for selecting these sites were that they are straight, uniform and as free from flow resistent factors other than particle size.

Limerinos (1970) related channel roughness to two elements: 1) a characteristic particle size of the bed material; and 2) the distribution of particle size in the channel bed. Limerinos (1970) recognized that the retarding effect in the channel depends on the particle size and the depth of flow and used the ratio of the hydraulic radius to the flow depth, R/d_{84}, as an index of relative smoothness. This ratio was compared with the ratio of $n/R^{1/6}$. Note that this parameter is directly proportional to the square root of the Darcy-Weisbach friction factor, *f*, another commonly used means of expressing boundary roughness. The results of Limerinos (1970) study yielded the following relationship for predicting Manning's roughness coefficient:

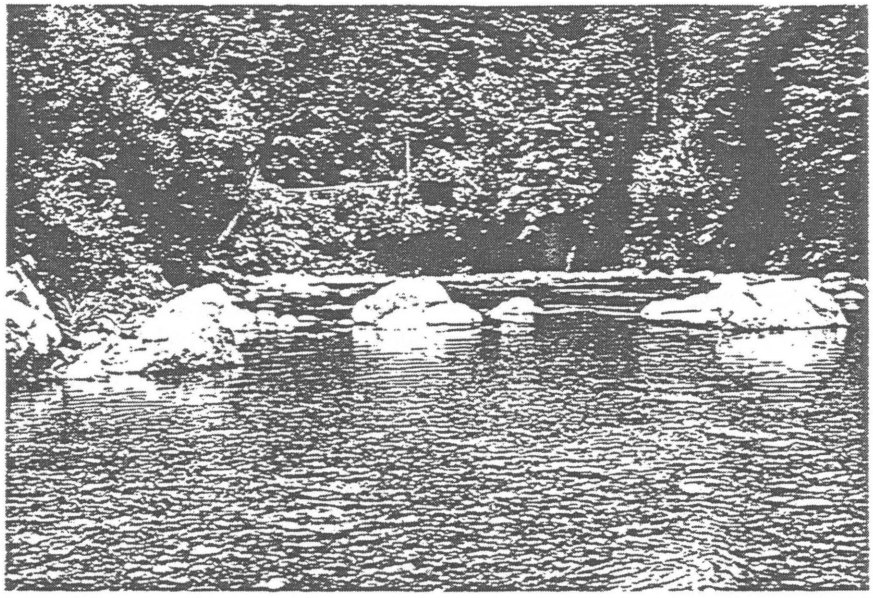

View downstream at middle of reach.

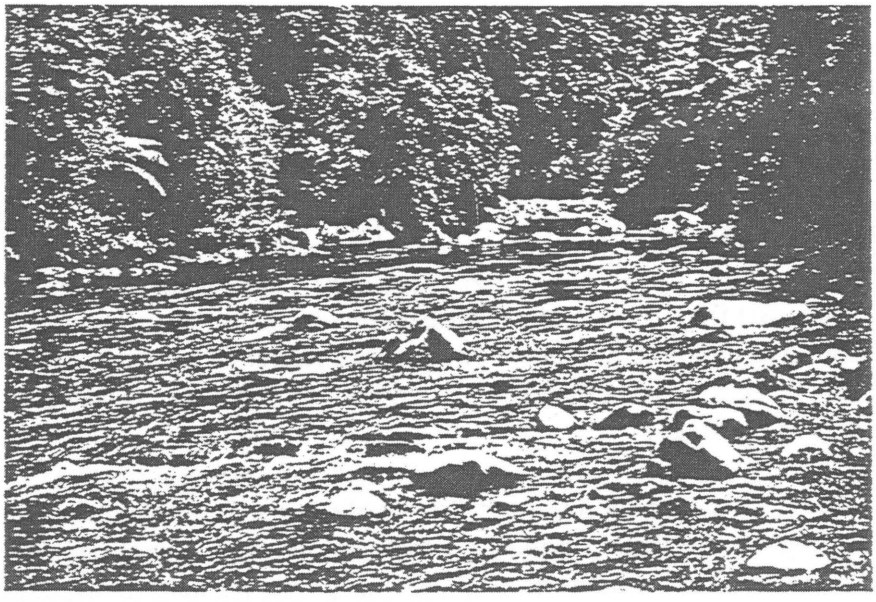

View upstream from bottom cross-section.

Figure 1. Typical stream reach used for comparison analysis.

Table 1. Summary of Hydraulic Parameters and Manning's n values

Site No.	Description	Q (m^3/s)	Sf	A (m^2)	R (m)	V (m/s)	Fr	d84 (mm)	R/d84	n Measured	n Limerinos	n Jarrett	n Madrid
1	Waian Water Race	0.33	0.00455	0.71	0.18	0.47	0.35	80	2.25	0.045	0.046	0.066	0.053
2	Hutt at Kaitoke	8.38	0.00359	11.8	0.42	0.79	0.39	212	1.98	0.039	0.056	0.053	0.052
3	Hutt at Taita Gorge	59.4	0.00183	52.3	0.97	1.14	0.37	170	5.71	0.038	0.042	0.036	0.046
4	Jollie at Mt. Cook Station	9.25	0.00846	8.6	0.44	1.16	0.56	90	4.89	0.046	0.039	0.073	0.048
5	Waipapa at Forest Ranger	4.55	0.00268	10.2	0.39	0.45	0.23	91	4.29	0.063	0.040	0.048	0.067
6	Ruakokapaptuna at Iraia	0.2	0.00568	0.98	0.17	0.22	0.17	119	1.43	0.100	0.057	0.073	0.092
7	Cobb at Trilobite	0.78	0.00153	5.12	0.44	0.15	0.07	200	2.20	0.130	0.053	0.038	0.121
8	Pelorus at Bryants	11.8	0.00352	31.7	0.83	0.44	0.15	175	4.74	0.110	0.044	0.047	0.100
9	Okarito at Lake Wahapo	17.4	0.0387	22.9	0.78	0.80	0.29	800	0.98	0.200	0.095	0.118	0.170
10	Butchers Creek at Lake Kaniere Road	0.29	0.0146	0.85	0.16	0.36	0.29	168	0.95	0.093	0.074	0.105	0.095

$$n = \frac{0.113\ R^{1/6}}{1.16 + 2.00\ \log[\frac{R}{d_{84}}]} \quad (3)$$

The above equation is generally valid for:

1) streams that convey flow in the subcritical regime, Froude number less than one;
2) Hydraulic radii of cross-sections studied ranged from 1.02-10.9 ft (0.33-3.6 m);
3) intermediate particle diameter, d_{84}, ranging from 0.062-2.45 ft (20-800 mm); and
4) index of relative smoothness, R/d_{84}, ranging from 0.9-68.5.

Limerinos (1970) provides no data regarding the friction slope of the study reaches. In addition, the study did not consider the spacing pattern of streambed particles. While this was considered an important factor, the spacing pattern is difficult to quantify. Since this effect was not considered, other factors considered to be of lesser importance were also neglected such as Froude number, width to depth ratio, and sediment transport.

Jarrett (1984) used seventy-five current-meter measurements of discharge were made at 21 high-gradient natural stream sites in the Rocky Mountains of Colorado for the purpose of computing channel roughness by the Manning formula. The selected reaches were straight and uniform and had a connected water surface and a stable bed and banks with minimal vegetation. The roughness measured was primarily due to the effects of bed and bank-material roughness. His multiple-regression analysis yielded the following expression:

$$n = 0.39\ S^{0.38}\ R^{-0.16} \quad (4)$$

where S is the stream gradient and R is the hydraulic radius. This equation is generally valid for:

1) streams that convey flow in the subcritical regime, Froude number less than one;
2) channel slopes from 0.002-0.04;
3) Hydraulic radii of cross-sections studied ranged from 0.5-7 ft (0.15-2.1 m);
4) natural main channels having stable bed and bank materials (gravels, cobbles, and boulders) without backwater and small amounts of suspended sediment.

Jarrett's (1984) equation is dependent on the relationship between friction slope and roughness. He recognized that as channel gradient increases, the effect of increased turbulence and resistance results in increased friction slope. For similar bed size material, channels with lower slopes have lower Manning's roughness coefficients than channels with steeper slopes. Although Jarrett's (1984) equation does not depend on the particle size, it is appropriate to note that the index of smoothness ranged from 0.5-10.8 and d_{84} ranged from 0.3-2.6 ft (98-850 mm) in his study.

Ugarte and Madrid (1992) developed two prediction equations characterizing flow from the large-scale ($0<R/d_{84}<1$) and intermediate-scale ($1<R/d_{84}<12$) roughness regions. These equations are depended on the friction slope, hydraulic radius, d_{84}, and Froude number. The first equation was developed from data collected by Bathurst (1985) for 16 rivers in the United Kingdom and Colorado River data published by Jarrett (1970). The following equation for predicting Manning's roughness coefficient was developed for flow in the region of large-scale roughness.

$$n = [0.183 + \ln (\frac{1.7462\ S_f^{0.1581}}{Fr^{0.2631}})] \frac{(d_{84})^{1/6}}{\sqrt{g}} \qquad (5)$$

where Fr is the Froude number and the other variables are as previously defined.

The following equation was developed on the basis of 62 measurements collected in 19 Chilean rivers (Madrid, 1992) for the region of intermediate-scale roughness.

$$n = [0.183 + \ln (\frac{1.3014\ S_f^{0.0785} (\frac{R}{d_{84}})^{0.0211}}{Fr^{0.2054}})] \frac{(d_{84})^{1/6}}{\sqrt{g}} \qquad (6)$$

Equation (6) was developed based on a range of flow from 77-10,500 ft^3/s (2.71-371 m^3/s) and is valid for friction slopes ranging from 0.002-0.04. Other than these data, Ugarte and Madrid (1992) provide no information regarding the data collection and development of Equation (6). A full description of the field survey is given in Madrid (1992); however, that document was unavailable at the time of this writing.

COMPARISON OF RESULTS

Figures 2 through 4 are plots of the Manning's *n* values predicted using Limerinos (1970), Jarrett (1984) and Ugarte and Madrid (1992), respectively, verses the measured values from Hicks and Mason (1991). If the prediction function exactly predicts the roughness coefficient for a given stream reach, the point will fall on the line of perfect agreement. Points that fall above and below the line indicate overprediction and underprediction, respectively. In general, these plots suggest that Ugarte and Madrid's (1992) equation provides the most accurate estimates of channel roughness. Ugarte and Madrid's (1992) equation predicted Manning's *n* with an average error of 12.9%. While all three equations provide reasonable estimates for low values of Manning's *n*, Limerinos and Jarrett

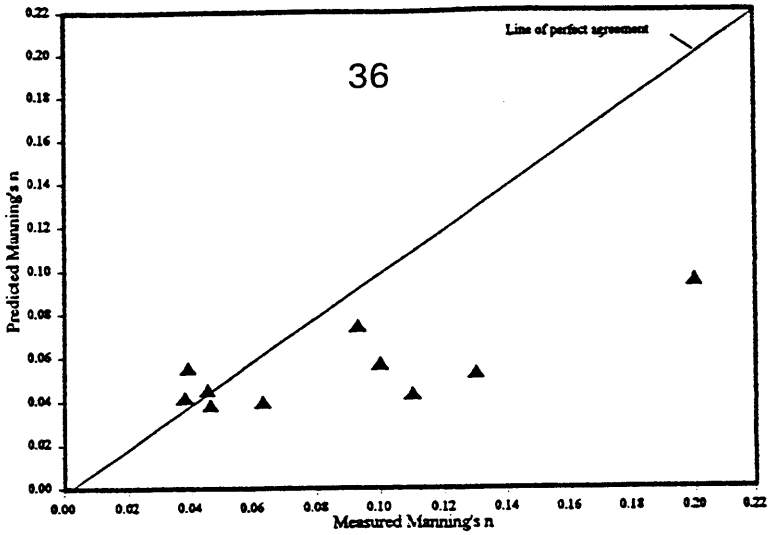

Figure 2. Predicted Manning's n using Limerinos' Equation verses Measured Manning's n from Hicks and Mason (1991)

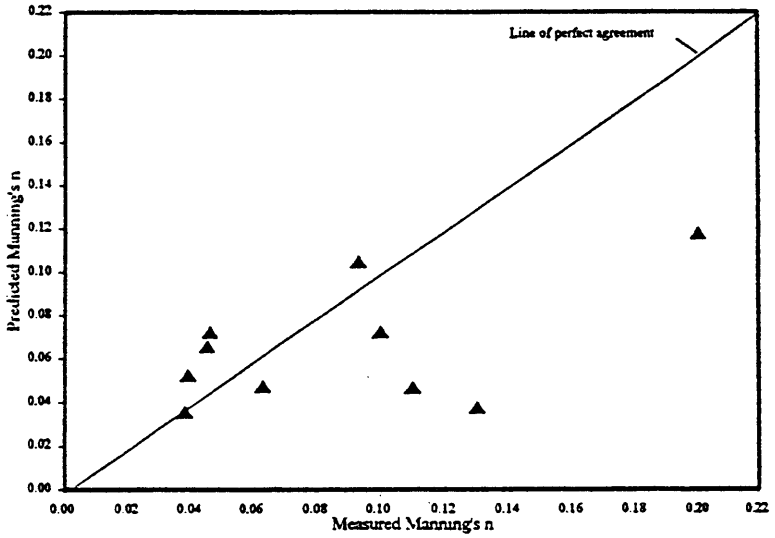

Figure 3. Predicted Manning's n using Jarrett's Equation verses Measured Manning's n from Hicks and Mason (1991)

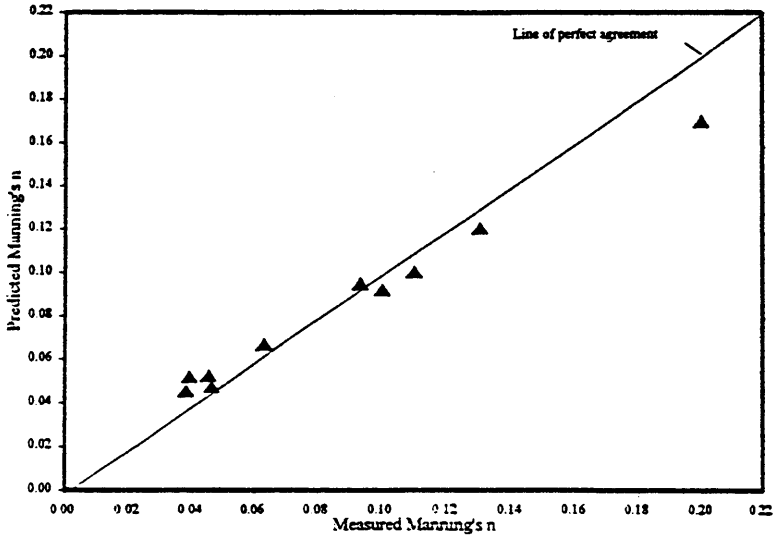

Figure 4. Predicted Manning's n using Ugarte and Madrid's Equation verses Measured Manning's n from Hicks and Mason (1991)

considerably underpredict Manning's *n* as the measured roughness increases. The average error associated with Limerinos' (1970) and Jarrett's (1984) equations is 34.2% and 37.9%, respectively.

With regard to Ugarte and Madrid's (1992) equation, two important points should be noted. First, the reason that Ugarte and Madrid's equation appears to yield more accurate results than Limerinos and Jarrett is due to the form the equation. Both equations developed by Ugarte and Madrid are dependent on Froude number (Fr) and friction slope (Sf). The general equation for the Froude number is

$$Fr = \frac{V}{\sqrt{gD}} \tag{7}$$

where D is hydraulic depth, defined as cross-sectional area divided by water surface top width, A/T. For wide channels, D is approximately equal to the hydraulic radius, R. If this equation is rearranged and substituted into the general Manning's equation for velocity, Fr can be expressed in terms of *n* as shown below.

$$Fr = \sqrt{\frac{\phi\, D^{1/3}\, S_f}{n^2\, g}} \tag{8}$$

This derivation demonstrates that the Froude number can be expressed in terms of Manning's *n*; therefore, Manning's *n* appears on both sides of Ugarte and Madrid's equations. As a result, there is an inherent, spurious correlation in this function that causes the data to collapse in the form of a straight line.

Second, the Froude number is not a measured quantity. Rather, it is obtained indirectly from measured cross-sectional geometry and discharge or velocity. If the velocity, cross-sectional geometry and friction slope are known, the roughness coefficient can be computed directly from Manning's equation.

Limerinos' (1970) equation is in a form commonly referenced as *logarithmic law* for turbulent flow. Equations in this form are often used to describe the logarithmic average velocity distribution for steady, uniform flow over hydraulically rough surfaces. An equation in this form is only valid for values of R/d greater than one, where d is the height of the roughness elements. That is, the roughness elements cannot protrude through the water surface. Since this condition was violated in 8 of the 10 streams used in this comparison analysis, this may explain the underestimation of Manning's *n* using Limerinos' equation at high roughness values. It should be noted that Limerinos (1970) does not include photographs or descriptions of the individual stream reaches used to develop his equation. The paper provides little information regarding this matter; however, in one of the streams studied by Limerinos (1970), the ratio of R/d_{84} is less than one.

Jarrett's (1994) equation also underestimated Manning's *n* for high measured values. Jarrett's data was collected from high-gradient mountain streams in which particles protruding from the water surface are clearly illustrated in the photographs provided in his paper. With regard to this condition, Jarrett states

> "The *n*-values having the greatest error are typically low-flow measurements when the ratio of R-d_{50} is less than 7. The concept of flow resistance at low flows may be subject to question due to nonconnection of the water surface."

Jarrett's (1984) equation has one advantage over both Limerinos (1970) and Ugarte and Madrid (1992). It is only dependent on friction slope and hydraulic radius while the other equations require particle size data. Accurate particle size data is difficult to obtain and may not be available due to hydraulic conditions of the stream, and economic and time constraints. Conversely, friction slope can usually be measured with considerable accuracy in high-gradient coarse bed streams.

CONCLUSION

The available techniques for selecting appropriate roughness coefficients for coarse bed streams are based on limited verified roughness data. Ugarte and Madrid (1992) equation for intermediate scale roughness was developed on the basis of 62 measurements with an average error of 2.2% The equation for large-scale roughness was developed on the basis of 119 measurements with and average error of 5.7%. Based on the 10 measurements used in this study, the average error of prediction using Ugarte and Madrid's (1992) equations was found to be 12.6%. These results are subject to question due to the spurious correlation inherent in Ugarte and Madrid's (1992) equations.

Limerinos' (1970) equation was developed based on 50 measurements with an average error of 15.5%. In this study, Limerinos' equation yielded an average error 34.2% Jarrett's (1984) equation was developed on the basis of 75 measurements with an average error of 28%. The average error found in this study using Jarrett's equation was 37.9%. Both equations provide reasonable estimates under conditions of low resistance but underestimate Manning's *n* as the measured roughness increases. The larger error may be explained by the low indices of relative smoothness of the comparison reaches or by the small data set used in this study.

The primary objective of this paper was to assess the progress or lack of progress made in our ability to predict Manning's *n* in coarse bed streams using quantitative methods. However, given the spurious correlation inherent in Ugarte and Madrid's (1992) equation, this objective could not be completely fulfilled. While it would be desirable to examine other "new" quantitative methods, this is beyond the scope of this study. It can be concluded Limerinos' (1970) and Jarrett's (1984) equations appear to yield comparable results; however, Jarrett's (1994) equation may be more practical from an economic viewpoint since the data required may be more accurately and easily obtained. While the quantitative methods discussed in this paper are useful tools and provide guidance for the practicing engineer, the author believes that no available technique for estimating Manning's *n* in cobble bed streams can replace experience and sound judgement.

APPENDIX I. REFERENCES

(1) Arcement Jr., G.J, and Schneider V.R. 1994. Guide for selecting Manning's roughness coefficients for natural channels and flood plains. *U.S. Geological Survey Water-Supply Paper 2339*, 37 p.

(2) Barnes, H.H., Jr. 1967. Roughness characteristics of natural channels. *U.S. Geological Survey Water-Supply Paper 1849*, 213 p.

(3) Bathurst, J.C. 1985. Flow resistance estimation in mountain rivers. *Journal of Hydraulic Engineering*, ASCE, Vol. 111, No. 4, April, 1985.

(4) Chow, V.T. 1959. *Open-Channel Hydraulics*. McGraw-Hill Book Co., New York, 680 p.

(5) Hicks, D.M. and Mason, P.D. 1991. *Roughness Characteristics of New Zealand Rivers*. Water Resources Survey, DSIR Marine and Freshwater, Private Bag, Kilbirnie, Wellington, New Zealand, 329 p.

(6) Jarrett, R.D. 1984. Hydraulics of high gradient streams. *Journal of Hydraulic Engineering*, ASCE, Vol. 110, No. 11., November, 1984.

(7) Limerinos, J.T. 1970. Determination of the manning coefficient from measured bed roughness in natural channels. *Geological Survey Water-Supply Paper 1898-B*, U.S. Geological Survey, Washington, D.C.

(8) Madrid, M. 1992. Hidraulica de Rios con Gran Pendiente, Universidad Santa Maria, Chile.

(9) Ugarte A. and Madride M. 1992. Roughness coefficient in Mountain Rivers. *Hydraulic Engineering '94, Proceedings of the 1994 Conference Vol. 2*, ASCE, Edited by G.V. Cotroneo and R.R. Rumer.

ESTIMATING FLOW RESISTANCE IN VEGETATED CHANNELS

J. Craig Fischenich

Abstract

Channel design and restoration efforts frequently include vegetation establishment or maintenance in the floodway. Evaluation of the hydraulic condition and stability of vegetated floodways requires an adequate prediction of flow resistance. Existing methods for estimating resistance coefficients are presented and evaluated by comparing resistance coefficients obtained by the application of each existing method to coefficients computed from measured friction slopes for several river reaches containing vegetation in the floodway. Results of the comparison are presented, each method is discussed, and the attributes of an appropriate resistance relation are proposed.

Introduction

Hydraulic engineers have become increasingly involved in channel restoration projects and modifications to existing flood control projects as the conventional "flood control" ideology is replaced with a new "flood management" philosophy. The incorporation of vegetation into these projects is often mandated. Healthy riparian vegetation tends to stabilize stream banks, provides shade that prevents excessive water temperature fluctuations, performs a vital role in nutrient cycling and water quality, improves aesthetic and recreational benefits of a site, and is immensely productive as wildlife habitat.

Concurrent with these benefits are impacts to the channel and floodway conveyance with subsequent sedimentation and stability impacts. Proper evaluation of these impacts requires an analysis of flow depths and velocities in the channel and floodplain. Although more complicated analyses are often warranted and sometimes performed, engineers typically evaluate river systems using one-dimensional, steady, gradually-varied flow models. Depending upon the model used, engineers can account for the effects of dense vegetation by adjusting one or more of the following parameters: channel cross section, velocity coefficients, momentum coefficients, flow area subdivision, or resistance coefficients.

Virtually no guidance exists for the adjustment of the first four parameters and only limited guidance is available for the selection of resistance coefficients in vegetated floodways. In the U.S., it is customary to express the flow resistance in terms of the resistance coefficient from Manning's Monomial Equation:

$$V = \frac{k_n}{n} R^{\frac{2}{3}} S_f^{\frac{1}{2}} \quad (1)$$

where V = cross-sectional average velocity, R = hydraulic radius, S_f = friction slope, k_n = 1.486 for English units and k_n = 1 for SI units, and n = Manning resistance coefficient.

Existing Techniques

Procedures for the computation or estimation of Manning's n in vegetated channels can be grouped into four general categories: direct measurement, analytical approaches, and handbook methods. Direct measurement, although important for model calibration and verification, is of little practical use in prediction and is not presented.

Analytical Approaches: Cowan (1956) proposed a procedure for estimating Manning's n that takes into account the contributions of various factors, including vegetation, to total flow resistance. The procedure, assumes that the resistances induced by various contributing factors can be summed to establish total resistance as follows:

$$n = (n_b + n_1 + n_2 + n_3 + n_4)m \quad (2)$$

where m = ratio for meandering, n_b = base n value, n_1 = addition for surface irregularities, n_2 = addition for variation in channel cross section, n_3 = addition for obstructions, and n_4 = addition for vegetation. Arcement and Schneider (1989) summarize estimates for each of the factors as presented by several previous investigators. Adjustment factors for vegetation vary from 0.002 to 0.100 and, as with the other factors, selection of an appropriate adjustment is based upon interpretation of qualitative descriptions of channel conditions. Adjustment factors for vegetation in the channel and floodplain are presented in Tables 1 and 2, respectively.

Table 1. Adjustment values for factors that affect the roughness of a channel.
(Modified from Aldridge and Garrett 1973)

Amount of vegetation	Adjustment in n value (n_4)	Example
Small	0.002-0.010	Dense growths of flexible turf grass, such as Bermuda, or weeds growing where the average depth of flow is at least two times the height of the vegetation; supple tree seedlings such as willow, cottonwood, arrowweed, or saltcedar growing where the average depth of flow is at least three times the height of the vegetation
Medium	0.010-0.025	Turf grass where the average depth of flow is from one to two times the height of the vegetation; moderately dense stemmy grass, weeds, or tree seedlings growing where the average depth of flow is from two to three times the height of the vegetation; brushy, moderately dense vegetation, similar to 1- to 2-year-old dormant willow trees, growing along the banks, and no significant vegetation is evident along the channel bottoms where the hydraulic radius exceeds 2 ft

Large	0.025-0.050	Turf grass growing where the average depth of flow is about equal to the height of the vegetation; 8- to 10-year-old willow or cottonwood trees intergrown with some weeds and brush (none of the vegetation in foliage) where the hydraulic radius exceeds 2 ft; bushy willows about 1 year old intergrown with some weeds along side slopes (all vegetation in full foliage), and no significant vegetation exists along channel bottoms where the hydraulic radius is greater than 2 ft
Very Large	0.050-0.100	Turf grass growing where the average depth of flow is less than half the height of the vegetation; bushy willow trees about 1 year old intergrown with weeds along side slopes (all vegetation in full foliage), or dense cattails growing along channel bottom; trees intergrown with weeds and brush (all vegetation in full foliage)

Table 2. Adjustment values for factors that affect the roughness of floodplains.
(Modified form Aldridge and Garret 1973, Table 2)

Amount of vegetation	Adjustment in n value (n_4)	Example
Small	0.001-0.010	Dense growths of flexible turf grass, such as Bermuda, or weeds growing where the average depth of flow is at least two times the height of the vegetation; supple tree seedlings such as willow, cottonwood, arrowweed, or saltcedar growing where the average depth of flow is at least three times the height of the vegetation
Medium	0.011-0.025	Turf grass growing where the average depth of flow is from one to two times the height of the vegetation; moderately dense stemmy grass, weeds, or tree seedlings growing where the average depth of flow is from two to three times the height of the vegetation; brushy, moderately dense vegetation, similar to 1- to 2-year-old willow trees in the dormant season
Large	0.025-0.050	Turf grass growing where the average depth equals the height of the vegetation; 8- to 10-year-old willow or cottonwood trees intergrown with some weeds and brush (none of the vegetation in foliage) where the hydraulic radius exceeds 2 ft; mature row crops such as small vegetables, or mature field crops where depth of flow is at least twice the height of the vegetation
Very large	0.050-0.100	Turf grass growing where the average flow depth is less than half the vegetation height; moderate to dense brush,or heavy stand of timber with few down trees and little undergrowth where depth of flow is below branches; mature field crops where depth of flow is less than the height of the vegetation
Extreme	0.100-0.200	Dense bushy willow, mesquite, and saltcedar (all vegetation in full foliage): heavy stand of timber, few down trees, depth of flow reaching branches

Petryk and Bosmajian (1975) proposed a modification to Cowan's approach that more quantitatively addresses the effect of vegetation. By summing the forces in the longitudinal direction and substituting into the Manning formula, they developed the following equation:

$$n = n_0 \sqrt{1 + \left(\frac{C_* \Sigma A_t}{2gAL}\right)\left(\frac{k_n}{n_0}\right)^2 R^{4/3}} \qquad (3)$$

where n_0 = Manning's boundary-roughness coefficient excluding the effect of the vegetation, C_* = the effective-drag coefficient for the vegetation in the direction of flow, ΣA_t = the total frontal area of trees in the flow section, g = the gravitational constant, A = the cross-sectional area of flow, L = the length of channel reach, and other parameters are as previously described. The total boundary roughness n_0 is determined from a modified form of Cowan's equation:

$$n_0 = n_b + n_1 + n_2 + n_3 + n_4' \qquad (4)$$

The drag coefficient can be approximated from the relation $C_* = 22 - (3.75)R$. The roughness factors n_b and n_1 through n_3 are the same as those for Cowan's method. The n_4' factor is for vegetation such as shrubs, brush and grass, which was not accounted for in the vegetation density computations, and ranges from 0.001 to 0.025.

Ree and Palmer (1949) summarized research of flow in vegetated channels conducted by several SCS researchers from 1935 to 1943 at Spartansburg, GA and Stillwater, GA. The investigators found that most flow data for a particular grass, when plotted with n as a function of the product of velocity and hydraulic radius, would fall approximately along a single line. A frequently reproduced graph from these experiments (Figure 1) summarizes the n - VR curves for five "classes" of vegetation, each class considered to have similar properties. Use of this graph is referred to as the SCS method.

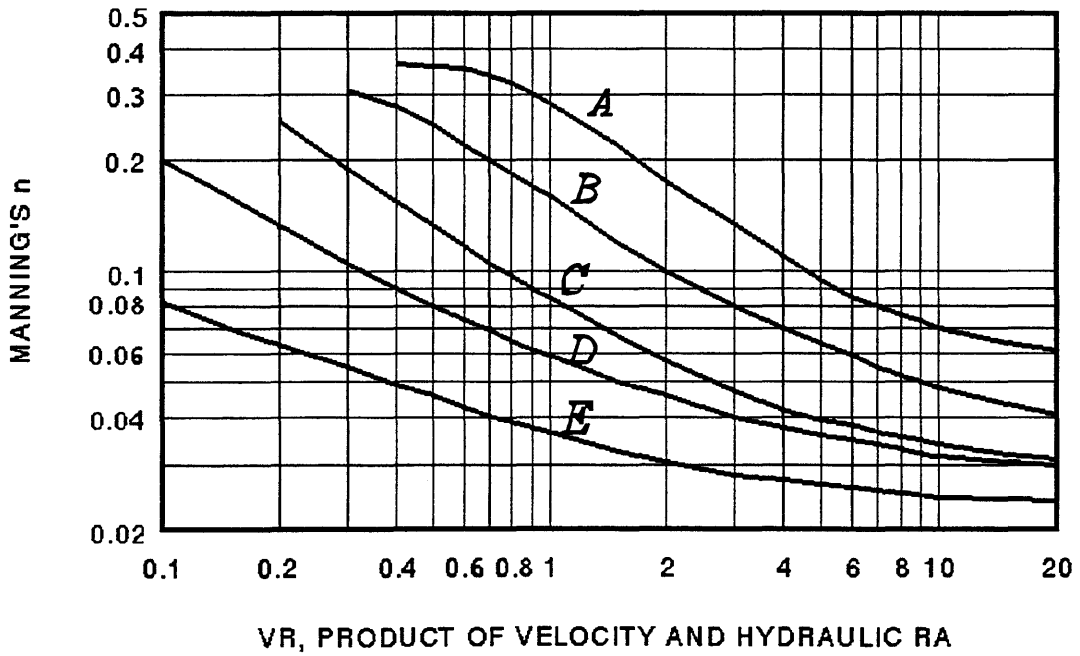

Figure 1. n - VR relationships for grass cover.

Kouwen and Unny (1973) proposed an improvement to the SCS method by suggesting that vegetation be classified on the basis of its flexural rigidity, defined by the product MEI. Kouwen, Li, and Simons (1981) present tables of MEI values for several species of vegetation. Kouwen (1988) presents a methods for estimating the value of MEI based on grass length. The relationship between MEI and h for green and dormant vegetation respectively are:

Green Vegetation:

$$MEI=319h^{3.3} \quad (5)$$

Dormant Vegetation:

$$MEI=25.4h^{2.26} \quad (6)$$

Handbook Methods: Establishment of flow resistance with procedures that do not rely on direct measurement or numerical analysis are referred to as "handbook methods". Included are tables of roughness values and compilations of photographs with descriptive information and calculated n values. Chow (1959) presented tables of minimum, normal, and maximum values of Manning's n for conduits, lined canals, and natural channels. This work is probably the most prevalent reference for the selection of n values. Other tables of roughness values have been compiled, but offer little additional insight. Of the 111 channel and floodplain types listed in Chow's table, 27 include vegetation, and for these Chow suggests values of n ranging from 0.022 to 0.200. Selection of an appropriate value is accomplished by interpreting brief anecdotal descriptions of channel conditions.

Barnes (1967) presents color photographs and descriptive data for 50 stream channels, nearly all of which have vegetation on the banks. Unfortunately, nearly all of the data presented in Barnes' report pertains to the main channel only. Where overbank flow existed, it was omitted from the calculations. Hicks and Mason (1991) presented similar information for 78 rivers reaches in New Zealand encompassing a broad range of conditions. Unlike Barnes, Hicks and Mason use multiple photographs for each reach, present bed material gradations, summarize all pertinent hydraulic data, compute values for both Manning's n and Chezy's C, and provide an estimate of computation error. They also evaluated multiple discharges for each reach. Like Barnes, Hicks and Mason avoided computation of flow resistance in floodplains, although their work does provide some insight into the contribution of bank vegetation to channel roughness.

Arcement and Schneider (1989) presented photographs for 15 densely vegetated floodplains for which roughness coefficients have been verified. Using Cowan's procedure and the method proposed by Petryk and Bosmajian, they used measured vegetation density in the floodplain and an effective drag coefficient to calculate the contribution of vegetation to the total roughness. Values for Manning's n ranged from 0.10 to 0.20. The contribution due to vegetation ranged from 0.065 to 0.145 which constituted 64 to 81 percent of the total value.

Evaluation of Techniques

Fifteen channel reaches with measured n values were used to assess the prediction methods described above. Four of the reaches were excavated canals, one was a laboratory flume and the remainder were natural channels. Six of the channels were evaluated for a discharge contained within the banks and seven for overbank flows. Three general cases of vegetal retardence were represented; 1) dense vegetation on the streambanks, 2) submerged or partially submerged aquatic vegetation, and 3) dense vegetation on the floodplains. Figure 2 is a photograph of the reach investigated on the Gila River near Yuma, AZ. Accompanying the figure are the computations and assumptions made in deriving the n values using each of the techniques.

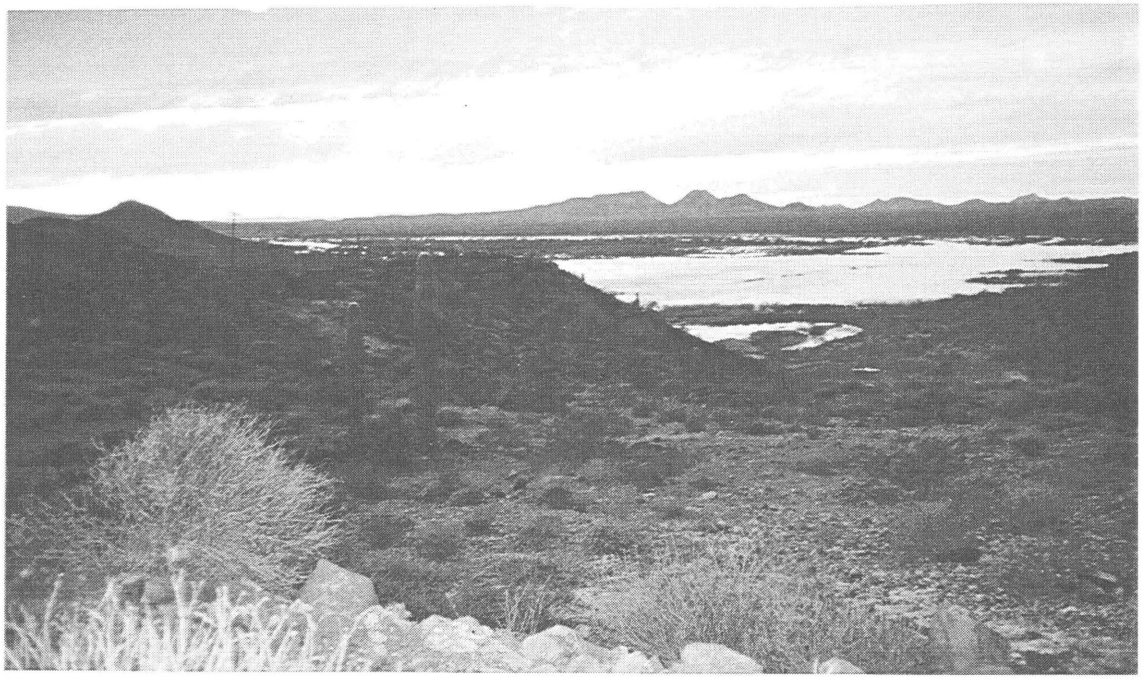

Figure 2. Gila River near Yuma, AZ

Computations and Assumptions for the Gila River:

Date: 8/17/65, Overbank flows in dense salt cedar/mesquite complex, Computed n = 0.082
Q = 40,000 cfs, V = 2.2 fps, S_o = 0.002, B_c = 140 ft, B_f = 2600 ft, R = 7.0 ft
d50 = 0.7 mm (est.), Veg_d = 0.0125 (est.), C* = 1.5 (est),
Chow - nc = 0.030, nf = 0.100, Composite n = 0.078
Hicks & Mason - Best match w/ Sec 43433 (note flows in bank) n = 0.046
Barnes - Best match w/ Sec 1005 (note flows in bank) n = 0.049
Cowan - Channel: n_b = 0.028, n_1 = 0.002, n_2 = 0.001, n_3 = 0.005, n_4 = 0.005, m = 1
Floodplain: n_b = 0.025, n_1 = 0.002, n_2 = 0, n_3 = 0.005, n_4 = 0.050, m = 1
nc = 0.041, nf = 0.082, Composite n = 0.069
Petryk & Bosmajian - nc = 0.041, nf = 0.111, Composite n = 0.097
n-VR - Not Applicable
MEI - Not Applicable

Measured n values and those predicted using each of the methods are presented in Table 3. Blanks in the table signify that an n value could not be estimated because a) the method was not applicable to the given conditions, b) requisite data was not available for the site and could not be estimated, or c) the magnitude of one or more parameters was well outside the range of data upon which the given technique was developed. The table also presents the mean of the predicted n values and coefficients of variation for each technique.

Table 3. Summary of Measured and Predicted n Values.

Stream/Location	Measured n value	Computed n Values						Mean Predict.
		Chow	H&M	Barnes	Cowan	P&B	n-VR	
Pearl River nr. Slidell, LA								
Marshy Section	0.065	0.035			0.074		0.065	0.058
Wooded Section	0.095	0.100			0.109	0.190		0.133
Tug Fork R. nr. Williamson, WV								
Bankfull Flow	0.050	0.040	0.046	0.046	0.054			0.046
Overbank Flow	0.074	0.080		0.080	0.111	0.200		0.118
Chisolm Crk. nr. Park City, KS	0.056	0.035	0.032	0.026	0.043			0.034
Cypress Crk. nr. Downsville, LA	0.100	0.100			0.105	0.085		0.097
Thompson Crk. nr. Clara, MS	0.200	0.120			0.155	0.151		0.142
River Yare nr. Norwich, Norfolk	0.150	0.100	0.140		0.117		0.080	0.109
Gila River nr. Yuma, AZ	0.082	0.078	0.046	0.049	0.069	0.097		0.068
Flume w/ Bulrush	0.329	0.150			0.112	0.398	0.350	0.252
Don River nr. Toronto, Canada	0.225	0.150			0.150			0.150
Two-Mile Sl. nr. Sadorus, IL	0.120	0.070	0.066	0.070	0.093	0.065		0.073
Kaskaskia Chn. nr. Bondville, IL	0.080	0.070	0.041	0.045	0.089	0.057		0.060
Naanai Canal, Egypt	0.040	0.050	0.060		0.057			0.056
Port-Said Canal, Egypt	0.074	0.080	0.060		0.057			0.066
Coeff. of Var.		0.247	0.33	0.326	0.249	0.471	0.177	0.268

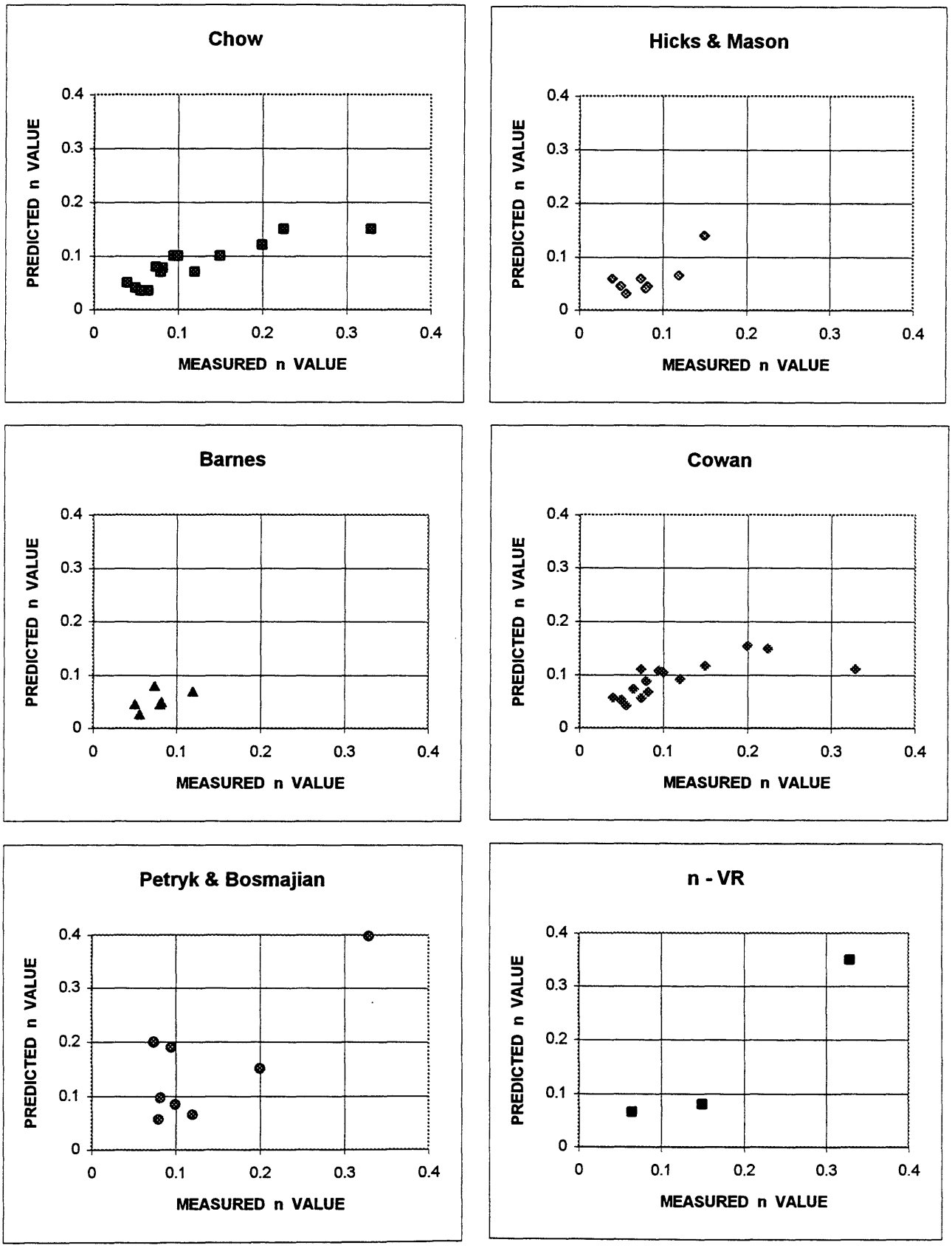

Figure 3 - Plots of Predicted vs. Measured n Values for Each Method

Figure 3 presents plots of the predicted n values against measured n values for each technique. In general, prediction error increased with increasing degree of resistance. Coefficients of variation for each method were: n-VR - 0.177, Chow - 0.247, Cowan - 0.249, Barnes - 0.326, Hicks and Mason - 0.330, and Petryk and Bosmajian - 0.471. Chow's method tended to underpredict resistance at higher values, as did Cowan's. The handbook methods of Barnes and of Hicks and Mason as well as the n-VR method displayed no trends relative to over- or under-predicting actual n values for the ranges in which they were applicable. The method of Petryk and Bosmajian tended to overpredict resistance, and had the greatest degree of variation.

This analysis highlighted the inadequacies of the various methods for predicting resistance values for typical field applications. Of particular note is the limited number of cases for which many of the methods were applicable. While estimates could be made for all 15 reaches using the methods by Chow and Cowan, the others proved far less applicable. Reasonable matches in Hicks and Mason's handbook could be found for only eight cases, and Barnes' handbook could be used for only six. Measurements of vegetation density were available for only four sites, but were estimated for an additional four, allowing the method by Petryk and Bosmajian to be used on eight reaches. The n-VR method was applicable to only three of the fifteen cases investigated, and these were somewhat outside the range of data for which the method was developed.

Conclusions

Most engineers rely upon experience and judgement, along with a standard reference such as Chow's tables, to select resistance coefficients for hydraulic and channel stability analyses. Presumably, a more quantitative approach would improve accuracy and prove more useful for investigations where dense vegetation is present in the floodway. A predictive method incorporating variables such as flow depth, percentage of the wetted perimeter covered by vegetation, vegetation density, vegetation response to flow, and vegetation alignment would be expected to yield more accurate predictions than methods based upon judgement or the interpretation of qualitative descriptions. No such predictor has been proposed, but the methods evaluated in this investigation include some of these variables.

Since each of the methods require some degree of interpretation or the estimation of parameters, other investigators attempting to reproduce the results of this evaluation would likely arrive at different n values than those obtained by the author for each method. Nevertheless, general conclusions about the applicability and estimation error of each method can be drawn from the analysis.

Though Chow's handbook tables and Cowan's procedure rely upon interpretation of qualitative descriptions for the assignment of resistance values, they proved to be the most applicable techniques and had lower prediction errors than all but the n-VR method (which only applied to three cases). However, these methods clearly underpredict resistance for n values in excess of 0.1. They are probably best suited to conditions in which vegetation is not present or is confined to the banks. When flows in densely vegetated floodplains are anticipated, alternative procedures should be used or the predicted values should be adjusted.

Handbook methods relying upon pictoral descriptions of channels are convenient and offer the advantage of implicitly compositing channel resistance, but they offer little utility in cases where vegetation is present or where floodplain flows are anticipated. Only a dozen such circumstances are addressed in the collective works of the handbooks cited. The author found that reliance upon these handbooks can actually be misleading, resulting in greater errors than simply using qualitative channel and floodplain descriptions. In many cases, more than one channel in the references appeared to have characteristics similar to those for the channel being investigated, and the reference channels had substantially different resistance values.

Petryk and Bosmajian's vegetation density technique is hindered by the additional data collection requirements and is only applicable to densely wooded floodplains. In cases where vegetation is limited to the banks, or is not continuous throughout the floodplain, the method greatly overpredicted resistance. However, for wooded floodplains with little undergrowth, this method yielded the best estimates. It is recommended that its use be limited to these conditions.

The n-VR method is limited by the range of slopes over which data were collected (greater than three percent), the types of vegetation used (grasses only), and difficulties in selecting an appropriate curve. The method yielded good estimates of resistance for the three cases in which it was applicable, although the channel slopes were less than three percent. The MEI analyses proposed by Kouwen et. al. explicitly includes the geometric and physical properties of the vegetation in the analysis of flow resistance. Though not substantially verified, this method appears to provide a sound process for the assessment of resistance due to some types of vegetation. Unfortunately, the method could not be applied to any of the reaches in this investigation because of a lack of data.

Additional work on the development of resistance relationships for vegetated floodways should focus on a procedure that exhibits the following characteristics: resistance should be related to readily defined, measurable characteristics of the channel, vegetation, and flow; resistance should be described as a continuous function of the independent variables involved; and the resistance function should be dimensionally homogeneous. None of the methods evaluated possess these qualities.

References

Arcement, G. J., Jr., and Schneider, V. R. (1989). Guide for selecting Manning's roughness coefficients for natural channels and flood plains, *U.S. Geological Survey Water-Supply Paper 2339*, Denver, CO.

Barnes, H.H. (1967) Roughness characteristics of natural channels. US Geological Survey, Water-supply Paper No. 1849, 214 pp. Washington, DC.

Chow, V.T. (1959) *Open-Channel Hydraulics*. McGraw-Hill Book Co., New York.

Cowan, W.L. (1956) Estimating hydraulic roughness coefficients. *Agricultural Engineering 37*, 473-475.

Hicks, D.M. and Mason, P.D. (1991) Roughness Characteristics of New Zealand Rivers. *Water Resources Survey*, 1-9.

Kouwen, N. and Unny, T.E. (1973). Flexible Roughness in Open Channels. *Journal of the Hydraulics Division, Proceedings of the American Society of Civil Engineers 99*, 713-728.

Kouwen, N., Li, Ruh-Ming, and Simons, D.B. (1981). Flow Resistance in Vegetated Waterways. *Transactions of the American Society of Agricultural Engineers 24*, 684-690, 698.

Petryk, S. and Bosmajian, G., III. (1975). Analysis of Flow Through Vegetation. *Journal of the Hydraulics Division, Proceedings of the American Society of Civil Engineers 101*, 871-885.

Ree, W.0. and Palmer, V.J. (1949) Flow of water in channels protected by vegetative linings. *US Department of Agriculture. Soil Conservation Service Technical Bulletin No. 967*, 115 pp.

Bridge Pier Scour: A Comparison of Various Scour Prediction Functions Using Field Data

John M. Carroll Jr.

Abstract

Six local scour prediction functions will be compared using forty-one sets of field data. These six functions represent three older established methods and three newer methods that have been presented at ASCE National Hydraulic Conferences over the past two years.

Introduction

Scour is the result of the erosive action of flowing water, excavating and carrying away material from the bed and banks of streams. Different materials scour at different rates. Loose granular soils are rapidly eroded by flowing water, while cohesive or cemented soils are more scour resistant. However, ultimate scour in cohesive or cemented soils can be as deep as scour in sand bed streams.

Total scour at a highway crossing generally consists of three components: long term aggradation or degradation; contraction scour; and local scour. Prediction of the riverine response to bridge constriction and other man-made modifications is a very complex process. The focus of this paper will be limited to predicting local scour at bridge piers, comparing several methods of predicting local scour with field data.

A factor in scour at highway crossings and encroachments is whether the scour is clear-water or live-bed scour. Clear water scour occurs where there is no transport of bed material upstream of the crossing or encroachment and live-bed scour occurs where there is transport of material from the upstream reach into the crossing or encroachment. In analyzing the field data for this paper, only measurements taken where there was live-bed scour were used for comparisons.

Historically, the equations for estimating contraction scour and local scour have been based on laboratory experiments with limited field verification. Research efforts aimed at gaining an understanding of scour at bridge piers have focused on laboratory testing. The basic mechanism causing local scour at piers or abutments is the formation of vortices. The flow pattern past a pier protruding from a plane boundary is complex. This complexity increases with the development of the scour hole. The flow pattern past a pier may be separated into its components:

1) Downflow in front of the pier
2) Horseshoe vortex
3) Cast-off vortices and wake
4) Bow wave

These are shown in diagrammatic form in Figure 1.

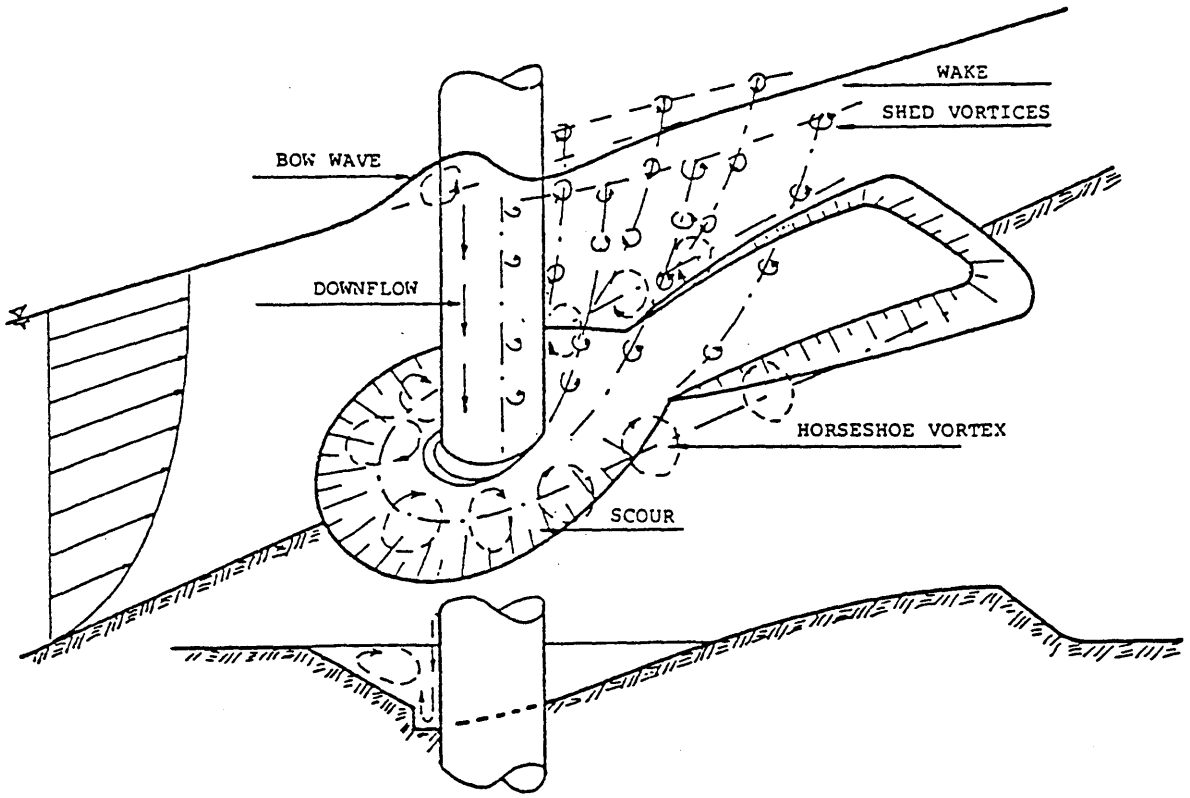

Figure 1 (Breusers, 1991). Flow Pattern Adjacent to a Cylindrical Pier.

The scour depth depends on variables which characterize the fluid, bed material, flow and bridge pier, e.g., fluid density, kinematic viscosity, gravity, sediment particle size, sediment particle density, flow depth, flow velocity, and pier width. The published formulae for scour at bridge piers are based on various combinations of these parameters, with varying results as shall be shown.

Field Data

The field data used for comparisons in this paper are the result of a U.S Geologic Survey (USGS) data collection effort as part of a cooperative National Scour Study with the U.S. Department of Transportation, Federal Highway Department (FHWA), initiated in 1987. This data set contains detailed measurements of flow depth and velocity, a measure of bed material size and gradation, information on pier type, shape, skew angle to flow direction, debris, and other pertinent information. Eighteen bridges are represented in the selected data sets, located in Alaska, Delaware, Indiana, Louisiana, Mississippi, New York, Ohio, and Virginia.

An attempt was made to select a fairly homogeneous data set to facilitate analyzing the differences in the scour prediction functions. Forty-one sets of field data were selected based on

the following criteria: the bridge piers are either cylindrical or have rounded noses; and live bed scour conditions prevail at the highway crossing. About 41% of the data sets did not have significant debris load on them, while for the balance the debris load was unknown. With regard to bridge skew with the direction of flow, only about 5% of the data sets represent bridges with significant skew of 15 degrees or more.

Scour measurement data have usually been obtained from physical models in laboratory flumes where bed elevations outside of the scour hole usually do not change significantly. The reference surface is usually taken as the average of several points measured in the unscoured region around the obstruction after equilibrium bed conditions are established and after the model run is completed. This ambient or mean equilibrium (in the case of dunes) bed level has been used as the reference surface in most flume studies of local scour. In the field, local scour measurements using reference surfaces other than concurrent ambient bed level may include significant amounts of contraction or general scour, which would significantly reduce the value of these data. Therefore, the concurrent ambient bed level is the preferred reference surface for measurements of local scour depth from scoured channel geometry. Figure 2 is a depiction of a scour hole and reference surface.

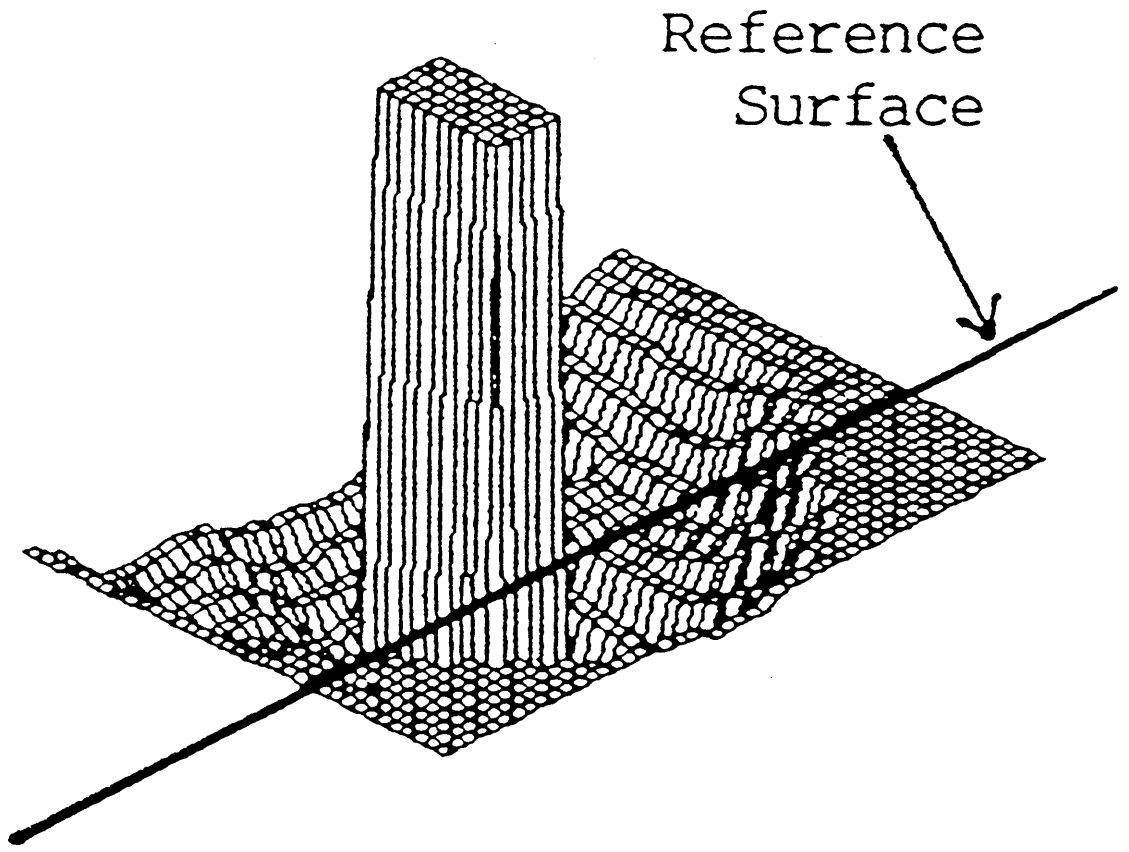

Figure 2 (Landers, 1993). Reference surface for Local Scour.

The reference surface based on concurrent ambient bed level can isolate the local scour component of total scour. Contraction scour would be identified as a separate component of total scour at a bridge. The data set used herein was developed applying this method of local scour depth measurement.

Scour Prediction Functions and Data Analyses

A number of equations for predicting local scour depth have been proposed by different researchers over the past fifty years. The equations have been developed generally following three methods of analysis. These methods are: 1) The regime approach, using the transport relations in the approaching flow and in the scour hole; 2) Regression analyses of available data, to present empirical equations; and 3) Dimensional analyses of the basic parameters affecting the local scour process.

The six methods to be compared cover this broad spectrum. The new and older methods are be contrasted in pairs because the pairs reflect similar approaches in the development of prediction functions, as outlined above. Please note that the variables in the prediction functions may have been revised from their original presentation in the references in order to have consistent symbols representing specific variables in this paper.

Breuser vs. Ansari

The methods of Breuser (as modified by Larras, see Shen 1969) and Ansari (1993) share a similar and defining characteristic. Both predict local scour as functions solely of the pier geometry. The following is an outline of the method of Breuser as modified by Larras.

For scour with continuous sediment motion (live-bed)

$$y_s = 1.42\, k\, b'^{0.75}$$

where y_s: maximum equilibrium scour depth (ft)

k : pier shape coefficient (k=1 for cylindrical or round piers)

b' : width of pier projected normal to direction of flow (ft)

Larras collected available scour data from various French rivers; however, these were point measurements of scour depth, and since there was no long record, it unlikely that these measurements correspond to equilibrium depths of scour. Larras states that measurements were made after the flood had passed, that the pier was generally aligned with the flow and the bed was not moving.

A plot of the prediction function versus field data is shown in Figure 3. If one needs a quick estimate this method provides adqequate results. It did under-predict about 1/4 of the

scour depth values, but generally not by more than 25% to 50%. From this it may be concluded that pier size is a very important factor in local scour. The data points most overestimated reflect bridges with significant skew such that effective pier width becomes large. It should be noted that Breuser's original function is simply y (scour depth) = 1.4*b (pier width).

The method of Ansari is the result of similar analyses of field data covering a wide range of variables to develop envelope curves. The method provides an estimate of the ultimate depth of local scour at a bridge pier.

Ultimate depth of scour is enveloped by curves having equations as:

$$y_s = 0.86\ b'^{3.0} \quad \text{for } b' < 2.20 \text{ m}$$

and

$$y_s = 3.6\ b'^{0.4} \quad \text{for } b' > 2.20 \text{ m}$$

where y_s : ultimate scour depth (m)

b' : width of pier projected normal to direction of flow (m)

In discussion of their results, Ansari and Qadar (Ansari, 1994) noted that no physical justification could be given to explain dividing the projected pier width criteria into two regimes, which was simply taken from the trends of the data and their enveloping curves.

As shown in Figure 3, this method provides similar results to that of Breuser-Larras except where the pier width exceeds the 2.2 meter parameter set forth by Ansari. For wide piers or when significant skew is present this method predicts much more conservative values of local scour than Breuser-Larras. Also, it tended to underpredict scour by a wider margin than did Breuser- Larras. In the present narrow analysis, for cylindrical or round-nose piers with little skew, the Breuser-Larras function appears to be more consistent.

CSU Equation versus Richardson & Richardson

These two functions represent very similar approaches, as both contain major contributions by E.V. Richardson. The former is the preferred method for local scour prediction in the U.S. Department of Transportation's "Highways in the River Environment," (Richardson, 1990). The following is a presentation of the CSU Equation.

For local scour with either clear-water or continuous sediment motion (live-bed)

$$y_s = 2.0\ y_1\ k_1\ k_2\ (b/y_1)^{0.65}\ Fr_1^{0.43}$$

where y_s : equilibrium scour depth (ft)

b : pier width (ft)

k_1 : pier shape factor (k=1 for cylindrical or round piers)

k_2 : angle of attack factor, a function of the ratio of pier length to width and the attack angle, value taken from a table, varies from 1 to 5, maximum value for the data set was 3

y_1 : approach flow depth (ft)

Fr_1 : approach flow Froude number

The CSU Equation was developed from a dimensional analysis of the parameters affecting pier scour and analysis of laboratory data. It does not account for effects of bed material size or gradation. The equation incorporates the upstream flow conditions including the upstream flow velocity in the Froude number, and the modifies the bridge skew using the angle of attack factor.

The CSU Equation enveloped the field data but for one point. It gave a few rather conservative values but was in general very consistent, as shown in Figure 3. Where approach depth is deep with high velocity and pier is wide, the equation yields very conservative values. With required data on flow conditions, the method is straightforward in application.

The method of Richardson and Richardson appears to be a refinement of the CSU Equation with additional factors to account for bed condition (plane bed, ripples, or dunes) and the potential for bed armoring. The following is a presentation of the Richardson and Richardson method.

For local scour with either clear-water or continuous sediment motion (live-bed)

$$y_s = 2.0\, b\, k_1\, k_2\, k_3\, k_4\, (y_1/b)^{0.35}\, Fr_1^{0.43}$$

where y_s : equilibrium scour depth (ft)

b : pier width (ft)

k_1 : pier shape factor - from table, k=1 for cylindrical or round piers

k_2 : angle of attack factor, a function of the ratio of pier length to width and the attack angle, value taken from a table, varies from 1 to 5, maximum value for the data set was 3

k_3 : bed condition factor - from table, based on bed dune height; value ranges from 1.1 for clear water or plane bed to 1.3 for large dunes

k_4 : bed material factor - from table, based on ratio of D_{50}/D_{90} and ratio of v_1/v_c (see equation below); value ranges from 1 for sands to 0.8 for cobbles

y_1 : approach flow depth (ft)

Fr_1 : approach flow Froude number

v_1 : approach flow velocity (ft/s)

v_c : critical velocity to move a sediment particle (ft/s),

where the critical velocity of the D_{90} bed material size when the specific gravity of the sediment G=2.65 is as

$$v_c = 10.95\, y_1^{(1/6)}\, D_{90}^{(1/3)}$$

For piers aligned with flow, without pressure flow or debris, the maximum depth of scour calculated by this method is limited by the following:

$$y_s = 2.4\ b \quad \text{for } Fr_1 < 0.8$$

$$y_s = 3.0\ b \quad \text{for } Fr_1 > 0.8$$

This equation is very similar to the CSU Equation. Both contain (pier width)$^{0.65}$ but Richardson & Richardson incorporates the flow depth as $y_1^{0.35}$ versus $y_1^{-0.65}$ in the CSU Equation. In application to this particular field data set, the bed material and bed condition factors had little impact on predicted scour values.

The Richardson & Richardson method provides results that are very similar to the CSU Equation. In general, for this data set with its rather limited scope of conditions, it is slightly more conservative than the CSU Equation, and rather more involved in application. The incorporation of the bed conditions was not a factor for these data.

Froelich vs. Gao

These two prediction functions were developed through regression analyses of field data with an attempt to incorporate additional influences beyond that of pier width and approach flow conditions. The method of Froelich (Froelich, 1988) is of relatively recent origin and appears as an alternative method for local scour prediction in the U.S. Department of Transportation's "Highways in the River Environment," (Richardson, 1990). The following is a presentation of Froelich's function.

For local scour with continuous sediment motion (live-bed)

$$y_s = 0.32\ b\ k\ (b'/b)^{0.62}\ (y_1/b)^{0.46}\ Fr_1^{0.20}\ (b/D_{50})^{0.08}$$

where y_s : equilibrium scour depth (m)

b : pier width (m)

b' : width of pier projected normal to direction of flow (m)

k : pier shape coefficient (k=1 for cylindrical or round piers)

y_1 : approach flow depth (m)

Fr_1 : approach flow Froude number

D_{50} : equivalent sediment particle diameter for finer than 50% size fraction (mm)

Froelich's function underestimated about 73% of the measurements and the function generally yields low values with respect to measured scour depth, as shown in Figure 3. The regression factor of 0.32 limits the applicability of the function. The pier width is important, as Froehlich has also determined a "Design Equation" that would add 0.32*(pier width) to the design scour depth. Using the "Design Equation," the function underestimated only 8% of the measured values. The "Design Equation" is thus apparently more effective in scour prediction.

The Froehlich method incorporates the upstream flow conditions including the upstream flow velocity in the Froude number, and the bed material size. It was developed using regression analysis from 83 groups of field data.

The method of Gao (Gao, 1993) was originally developed in the People's Republic of China in 1964, and the method presented here represents recent improvements to their equations, which have been developed from model and field data.

For local scour with continuous sediment motion (live-bed)

$$y_s = 0.46\, k\, b'^{0.60}\, y_1^{0.15}\, D^{-0.07}\, [(v-v_c')/(v_c-v_c')]^{eta}$$

where y_s : equilibrium scour depth (m)

b' : width of pier projected normal to direction of flow (m)

k : pier shape coefficient (to be determined from special curves and figures; simplified to k=1 for cylindrical piers; 0.8 for round-nosed piers)

y_1 : approach flow depth (m)

D : median sediment particle diameter (m)

v : mean velocity of approach flow (m/s)

v_c : critical velocity for initiation of motion of bed material (m/s) - see below

v_c' : initial velocity of local scour of pier (m/s) - see equation below

eta : a power related to bed load as

If $v <= v_c$ then eta = 1.0 (clear water scour)

If $v >= v_c$ then eta < 1.0 (live-bed scour)

where eta = $(v_c/v)^{9.35 + 2.23\log D}$

According to the model studies of China, the magnitude of the initial velocity of local scour at the pier, v'_c, varies from about 0.4 to 0.6 times the critical velocity for initiation of motion of bed material, v_c. The equation for v_c is

$$v_c = (y_1/D)^{0.14} \{17.6 (G-1) D + 0.000000605 [(10 + y_1)/D^{0.72}]\}^{0.5}$$

where G : the specific gravity of the sediment

From model experimental data, the equation for v'_c is

$$v'_c = 0.645 (D/b')^{0.053} v_c$$

The pier shape coefficient reflects the influence of pier shape and flow attack angle on scour depth. Assuming the scour depth of a cylindrical pier is unity, the ratio of scour depth to any other shaped pier is the pier shape coefficient K. A table of pier shape coefficients which includes 10 kinds of pier types was formulated according to a great number of model data by the Academy of Railway Sciences of China. Determination of the pier shape coefficient has been simplified (Gao, 1994).

The method of Gao incorporates not only upstream flow conditions and bed material size, but a sophisticated method of accounting for incipient motion of sediment at the pier itself incorporating the influence of pier width, upstream flow depth, and sediment particle size. The equation for eta was developed from 212 groups of live bed scour data using regression analysis.

As can be seen in Figure 3, these two methods provide quite similar results. The Chinese method modified by Gao provides relatively less error and appears to err on the conservative side. However, the Froehlich "Design Equation" would seem the preferable alternative to either method.

Summary and Conclusions

Historical investigations used flume experiments in the initial pursuit of understanding scour phenomena. As the physical factors affecting pier scour have been revealed, mathematical approaches to combining these factors have allowed for refinement of prediction methods.

There are more than twenty methods commonly noted in the literature, providing a rather broad spectrum of approaches to the analysis of local scour. Early efforts relied on laboratory flume tests. With the current interest in collecting field data, more complex behaviors can be studied in the effort to more fully understand and predict the riverine response to highway crossings.

Pier width is the most significant factor in the development of the local scour hole. As prediction methods have become more complex researchers have incorporated the contribution of other elements, notably flow depth and approach velocity. The most recent developments have used regression analysis and attempted to account for a variety of factors, adding bed particle size, complex derivations concerning the impact of the pier on the incipient motion of particles, or simplified bed condition factors.

The methods of Breuser-Larras and Ansari serve to illustrate the importance of pier width to the ultimate scour depth. They may have limited applicability when a quick answer is required, or when data is limited.

The approaches of Froehlich and Gao attempt to rationalize the affect of several parameters. This approach yields a population of values that reflect actual values, with attendant scatter of data. However, for design purposes a more conservative approach is advisable. As more field data is acquired, a better understanding of the physical processes will improve such methods.

The CSU Equation and the similar approach by Richardson and Richardson tend to envelope local scour depths for a wide range of conditions, making them attractive in terms of design applications. The application of the CSU Equation to the field data herein confirms its status as the preferred prediction method.

In terms of design application, the three types of predictors would provide for a comprehensive analysis of local scour phenomena. In comparison with the established methods, the new methods applied in this study do not appear to appreciably refine the prediction process. However, they do present interesting approaches.

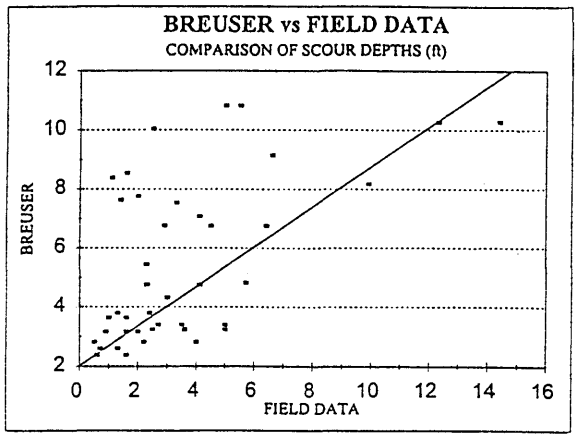

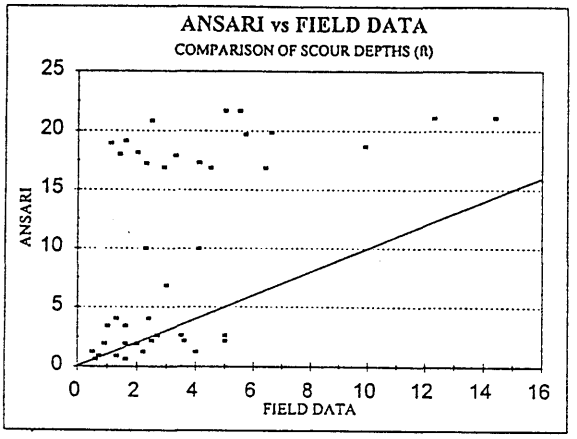

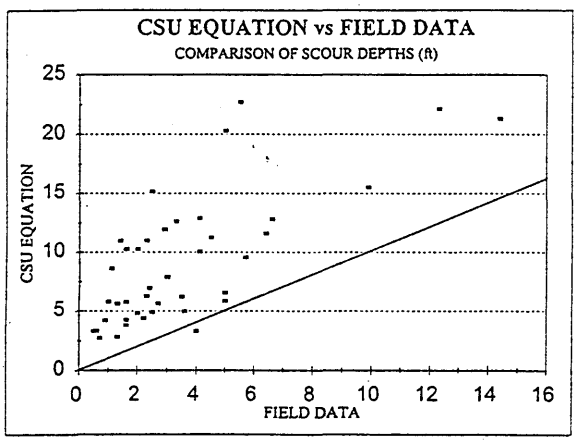

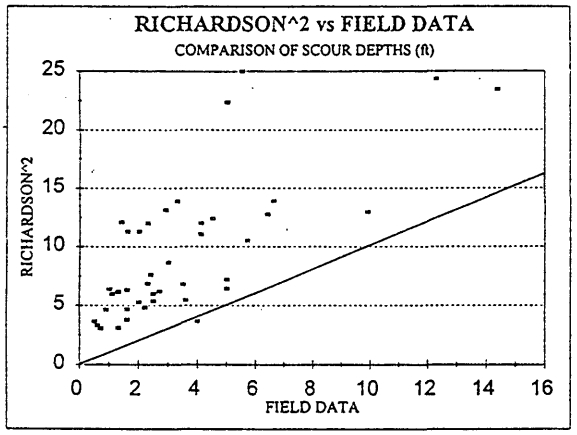

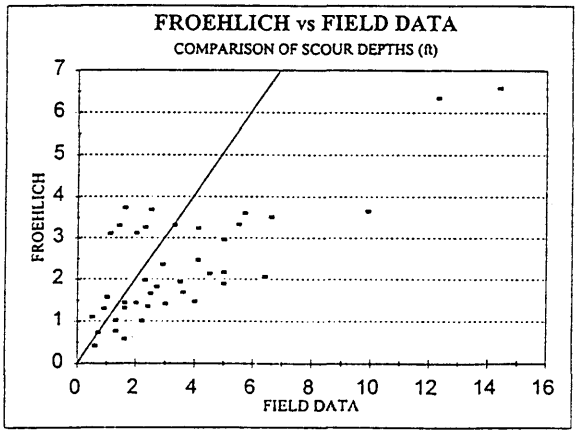

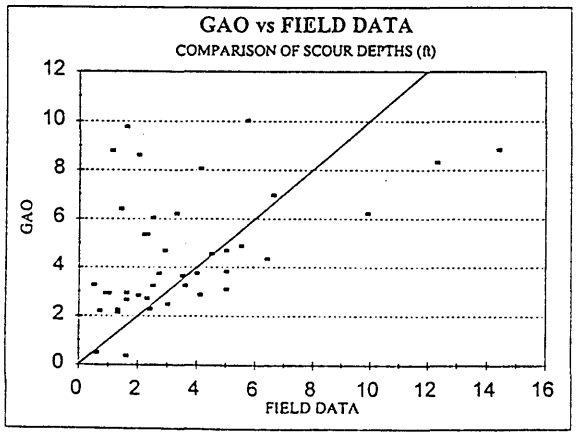

Figure 3. Comparisons of Various Prediction Methods with Field Data.

References

Ansari, S.A., and Qadar, A., 1994, "Ultimate Depth of Scour Around Bridge Piers," Hydraulic Engineering - Proceedings of 1994 National Conference, ASCE, p. 51-55.

Breusers, H.N.C, Nicollet, G., and Shen, H.W., 1977, "Local Scour Around Cylindrical Piers," Journal Of Hydraulic Research, 15 (3), p.211-252, IAHR.

Breusers, H.N.C, and Raudkivi, A.J., 1991, "Scouring," International Association for Hydraulic Research, A.A. Balkema, Rotterdam.

Froelich, D.C., 1988, "Analysis of Onsite Measurements of Scour at Piers," Hydraulic Engineering - Proceedings of 1988 National Conference, ASCE, p.534-539.

Gao, D., Posada, L., and Nordin, C.F., 1993, "Pier Scour Equations used in China," Hydraulic Engineering - Proceedings of 1993 National Conference, ASCE, p.1031-1036.

Gao, D., Posada, L., Nordin, C.F., 1994 (draft), "Pier Scour Equations used in China - Review and Summary," Dept. Of Civil Engineering, Colorado State University, Ft. Collins, CO.

Landers, M.N., and Mueller, D.S., 1993, "Reference Surfaces for Bridge Scour Depths," Hydraulic Engineering - Proceedings of 1993 National Conference, ASCE.

Landers, M.N., Jones, J.S., and Trent, R.E., 1994a, "Brief Summary of National Bridge Scour Data Base," Hydraulic Engineering - Proceedings of 1994 National Conference, ASCE.

Landers, M.N., and Mueller, D.S., 1994b (draft), "Channel Scour at Bridges in the United States," U.S. Dept. of Trans., FHWA.

Noshi, H.M., 1993, "Experimental Study on the Effects of Sediment Gradation and Flow Hydrograph on Clear Water Local Scour Around Circular Bridge Piers," (Master's Thesis), Colorado State University, Ft. Collins, CO.

Richardson, E.V, Simons, D.B., and Julien, P.Y., 1990, "Highways in the River Environment," U.S. Dept. of Transportation, FHWA.

Richardson, E.V., Harrison, L.J., Richardson, J.R., and Davis, S.R., 1993, "HEC-18: Evaluating Scour at Bridges, Second Edition," U.S. Dept. of Transportation, FHWA.

Richardson, E.V., and Richardson, J.R., 1994, "A Practical Method for Scour Prediction at Bridge Piers," Hydraulic Engineering - Proceedings of 1994 National Conference, ASCE, p.1-5.

Shen, H.W., Schneider, V.R., and Karaki, S., 1969, "Local Scour Around Bridge Piers," Journal of Hydraulics Division, ASCE, V. 95, p. 1919-1940.

Evaluation of Selected Pier-Scour Equations Using Field Data

by Mark N. Landers

for CE 717: River Mechanics, Spring 1995
Colorado State University

Introduction

River channels scour and aggrade due to complex interrelated natural processes. Bridge crossings frequently disrupt and intensify the natural river processes by constricting the flow area of the stream at flood stage, by constricting the portion of the channel from which sediment is supplied, and by disturbing the flow with local obstructions (i.e. piers) which locally constrict and redirect the flow. Estimates of the potential scour at bridge sites are essential for both the design of new bridges and for the evaluation of existing bridges to provide safe reliable public transportation corridors.

There are more than 580,000 bridges in the United States and about 84 percent of these are over waterways. Channel-scour around bridge foundations is the leading cause of bridge failure; exceeding all other causes combined. In a survey of 823 bridge failures since 1950, Shirhole and Holt (1991) found that 60 percent were associated with hydraulics, which includes channel bed scour around bridge foundations and channel instability. The predominance of the hydraulics failure mode indicates the need for improved scour analysis and prediction techniques.

The need for improved scour design techniques has long been recognized and scour processes have been extensively researched by many investigators. Numerous equations have been developed to predict contraction scour and local scour at bridges (Shen and others, 1969; Laursen, 1960; Melville and Sutherland, 1988; Richardson and others, 1993; Froehlich, 1988). Most of these equations are based on laboratory investigations. Scour predictions based on the many available equations produce a wide range of scour depths for the same set of conditions; probably due to the typically limited and somewhat unique conditions associated with each investigation. Scour predictions also differ from scour measurements at bridge sites; probably due to the range of deterministic scour variables in the field that are difficult to reproduce or measure in the laboratory, and due to dynamic dimensional dissimilarity between field conditions and laboratory investigations.

The recommendation of many scour investigations has been to measure scour data at bridges during floods to improve the understanding of scour processes and the bridge scour prediction methods. Cooperative investigations to collect bridge-scour data during floods have been initiated over the last several years between the U.S. Geological Survey (USGS) and many State Departments of Transportation.

Objectives and Scope

The objectives of this study are to evaluate and compare selected pier scour prediction equations using 38 field measurements of bridge scour made during active bed-load transport conditions during floods. The following equations are evaluated: Chinese (Gao and others, 1992), HEC-18 (Richardson and others, 1993), Larras (Larras,1963), and Shen-Maza (Shen and others, 1969). These equations are evaluated on the basis of their predictive versus the observed scour depths, and on the basis of the deterministic relations implied by their explanatory variables.

Summary of Scour Measurements at Bridge Piers

The measurements used in this evaluation were obtained at the upstream side of piers that were aligned to the flow, and had flow velocities greater than 1.5 times the critical shear velocity for the median bed material size. These 3 factors were the criteria used to select a subset of the nationwide scour data base compiled by Landers and Mueller (1995, in press). The data used here were measured at 25 piers at 16 sites in 10 States, as listed in Table 1. The scour measurement attributes are summarized in Table 2.

Piers are considered as aligned to the flow if the skew is 5 degrees or less. Pier width ranges from 2 to 14 feet in this data set. The flow velocity is a vertically averaged velocity measured just upstream of the accelerated flow region around the pier. Where the

Table 1. - Locations of scour measurement sites used in this analysis

SITE NO.	NAME	SITE NO.	NAME
2	Knik River at Old Glenn Highway near Palmer, AK	34	Badger Creek at U.S. 89 near Browning, MT
3	Knik River near Eklutna, AK	36	Chemung River at S.R. 427 at Chemung, NY
9	Red River at I-30 near Fulton, AR	41	Great Miami River at S.R. 128 at Hamilton, OH
13	Arkansas River at C.R. 613 near Nepesta, CO	47	Todd Fork at S.R. 22 at Morrow, OH
20	White River at S.R. 157 at Worthington, IN	48	Killbuck Creek at C.R. 621 at Killbuck, OH
21	Red River at east S.R. 3032 near Shreveport, LA	49	Pamunkey River at S.R. 614 near Hanover, VA
22	Red River at west S.R. 3032 near Shreveport, LA	52	Dan River at U.S. 501 at South Boston, VA
28	Homochitto River at U.S. 84 at Eddiceton, MS	53	Tye River at S.R. 56 near Lovingston, VA

Table 2. - Summary of attributes of scour measurements

Meas. No.	Site No.	Meas. Date	Pier ID	Pier Shape	Pier Length (ft)	Pier Width (ft)	Flow Velocity (ft/sec)	Flow Depth (ft)	D50 (mm)	D85 (mm)	Scour Depth (ft)	Error (ft)
1	2	07/11/65	5	SHARP	29.0	6.0	12.0	18.0	5	25	3.5	0.5
2	3	06/24/66	1	ROUND	36.9	5.0	5.0	7.0	1.8	13	2.0	0.5
3	3	06/24/66	2	ROUND	36.9	5.0	5.1	6.5	1.8	13	2.0	0.5
4	3	06/24/66	3	ROUND	36.9	5.0	5.2	10.0	1.8	13	3.0	0.5
5	3	06/24/66	4	ROUND	36.9	5.0	6.5	10.5	1.8	13	4.0	0.5
6	3	06/17/66	5	ROUND	36.9	5.0	2.9	4.0	0.58	7	1.0	0.5
7	3	06/24/66	5	ROUND	36.9	5.0	5.9	10.0	1.8	13	4.5	0.5
8	3	06/24/66	6	ROUND	36.9	5.0	6.8	8.5	1.8	13	3.5	0.5
9	3	06/24/66	7	ROUND	36.9	5.0	6.0	10.0	1.8	13	6.0	0.5
10	9	05/12/90	4	SHARP	*	7.0	9.5	35.3	0.18	*	14.6	0.5
11	13	06/05/84	1	ROUND	21.0	4.0	5.4	7.5	1.19	5.15	4.3	1.0
12	20	01/03/91	3	ROUND	43.0	3.0	4.2	16.7	0.9	4.2	2.2	0.5
13	21	05/19/90	4	SHARP	54.0	14.0	8.4	38.0	0.3	0.4	12.2	2.0
14	21	05/22/90	4	SHARP	54.0	14.0	6.9	30.9	0.3	0.4	11.4	1.0
15	21	05/19/90	5	SHARP	54.0	14.0	10.4	39.2	0.3	0.4	22.9	2.0
16	21	05/22/90	5	SHARP	54.0	14.0	9.5	32.1	0.3	0.4	25.1	1.0
17	22	05/17/90	4	ROUND	40.0	14.0	8.2	38.3	0.3	0.4	14.4	1.0
18	22	05/19/90	4	ROUND	40.0	14.0	8.4	35.5	0.3	0.4	10.8	2.0
19	22	05/22/90	4	ROUND	40.0	14.0	6.9	30.6	0.3	0.4	12.6	1.0
20	22	05/17/90	5	ROUND	40.0	14.0	9.8	39.5	0.3	0.4	14.9	1.0
21	22	05/19/90	5	ROUND	40.0	14.0	10.4	36.7	0.3	0.4	18.1	1.0
22	22	05/22/90	5	ROUND	40.0	14.0	9.5	31.8	0.3	0.4	12.3	1.0
23	28	08/27/92	4	CYLINDER	8.0	8.0	7.4	8.7	7.51	23.2	6.4	1.0
24	34	05/21/91	P3	SHARP	36.0	3.4	5.4	1.3	8	30	3.2	0.3
25	36	06/24/72	1	ROUND	48.0	5.0	13.4	27.3	27	58	5.1	0.5
26	41	05/16/90	3	ROUND	81.8	3.5	4.5	13.4	0.78	1.6	1.0	0.25
27	47	05/17/90	1	ROUND	39.0	3.7	7.0	9.4	5	16	2.4	0.25
28	48	05/17/90	1	ROUND	31.5	2.5	2.4	7.3	0.185	0.54	1.3	0.25
29	48	07/23/90	1	ROUND	31.5	2.5	3.0	9.1	0.185	0.54	1.4	0.25
30	49	05/31/90	C	ROUND	35.0	3.0	4.6	28.7	0.7	1.6	5.0	1.0
31	52	10/24/90	1	ROUND	83.0	3.2	5.2	20.5	0.28	0.46	3.5	1.0
32	52	10/25/90	1	ROUND	83.0	3.2	6.2	26.0	0.28	0.46	4.0	1.0
33	52	04/22/92	1	ROUND	83.0	3.2	4.3	19.1	0.28	0.46	2.7	1.0
34	52	10/25/90	2	ROUND	83.0	3.2	7.1	30.5	0.28	0.46	3.5	1.0
35	52	04/22/90	2	ROUND	83.0	3.2	5.5	27.5	0.28	0.46	5.0	1.0
36	53	05/03/89	2	ROUND	41.0	2.0	5.2	5.5	72	170	1.6	1.0
37	53	05/07/89	3	ROUND	41.0	2.0	5.3	5.0	72	170	1.2	1.0
38	53	04/22/92	3	ROUND	41.0	2.0	8.5	8.6	72	170	2.5	1.0

measurement could not be obtained upstream of the pier, velocities were measured on either side of the pier and averaged. A local reference channel bed elevation was determined for each local scour measurement. This is the bed level to which flow depth was measured and the level beneath which scour depth was measured. This reference surface is the ambient bed level around the scour hole, that represents the expected bed level in the measured flow conditions if the pier were absent. Bed-material samples were collected to characterize the channel reach, rather than the scour hole sediments. Measured scour depths range from 1.0 to 25.1 feet for the data set.

Contraction and local scour processes can occur under clear-water or live-bed conditions. Clear-water conditions occur when transport of bed material into the channel section at the bridge crossing is negligible. Live-bed conditions occur when transport of bed material into the channel section at the bridge crossing is not negligible. It is important to identify the condition in which the scour is occurring because both the rate at which scour develops over time and the relation between scour depth and approach flow velocity depend upon whether clear-water or live-bed conditions predominate (Shen and others, 1969).

Surficial bed-material movent usually does not begin suddenly at a critical or incipient condition. However, the transition from negligible (clear-water) to significant (live-bed) bed-material transport conditions will be centered over some critical shear stress condition. Shield's diagram is often used to estimate the critical shear stress at which bed particles just begin to move. Neill (1968) presented an equation based on Shield's diagram to compute the critical, channel mean velocity for the incipient motion of large particles, on which viscous boundary forces are not significant. On Shield's diagram, the dimensionless shear stress for this fully-turbulent condition is constant at 0.060 at grain Reynold's numbers greater than about 600. Neill and others have noted that marginal transport of bedload occurs at much lower dimensionless shear stress values. Andrews and Smith (1992) observed that bedload transport of individual particles by rolling (rather than saltating) occurs over a range of dimensionless shear stress between 0.020 and 0.060 and state that gravel transport is not significant in this range. Neill (1968) suggests that his equation may be applicable for dimensionless shear stress values greater than 0.03.

The Neill equation is probably a reasonable indicator of bed-load transport condition for the flow conditions of the scour measurements used in this investigation. Neill's (1968) equation for the critical velocity of incipient motion, in a slightly modified form as presented in "HEC-18: Evaluating Scour at Bridges" (Richardson and others, 1993), is:

$$V_c = 1.58\,[(S_s-1)g\,D_{50}]^{\frac{1}{2}}\,(y/D_{50})^{\frac{1}{6}} \quad (1),$$

where

V_c	is	critical velocity for incipient motion of the median (D_{50}) grain size of bed material;
S_s	is	specific gravity of bed material;
y	is	depth of flow; and
D_{50}	is	median grain size of bed-material.

The data base of 384 measurements presented by Landers and Mueller (1995) contains 266 measurements made on the upstream side of piers aligned to the flow, and 38 of these were made at velocities greater than or equal to 1.5 times Neill's critical shear velocity.

Description of Selected Bridge Pier Scour Equations

A literature review of bridge scour equations by McIntosh (1989) found more than 35 equations that have been proposed for estimating the local scour at bridge piers. Five equations were evaluated for this investigation. A consistent notation for variables is used for presentation and discussion of the equations in this report; consequently, the notation used here may not be identical to the notation in the references cited. The variables are defined in the text the first time they are introduced. If an equation is not dimensionless, the units are defined with the equation in which they are required.

Chinese Equation

Gao and others (1992) presented scour equations that have been used in China for more than 20 years by highway and railway engineers. These equations were developed from laboratory and field data for both live-bed and clear-water scour at bridge piers. Gao and others (1992) define critical velocity of the bed material by a complex equation that is not repeated here, but was used in this analysis. Many hydraulic model experiments were conducted to relate the critical shear velocity in the approach section (V_c) to that in the accelerated flow region around the pier (V_c'), as a function of the pier width, b, and the mean

bed-material size (D_m). Data from these experiments were analyzed using multiple regression analysis to develop the following relation:

$$V_c' = 0.645\left(\frac{D_m}{b}\right)^{0.053} V_c \qquad (2),$$

with units of V_c' in meters per second, and b and D_m in meters.

Equation 2 indicates that the accelerated flow velocity will be about 1.5 to 3 times the approach flow velocity, depending on the ratio of bed-material size and pier width. Gao and Xu (1989) used V_c' in defining the following dimensionless variable to account of the influence of flow intensity on local pier scour depth (y_{sp}):

$$y_{sp} \sim \left(\frac{V_o - V_c'}{V_c - V_c'}\right) \qquad (3).$$

Gao and Xu (1989) found scour depth to vary with this flow intensity variable in a linear relation for clear-water conditions, and in and exponential relation for live-bed conditions. In analyses of model experiment data in China, scour depth was found to relate weakly to flow depth (y_o) and bed-material size to exponents of 0.15 and -0.07, respectively. The relation of scour depth and pier width was defined using pier width with an exponent of 0.6. These relations were used to derive an equation that includes a coefficient for pier shape and flow alignment (K_ξ) that is difficult to evaluate. Gao and others (1992) defined a simplified pier shape coefficient and developed two simplified equations for clear-water and live-bed conditions. The simplified scour equation for live-bed conditions, referred to here as the "Chinese" equation is defined as:

$$y_{sp} = 0.65 K_s b^{0.6} y_o^{0.15} D_m^{-0.07}\left(\frac{V_o - V_c'}{V_c - V_c'}\right)^c \qquad (4),$$

where

K_s is the simplified pier shape coefficient defined as 1.00 for cylinders, 0.8 for round nose piers, and 0.66 for sharp nose piers;

D_m is the mean bed-material size, (estimated as the D_{50} value for this analysis; and y_{sp}, y_o, b, and D_m have units of meters.

The exponent c in equation 4 for live-bed conditions is computed using the following equation which was derived from a regression analysis of 212 groups of field data for live-bed scour conditions:

$$c = \left(\frac{V_c}{V_o}\right)^{9.35 + 2.23 \log D_m} \qquad (5),$$

with units of meters for D_m.

Hydraulic Engineering Circular 18 (HEC-18)

The Federal Highway Administration report "Hydraulic Engineering Circular 18 (HEC-18): Evaluating Scour at Bridges" (Richardson and others, 1993) presents the following equation that was developed at Colorado State University using a compilation of laboratory data for scour at circular piers.

$$\frac{y_{sp}}{y_o} = 2.0 K_1 K_2 K_3\left(\frac{b}{y_o}\right)^{0.65} F_o^{0.43} \qquad (6),$$

where

K_1 is a coefficient based on the shape of the pier nose (1.1 for square-nosed piers, 1.0 for circular- or round-nosed piers, 0.9 for sharp-nosed piers, and 1.0 for a group of cylinders);

K_2 is a coefficient based on the ratio of the pier length to pier width (L/b) and the alignment of the approach flow to the bridge pier; and

K_3 is a coefficient based on the channel bed conditions.

With the exception of the K_3 factor, equation 6 is the Colorado State University equation, as presented in "Highways in the River Environment" (Richardson, and others, 1990) and elsewhere. The channel bed condition coefficient, K_3, is defined in the following table:

Bed Condition	Dune Height	K_3
Clear-water scour	N/A	1.1
Plane bed or antidunes	N/A	1.1
Small dunes	0.6 to 3.0m	1.1
Medium dunes	3.0 to 9.1m	1.1 - 1.2
Large dunes	> 9.1m	1.3

Solving equation 6 for y_{sp} results in the "HEC-18 equation", defined here as:

$$y_{sp} = 2.0\,K_1\,K_2\,K_3\,b^{0.65}\,y_o^{0.35}\,F_o^{0.43} \qquad (7).$$

Consistent metric or British units may be used in the HEC-18 equation.

Froehlich Equation

Froehlich (1988) compiled field measurements of local scour at bridge piers from the reports of several investigations. All of the data sets were assumed to represent scour depth at equilibrium sediment transport conditions. Froehlich (1988) analyzed only measurements that appeared to have been made in live-bed conditions based on the critical mean-velocity relation presented by Neill (1968). Froehlich selected dimensionless variables and used linear regression analysis of these live-bed data to develop the following equation:

$$y_{sp} = 0.32\,b\,\phi\,F_o^{0.2}\left(\frac{b_e}{b}\right)^{0.62}\left(\frac{y_o}{b}\right)^{0.46}\left(\frac{b}{D_{50}}\right)^{0.08} \qquad (8)$$

where

b_e is the width of the bridge pier projected normal to the approach flow; and

ϕ is a coefficient based on the shape of the pier nose (1.3 for square-nosed piers, 1.0 for round-nosed piers, 0.7 for sharp-nosed piers).

This which will be referred to as the "Froehlich equation". The predicted scour using equation 8 is less than or equal to the measured scour for one-half of the data set from which it was developed; because it was developed using least-squares regression. A design scour depth, for which the predicted scour is greater than the measured scour for all cases in the data set, can be computed as the sum of the pier width (b) and y_{sp} from equation 8. Froehlich (1988) recommended, for design purposes, that the depth of scour computed by equation 9 be increased by the width of the pier. This will be referred to as the "Froehlich Design equation". Consistent metric or British units may be used in the Froehlich equations.

Larras

Larras (1963) compiled scour data from field investigations of several French rivers and scale-model investigations and developed the "Larras" equation:

$$y_{sp} = 1.42\,K_{S2}\,b^{0.75} \qquad (9),$$

where

K_{S2} is a coefficient based on the shape of the pier nose (1.0 for cylindrical piers and 1.4 for rectangular piers); and y_{sp} and b have units of feet.

The Larras equation is a function of pier width and shape only. Because Larras's field measurements were only point measurements of scour depth made after a flood had passed, those data may not represent the depth of equilibrium scour (Shen and others, 1969).

Shen-Maza

Shen and others (1969) analyzed the pier Froude number (F_p), described in Maza and Sanchez (1964), as an explanatory variable for scour depth. They found that for pier Froude numbers less than 0.2 and fine sands (D_{50} < 0.52mm), the depth of scour increased rapidly as the pier Froude number increases. However, for pier Froude numbers greater than 0.2 and coarser sands, the depth of scour increased only moderately for increases in the pier Froude number. From that analysis, Shen and others (1969) developed two equations, referred to as the "Shen-Maza" equations. For the data set of this analysis, all of the (F_p) values are greater than 0.2, and the applicable equation is defined as:

$$y_{sp} = 3.4\,b\,F_p^{0.67} \quad for \quad F_p > 0.2 \qquad (10);$$

where

F_p is the pier Froude number, defined as $\frac{V_o}{\sqrt{gb}}$;

and y_{sp} is in feet.

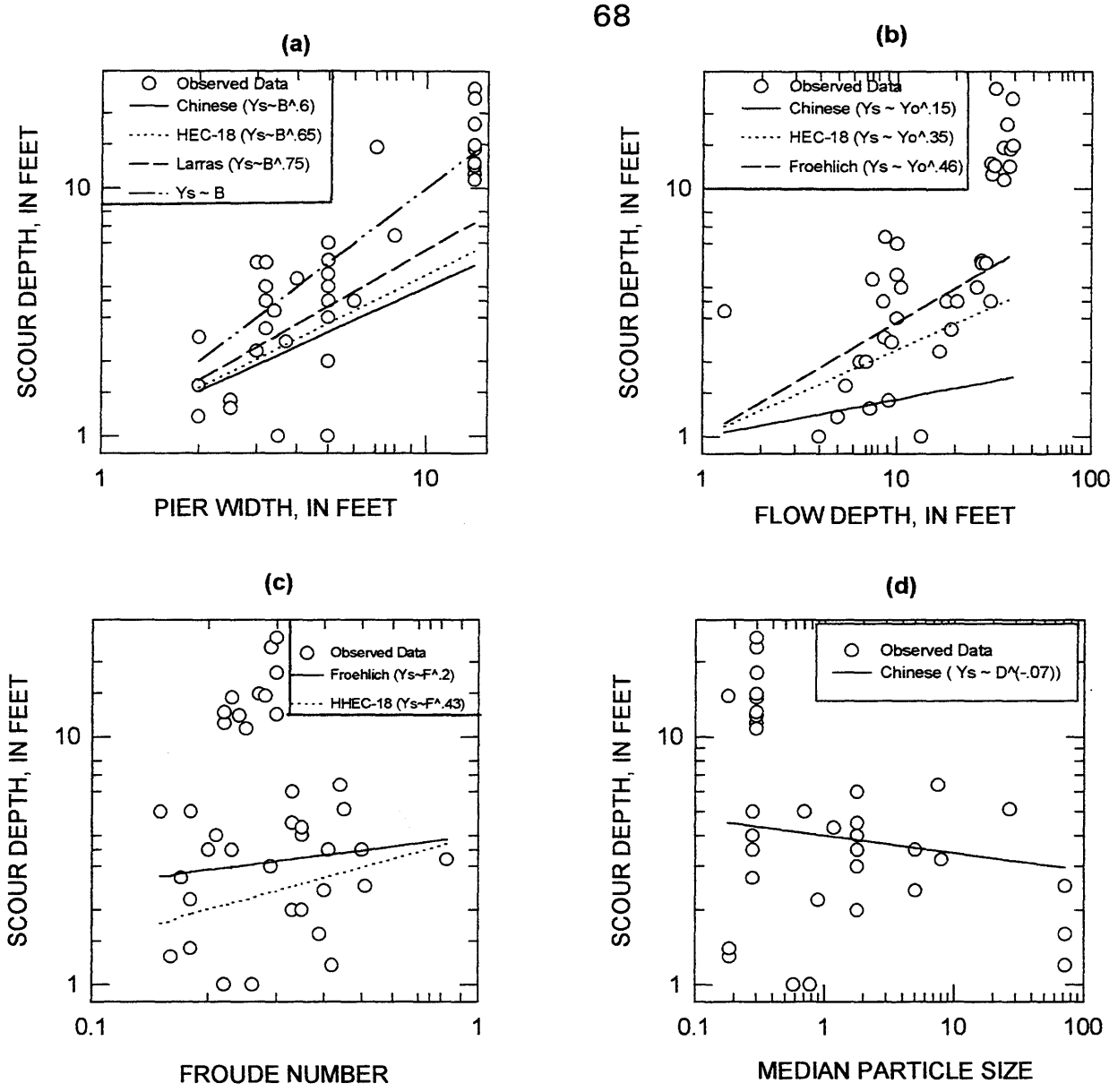

Figure 1- Relation of pier scour depth to selected explanatory variables for 38 scour measurements and for selected equations.

Evaluation of Selected Bridge Pier Scour Equations

Deterministic Relations Implied By Explanatory Variables

All of the selected equations were developed empirically, using some form of curve fitting. However, these empirically derived functions imply, and were developed in light of, deterministic relations between explanatory variables and scour depth. This discussion will consider these deterministic relations that, as they are better understood, provide the basis for improved predictive methods. Selected explanatory variables are plotted against scour depth in Figure 1. Curves are also shown for the relation of the explanatory variable to bridge scour as defined in applicable equations (with the $\log_{10}$ slope of its exponent).

Conclusions from this evaluation must be drawn cautiously because the functional relations for the explanatory variables within each equation were developed interdependently (with the exception of the Larras equation). For example, the HEC-18 and Froehlich equations contain both flow depth and

Froude number, and the implied relation with scour depth for each of these variables may be affected by their interdependence (correlation). Similarly there is correlation between flow depth and pier width, simply because wide piers are more typical of large, deep streams. With this caution in mind, the evaluation of deterministic relations implied by these equations helps us see how the variables 'explain' the scour quantitatively.

Pier Width Effects

The effective pier width is probably the most influential deterministic parameter for local pier scour, and estimated scour varies directly with pier width in many design equations. Measurements at piers skewed to the flow alignment were not selected for this investigation, so that the effects of other variables could be analyzed more directly. Figure 1(a) illustrates the relation between pier width and local scour depth for the 38 measurements of this investigation. These variables have a more linear relation when $\log_{10}$ transformed. The Pearson linear correlation coefficient for scour depth and effective pier width is 0.87 for the untransformed variables.

The slope of the relation shown in figure 1(a) indicates that the influence of pier width on scour depth is linear in logarithmic space and thus is decreasing at a slow, linear rate in untransformed space. The slope of the relation for the observed data generally appears steeper than the relation described in the equations. The local pier scour equation in HEC-18 includes pier width to the 0.65 power. Larras' local scour equation is a function of pier width to the 0.75 power, and the Chinese scour equation includes pier width to the 0.6 power. Froehlich nondimensionalized his analysis using pier width, however his equation may be rearranged to bring *b* into a single factor to the power of 0.62. The $\log_{10}$ slope of this relation was about 0.77 in the analysis by Landers and Mueller (1995) of 384 scour measurements. The apparently steeper sloped relation in this data set may imply that pier width is more significant for measurements where the flow is aligned and (or) the flow intensity is high.

Maximum y_{sp}/b values of 2.4 and 3.0 are suggested for Froude numbers in the range less than and greater than 0.8, respectively in HEC-18 (Richardson and others, 1993). The pier scour design method presented by Melville and Sutherland (1988) is based upon a maximum scour depth of 2.4 pier diameters for a cylindrical pier, which is then modified by coefficients that account for other scour variables. The maximum y_{sp}/b for the 212 live-bed scour measurements presented by Gao Dong Guang and others (1992) is 3.1. The maximum y_{sp}/b for the set of 384 measurements presented by Landers and Mueller is 2.6 and the maximum ratio for this data set is 2.1 for measurement number 10. These maximum y_{sp}/b values are useful 'rules of thumb' for bridge design engineers.

Flow Depth Effects

The effect of approach flow depth on local scour depth has been somewhat disputed in previous literature. Laursen and Toch (1956) stated that the principal hydraulic parameter affecting scour is the flow depth and not velocity. Shen and others (1969) found the effect of flow depth on equilibrium scour depth to be very slight. More recent laboratory studies for clear-water scour have found the influence of scour depth to be significant only for depth to pier width ratios (y_o/b) less than about 3 (Raudkivi and Ettema, 1983). At these smaller y_o/b ratios scour reportedly increases with increasing flow depth because of decreasing interference of the surface bow wave with the horseshoe vortex at the base of the pier. In the design method presented by Melville and Sutherland (1988), local scour is computed using a flow depth correction factor when y_o/b is less than 2.6 and is computed independent of flow depth where y_o/b is larger than 2.6.

Analysis of the effect of flow depth (y_o) on scour (y_{sp}) is difficult with field data because the flow depth is closely related to measured velocity and to pier width. Figure 1(b) illustrates the relation between y_o and y_{sp}, which has a linear correlation of 0.79 for the measurements used in this evaluation. The Chinese pier scour equation includes flow depth to the 0.15 power. The local pier scour equations in "HEC-18: Evaluating Scour at Bridges" (Richardson and others, 1993), and Froehlich (1986) include factors of flow depth to the power of 0.35 and 0.46, respectively. The trend of the observed data in figure 1(b) is clearly steeper than that of the predictive equations.

The effects of flow depth are often analyzed using y_o/b and y_{sp}/b so that scour depth is normalized for the effect of pier width and the factors are nondimensional. This is particularly desirable when working with scale model data where scale effects are a concern. The relation of y_o/b and y_{sp}/b has a $\log_{10}$ slope close to 0.4 for the observed data which tends to verify the exponents used in the Froehlich and HEC-18 equations.

This discussion implies that either the selected equations significantly underestimate the slope of this relation, or that it is important to normalize scour depth by pier width and nondimensionalize flow depth. This author believes the latter conclusion to be correct. The relations of y_o/b to y_{sp}/b and of y_o to y_{sp} for the observed data have $\log_{10}$ slopes less than 1., indicating that flow depth has a decreasing effect on scour depth in linear space. However, neither relation indicates that flow depth ceases to influence scour at some critical y_o/b ratio.

Flow Intensity Effects

Flow intensity influences the local scour because it effects the initiation and rate of bed-load transport, and the hydraulic pressure field, downward velocity, and vortices generated around the pier. Several researchers (Neill, 1964; Bruessers and others, 1977; and others) have found that scour depth increases with increasing flow velocity to a maximum value near threshold sediment transport conditions, then decreases slightly and tends toward an equilibrium scour depth that is independent of further increases in flow velocity. The data used in this analysis were measured under live bed conditions, with ratios of measured velocity to estimated critical shear (threshold) velocity greater than 1.5. Thus, it is not surprising that no relation was found between scour depth and velocity (or velocity squared) for these data.

The selected equations use three different variables to explain the effect of flow intensity on scour depth. The Chinese equation uses a ratio of approach velocity to the threshold velocity, adjusted for the effect of local flow acceleration around the pier. The Shen-Maza equation uses an interesting factor referred to as the 'pier Froude number', and computed as described previously. The Froehlich and HEC-18 equations used Froude number to account for flow intensity. Space in this report does not permit a detailed evaluation and comparison of these factors. However, we may note that Froude number does not appear to be a good explanatory variable, as indicated in Figure 1(c). It is somewhat surprising that Froude number was selected as a measure of flow intensity, since it is actually a ratio of inertial to gravitational forces, both of which appear to be positively related to scour depth.

Sediment Size Effects

The principal effect of sediment size on local scour is it's influence on the initiation and rate of bed-material transport. That effect is evaluated in computations of critical velocity for incipient motion. In laboratory investigations reported by several researchers (Raudkivi and Ettema, 1983; Chiew & Melville, 1987) equilibrium scour depth has been shown to decrease with increasing bed-material size, at pier width to median sediment size ratios (b/D_{50}) less than about 50, for both clear-water and live-bed conditions. According to these researchers, larger particles reduce the local scour because they more effectively dissipate the energy of the downward flow velocity where it intersects the bed, and because they are physically large with respect to the groove eroded by the downward velocity where it intersects the bed at the base of the pier. Chiew and Melville (1987) showed that y_{sp}/b increases with logarithmic b/D_{50} in a nearly linear relation up to a b/D_{50} value of about 50.

The effect of sediment size on local scour depth is not directly accounted for in most scour prediction formulas. Melville and Sutherland's (1988) design method uses a sediment size factor computed as a function of $\log(2.24(b/D_{50}))$. Froehlich (1988) used the ratio of pier width to median sediment size in his local scour regression analysis and computed an exponent of 0.08 for this ratio. Gao and others (1992) use a sediment size correction of D_{50} (or average D) to the -0.07 power, based on regression analysis of 40 field measurements of local scour under clear-water conditions. The results for the Chinese equation are similar to those of Froehlich, and are shown in Figure 1(d). The observed data plotted in Figure 1(d) do not clearly indicate a relation, however only 4 of the 38 measurements plotted in this figure had b/D_{50} values less than 1000.

The lack of correlation between sediment size and scour depth for this data set is inconclusive. The absence of a clear relation may be because bed-material sampling methods are typically designed to characterize the general stream channel and, as such, may not represent the scour hole sediments, although the two are typically similar. Observations and limited sampling of sediments both in local scour holes and in the channel indicate that differences may exist, with larger particles being found in the scour hole (Landers and Mueller, 1995). Larger particles may accumulate in a scour hole because it requires more energy to roll these particle upslope and out of the scour hole than along the bed (effectively increasing the critical shear stress at this location).

Comparison of Observed and Computed Scour

The criteria for evaluating equations using comparisons of computed and observed (measured) scour depths should not be based on minimized errors of estimate for most pier scour equations. Most of the selected equations were not developed to predict observed scour, but to estimate the maximum probable scour for a given set of conditions for design applications. Design curves and equations are generally developed to not underestimate the data, so that there is a bias for negative residual errors (observed minus computed scour). The Froehlich equation (but not the Froehlich Design equation) is an exception because it was developed from least-squared error regression analysis. Equations that accurately estimate the maximum depth of scour and rarely underestimate the scour will be preferred for most design applications. Methods that could predict observed scour for the broad range of measurement conditions would probably be more complex than those reviewed here and would include methods to account for the time-dependent scour processes such as soil erodibility.

The predictive performance of the selected equations is illustrated in the scatter plots of Figure 2, and in box plots of the ratios of computed scour to observed scour in Figure 3. All of the equations frequently computed scour that was at least twice the observed depth of scour and occasionally some computed scour that was more than 5 times the observed values. Only the Shen-Maza equation did not under predict the scour depth for any of the measurements. The HEC-18 equation under predicted the scour depth for only 2 of the measurements, and the Froehlich design equation for only 3. The Chinese and Larras equations significantly under predicted all of the scour depth measurements greater than about 10 feet (Figure 2.) None of the equations consistently computed a depth of scour that closely matched the observed depth of scour for the measured conditions, as illustrated in Figure 2. Figures 2 and 3 indicate that the HEC-18, Froehlich Design, and Shen-Maza equations predicted the observed scour more closely than did the other selected equations. These equations also were less likely to under predict the observed scour, which is important for the purposes of design.

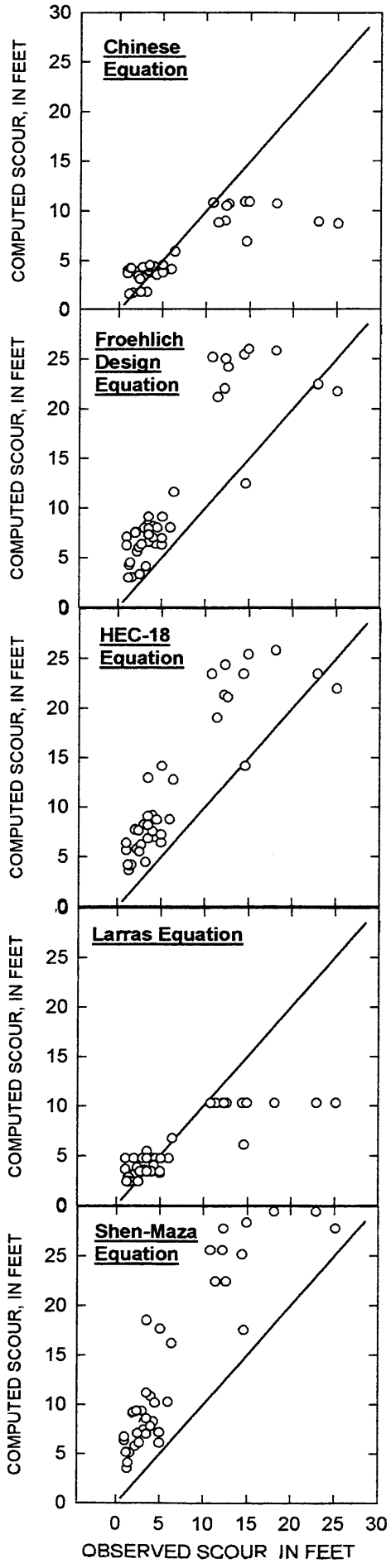

Figure 2 - Plot of observed and predicted pier scour depths for five design equations.

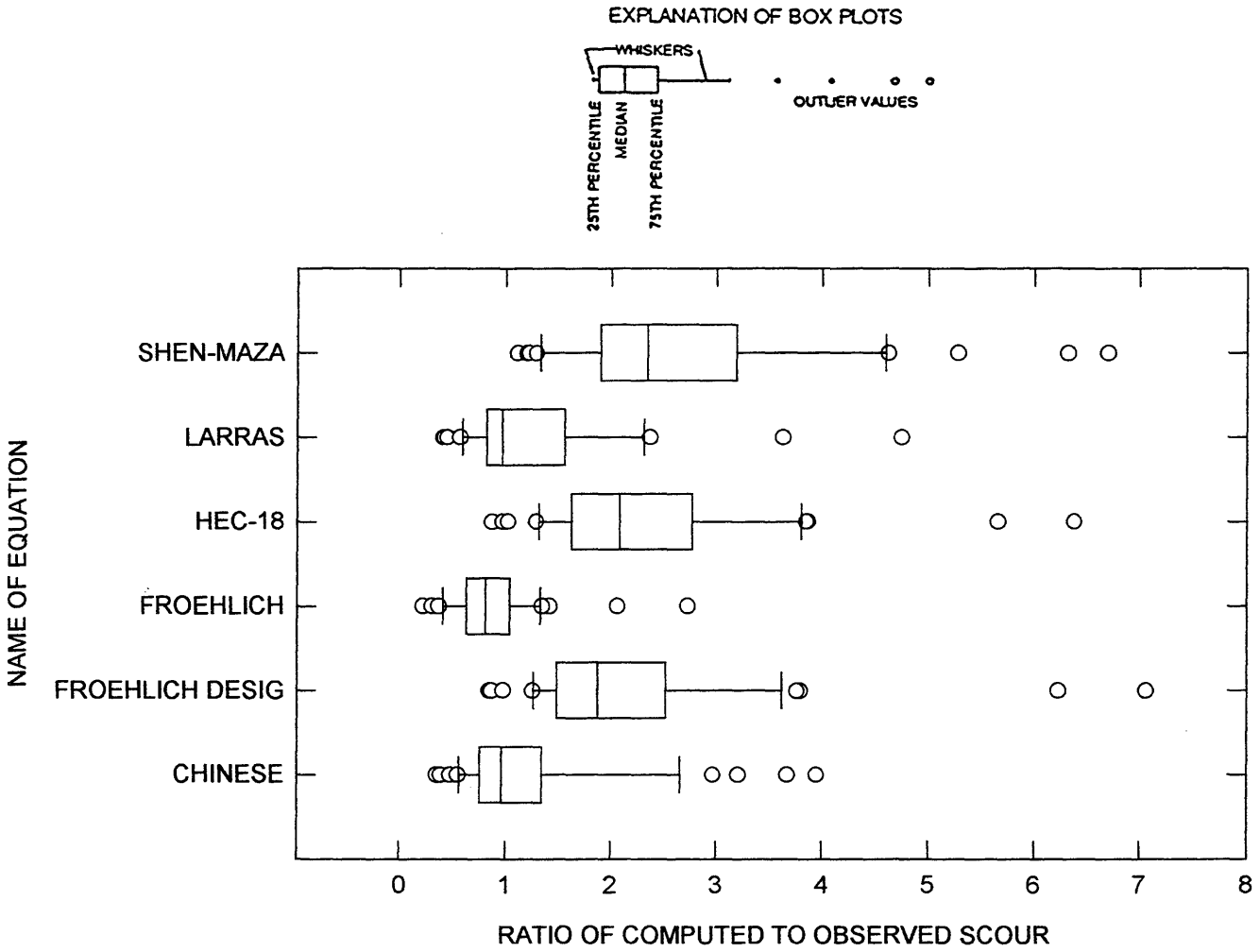

Figure 3 - Raito of computed to observed scour for six equations evaluated in this report

Summary

The processes of river channel scour at bridge foundations are complex and interrelated. Selected pier scour prediction equations are evaluated and compared in this study, using 38 field measurements of bridge pier scour made during active bed-load transport conditions during floods where the flow was aligned to the piers. These measurements all had velocities greater than 1.5 times the incipient motion velocity for the D_{50} particle size, as computed using Neill's (1968) method. Measured scour depths range from 1.0 to 25.1 feet for the data set.

Scour processes and the variables of selected equations are evaluated in relations of scour depth to individual explanatory variables. However, these processes are typically dependent on multiple, interrelated variables, so that the relation between scour depth and a single variable may have several curves that represent data subgroups defined by the values of a third variable. Scour depth and pier width have an approximately linear relation in logarithmic space, with a slope between about 0.65 and 0.8. The maximum ratio of scour depth to effective pier width for the data of this study is 2.1.

The influence of flow depth on scour appears to decrease at a uniform rate over the range of measured data, but does not become insignificant at large ratios of flow depth to pier width, which contradicts the findings of several laboratory investigations. The relation of scour depth and flow depth, where both variables are normalized for effective pier width, is

approximately linear in logarithmic space and has a slope between about 0.4 and 0.5. Measured scour depths appear independent of flow intensity for these live-bed conditions. The field data do not indicate any direct influence of sediment size on scour depth; however, this may be due to differences between the sampled bed-material and bed-material in the scour hole.

Comparison of computed and observed depths of scour showed that none of the selected equations accurately estimate the depth of scour for all of the conditions measured. As conservative design equations the HEC-18, Froehlich-Design, and Shen-Maza equations performed well; however they often over estimated the scour by large amounts, which would result in over-designed bridge foundations. The Larras and Chinese equations fit the data reasonably well for observed scour depths less than 10 ft, but significantly under estimate the depth of scour for observed depths of scour greater than 10 ft.

Additional field research, data collection, and data analysis are needed to understand and model the complex interrelated processes responsible for scour at bridges. Analysis and modeling of these processes will provide improved understanding of scour processes and contribute to the reliability and economy of bridge foundation designs that benefit the traveling public.

References

Andrews, E.D., and Smith, J.D., 1992, A theoretical model for calculating marginal bedload transport rates of gravel: *in* Dynamics of Gravel-bed Rivers, eds. Billi, P., Hey, R.D., Thorne, C.R., and Tacconi, P., John Wiley and Sons, Ltd, p. 41-52.

Breusers, H.N.C., Nicollet, G., and Shen, H.W., 1977, Journal of Hydraulic Research, v. 15(3), p. 211-252.

Chiew, Y.M., and Melville, B.W., 1987, Local scour around bridge piers: Journal of Hydraulic Research, v. 25(1), p. 15-26.

Froehlich, D.C., 1988, Analysis of on-site measurements of scour at piers, *in* Abt, S. R. and Gessler, Johannes, eds., Hydraulic Engineering--Proceedings of the 1988 National Conference on Hydraulic Engineering: New York, American Society of Civil Engineers, p. 534-539.

Gao Dong Guang, Posada G., Lilian, and Nordin, C.F., 1992, Pier scour equations used in the People's Republic of China; Colorado State University, Department of Civil Engineering, Draft.

Gao Dong Guang and Xu Guoping, 1989, Research on local scour mechanism of piers and revision of equations; Research report revision of Code of Investigation and Design of Highway Bridge Crossings in China, Xian Highway Transport University (in Chinese).

Landers, M.N., and Mueller, D.S., 1995, *(in press)* Channel Scour at Bridges in the United States: Federal Highway Administration, Publication FHWA-IP-95-xxx 94p.

Landers, M.N., Mueller, D.S., and Trent, R.E., 1993, Instrumentation for detailed bridge-scour measurements, *in* Shen, H.W., Su, S.T., and Wen, Feng, eds., Hydraulic Engineering '93: New York, American Society of Civil Engineers, p. 2063-2068.

Larras, Jean, 1963, Profondeurs maxmales d'erosion des fonds mobiles autour des piles en riviere [maximum depth of erosion in shifting bed around river piles]: Paris France, Annales des ponts et chaussees, v. 133, no. 4, p. 411-424.

Laursen, E.M., 1960, Scour at bridge crossings: Journal of the Hydraulics Division, American Society of Civil Engineers, v. 86, no. HY2, p. 39-54.

Laursen, E.M., and Toch, A., 1956, Scour around bridge piers and abutments: Iowa Highway Research Board, bulletin no. 4, Iowa Institute of Hydraulic Research, 60 p.

Maza Alvarez, J.A. and Sanchez Bribiesca, J.L., 1964, Contribucion al estudio de la socavacion local en pilas de puente: Porta Alegre, Brazil Universidade Federal do Rio Grande do Sul, August.

McIntosh, J.L., 1989, Use of scour prediction formulae, in Proceedings of the Bridge Scour Symposium: Federal Highway Administration Publication FHWA-RD-90-035, p. 78-100.

Melville, B.W. and Sutherland, A.J., 1988, Design method for local scour at bridge piers: Journal of the Hydraulics Division, American Society of Civil Engineers, v. 114, no. 10, p. 1210-1225.

Neill, C.R., 1968, Note on initial movement of coarse uniform bed material: Journal of Hydraulic Research, International Association of Hydraulic Research, v. 27, p. 247-249.

Neill, C.R., 1964, River-bed scour: Research Council of Alberta Contribution No. 281, Canadian Good Roads Association, 37 p.

Raudkivi, A.J., and Ettema, Robert, 1983, Clear-water scour at cylindrical piers: Journal of the Hydraulics Division, American Society of Civil Engineers, v. 109, no. 3, p. 338-350.

Richardson, E.V., Harrison, L.J., Richardson, J.R., and Davis, S.R., 1993, HEC-18: Evaluating Scour at bridges: Federal Highway Administration Hydraulic Engineering Circular 18, Publication FHWA-IP-90-017, revised April 1993, 238 p.

Richardson, E.V., Simons, D.B., and Julien, P.Y., 1990, Highways in the river environment: Federal Highway Administration Publication FHWA-HI-90-016, 719 p.

Shen, H.W., Schneider, V.R., and Karaki, Susumu, 1969, Local scour around bridge piers: Journal of the Hydraulics Division, American Society of Civil Engineers, v. 95, no. HY6, p. 1919-1940.

Shirole, A.M., and Holt, R.C., 1991, Planning for a comprehensive bridge safety assurance program: Transportation Research Record 1290.

CE 717 Project
Judith D. Sunantara
Spring 1995

REVIEW ON BRIDGE ABUTMENT SCOUR FORMULAS

Abstract

Abutment scour computation methods are presented. Abutment scour case of Razor Creek Bridge at Montana is taken for an example. The abutment scour depth is computed using several methods. Comparison between the calculated scour depths and the observed one is also presented as well as the comparison of the result of each computation method.

Introduction

The problem of scour at bridge is the most common cause of bridge failure. Research on scour began in the early 1900s with efforts concentrating on understanding the mechanics of scour. Started in early fifties, research efforts focussed on developing equations to predict maximum scour depth for design purposes. Researches on this matter has been going on since then, resulted in more than 30 scour prediction equations, developed based on laboratory tests and field data observations for various conditions.

This paper will concentrate only on abutment scour. The most widely used equations will be reviewed and applied to the case of bridge scour of Razor Creek Montana. The 100 year design flood had been exceeded twice (1988 and 1991), resulted in significant scour around the piers and abutment. In this paper, the scour depth will be calculated using several different methods.

Most of the equations for estimating local abutment scour at bridges are based on physical model studies in laboratory flumes. Unfortunately, existing laboratory model studies for predicting local abutment scour have deviated significantly from typical field conditions. All of existing laboratory data for abutment scour has been conducted by extending an abutment of known length into a shallow flow on a flat sand bed as shown in Figure 1. It is obvious that the approaching flow is essentially uniform, that is, lateral velocity profile is nearly the same at all locations across the flume. In laboratory condition, most of the overbank flow is forced to return to the bridge opening. As a result, two component of velocities converge near the end of abutment, creating turbulence and vortex which cause local scour at the abutment.

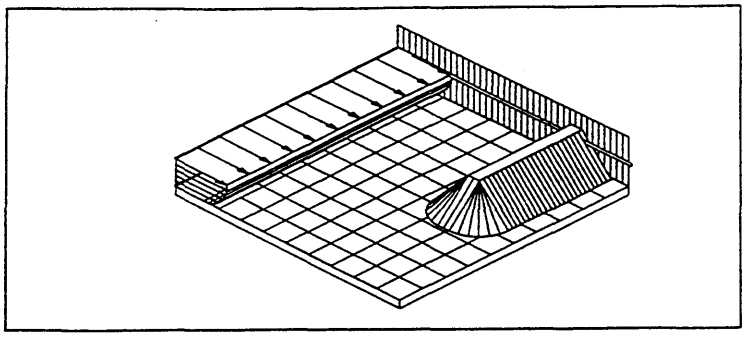

Fig. 1 Typical Laboratory Conditions for Abutment Scour Tests (after Richardson and Richardson 1993)

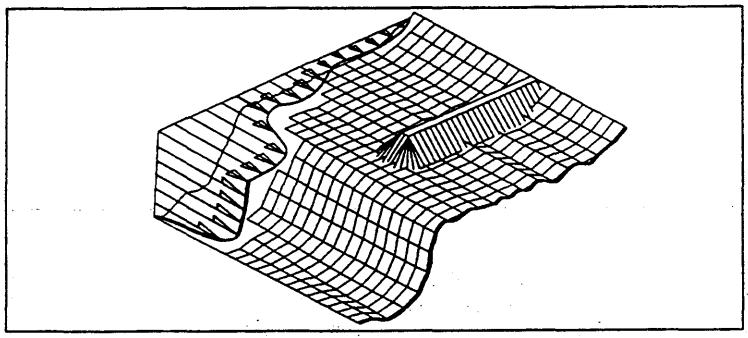

Fig. 2 Typical Field Conditions (after Richardson and Richardson 1993)

The most common real field condition is shown in Figure 2. It can be seen that abutment intercept flow on the floodplain where overbank flow is not uniformly distributed. As a result, the overbank flow which is returned to the bridge opening creates less vortex and turbulence. In the actual field condition, flow on the floodplain is also inhibited by vegetation, structures, and other features which tend to slow the overbank flow.

The actual characteristics of field conditions have not been represented by laboratory models. Because of these differences, predictive abutment scour equations result in excessive scour depths. In the following sections, several abutment scour formulas will be discussed.

General Framework for Abutment Local Scour Analysis

There are three ways of abutment scour formula development. The first one is the dimensional analysis, the second one is the sediment transport formula utilization, and the last one is regression analysis.

Hydraulically, there are two types of abutment scour equations, clear-water condition equations, and live-bed condition equations. Which one to be used depends on the ratio between actual shear stress and critical shear stress. If this ratio is larger than one, live-bed equations should be used. The main difference between live-bed and clear-water scour depth equations is, live-bed equations were developed by measuring the equilibrium scour depth, which is smaller than its maximum value (30% is recommended to be used for safety factor), while clear-water equations were developed by measuring the maximum scour depth, so we do not need to apply any safety factor. In general, maximum scour depth for clear-water condition is about 10% larger than equilibrium scour

depth for live-bed condition with the dune formation upstream of the bridge section, and they have equal values under the plain bed condition. The maximum live-bed scour depth is 20% to 30% larger than its equilibrium value.

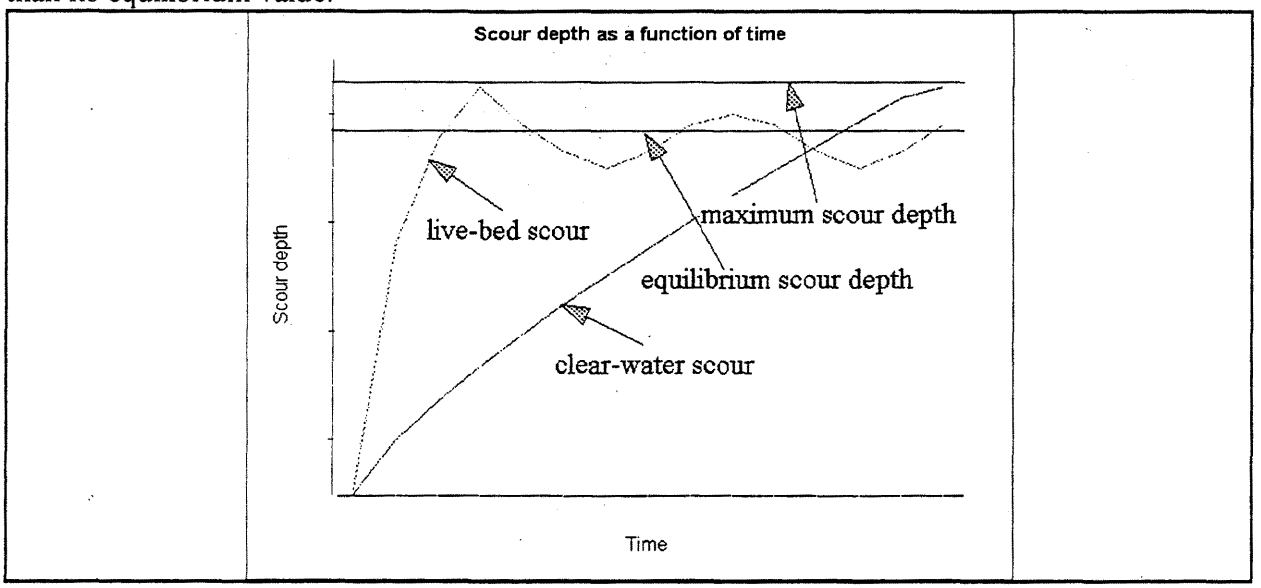

Figure 3

Another aspect that should be taken into account before choosing the equations is the abutment position. In general there are four main positions of the abutment:

- abutments projected into the channel without overbank flow
- abutments projected into the channel with overbank flow
- abutments on the flood plain with overbank flow
- abutments on the edges of the channel

It is possible that there are more than one equations applicable to the condition under consideration. In this case, we have to use all of them and make our decision based on the outcomes and other considerations such as economic and environmental considerations.

In general, under the assumption of constant relative density of sediment and the absence of viscous effects, equation for local scour at an abutment can be written as:

$$y_s = f\left(\frac{U^2}{gd_{50}}, \frac{y}{L}, \frac{d_{50}}{L}, \sigma_g, Sh, Al, G\right) \quad (1)$$

or:

$$y_s = f\left(Fr^2, \frac{y}{L}, \frac{d_{50}}{L}, \sigma_g, Sh, Al, G\right) \quad (2)$$

where:

Fr	=	Froude number
y	=	approaching flow depth
L	=	Abutment length projected to the flow
d_{50}	=	median grain size
σ_g	=	standard deviation of grain size distribution
Sh	=	shape parameter
Al	=	alignment parameter
G	=	parameter describing distribution of lateral flow and cross-sectional shape of the approach channel

In more general form, scour depth can be expressed as:

$$y_s = f(K_I.K_y.K_L.K_d.K_\sigma.K_s.K_\theta.K_G) \quad \textbf{(3)}$$

where:

K_I	=	parameter representing the effect of flow intensity
K_y	=	parameter representing the effect of approach flow depth
K_L	=	parameter representing the effect of abutment length
K_d	=	parameter representing the effect of sediment size distribution
K_σ	=	parameter representing the effect of standard deviation of sediment size distribution
K_s	=	parameter representing the effect of abutment shape
K_θ	=	parameter representing the effect of abutment alignment
K_G	=	parameter representing the effect of lateral flow distribution and cross-sectional shape of the bridge opening

In 1988, Kwan measured the velocity field around a short wing wall abutment. It was found that the primary vortex, which is analogous to horse-shoe vortex at bridge piers, is primarily responsible for scour hole development at the abutment. Furthermore he also found another similarity to bridge piers scour, that is, the flow pattern is relatively unaffected by changes in approach flow depth. Kwan's research also discovered that for short abutment scour depth scales with abutment length, on the other hand, for long abutment, scour depth scales with approach flow depth. Kwan's research has lead Melville (1992) to developing abutment scour formulas for two limiting cases, short abutment ($1 < l/y < 25$) and long abutment ($L/y > 25$).

In 1989, Froehlich developed a local abutment scour formula under clear-water condition, based on 164 laboratory experiments. In the same time, he also developed similar formula for live-bed condition based on 170 experiments. The latter is now recommended to be used for design purpose by FHWA (HEC-18, 1993).

In 1993, Melville conducted an experiment for developing formula to predict abutment scour depth, taking into account irregularity of a cross-sectional shape, by considering it as a compound channel. This model try to represent actual field condition as close as possible in order to improve the excessive scour depth prediction.

In the following sections, parameters involved in the scouring process will be explained in detail.

Abutment Shape and Alignment

The geometry of bridge abutment can be described in terms of the size of the obstruction (the length L) together with the shape factor to account for differences in shape, and the angle between the approach flow and the abutment (the alignment).

The effect of shape factor K_s is determined based on laboratory tests. The simplest abutment shape is vertical wall built perpendicular to the flow direction. This type is used as reference. It is understandable that streamlined shaped abutment s create less disturbance, hence produce less scour than blunt shapes. Therefore, all other abutment shapes have less scour depth for the same flow conditions. Figure 4 shows the most common abutment shapes and the value of K_s for these shapes is presented in Table 1

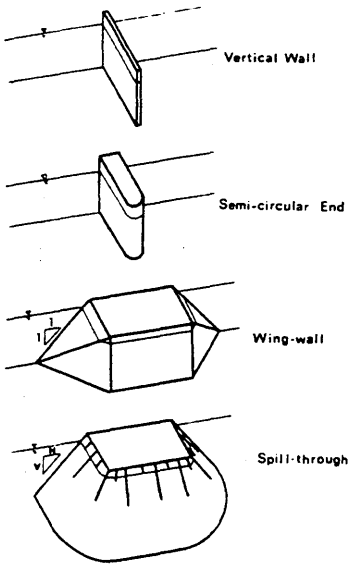

Figure 4

Table 1

Abutment Shape	Shape factor Kθ
Vertical plate or narrow vertical wall	1.00
Vertical wall with semicircular end	0.75
45° wing wall	0.75
Spill-through (H:V) :	
0.5:1	0.60
1:1	0.50
1.5:1	0.45

Abutment alignment is described by angle θ, as follows:

$$K_{(\theta)} = (\theta/90)^{0.13} \quad (4)$$

where $\theta < 90°$ abutment points downstream, and $\theta > 90°$ abutment points upstream. It has been found that generally, scour depth increase at the angle θ increase. Abutments pointed upstream are seem to produce deeper scour. On the other hand, abutments pointed downstream produce less scour depth .Most scour equations were developed for K_s and K_θ equal to 1. Therefore we need to multiply the results by appropriate value of K_s and K_θ

Sediment Size and Gradation

This paper will only deal with alluvial sediments. The simplest means of describing alluvial river sediment is the median particle size, d_{50}. For uniform material, d_{50} is adequate, for nonuniform material it is inadequate. To describe the nonuniformity of the material, parameter K_σ is used. This parameter represent the standard deviation of sediment size distribution. For standard deviation less than 1.3, the material can be treated as uniform.

Very limited data available on the effects of nonuniformity of sediment size distribution on the scour depth. For this reason, so far the nonuniformity of the sediment size effect is judge using experience and engineering judgments. Following is the review on several abutment scour depth formulas.

Liu's Formula (1961)

Based on dimensional analysis and laboratory tests, Liu et al. developed an abutment scour depth formula by referring to the Froude number of the approaching flow. For live-bed condition, his equation for equilibrium scour depth is:

$$\frac{d_s}{y_0} = 2.15\left(\frac{L}{y_0}\right)^{0.40} Fr_1^{0.33} \quad (5)$$

The experiments were based on standard abutment shape and alignment which is vertical wall perpendicular to the flow direction. To apply this formula for different abutment shape and alignment, we can use adjustment factor K_s and K_θ.

Laursen (1963)

In 1963 Laursen proposed the following implicit formula for local abutment scour depth under live-bed condition.

$$\frac{L}{y_0} = 2.75\frac{d_s}{y_0}\left[\left(\frac{d_s}{11.5y_1}+1\right)-1\right] \quad (6)$$

For clear-water condition, his equation is as follows:

$$\frac{L}{y_1} = 2.75\left(\frac{d_s}{y_0}\right)\left[\frac{\left(\frac{d_s}{11.5y_0}+1\right)^{7/6}}{\left(\frac{\tau_1}{\tau_c}\right)}-1\right] \quad (7)$$

where τ_1/τ_c is the ratio between actual shear stress and the critical Shields shear stress. In clear-water condition this ratio is less than one.

Zaghloul (1983)

In 1983 Zaghloul derived a scour depth equation under live-bed condition in terms of Froude Number based on regimes methods.

$$\frac{d_s}{y_0} = 2.62\frac{B}{B-L}Fr^{2/3} \quad (8)$$

Froehlich (1989)

In 1989 Froehlich developed scour depth formulas for clear-water and live-bed conditions based on 164 and 170 experiments, respectively. His proposed regression equation for scour under clear-water condition is as follows:

$$\frac{d_s}{y_0} = 0.78K_s K_\theta \left(\frac{L}{y_0}\right)^{0.63} Fr_0^{1.16} \left(\frac{y_0}{d_{50}}\right)^{0.43} \sigma_g^{-1.87} \quad (9)$$

in which Fr_0 and y_0 are Froude Number and depth of approaching flow, σ_g is the standard deviation of grain size distribution.

His formula for live-bed condition is now adopted by FHWA for abutment design purpose. This formula was developed based on 170 laboratory experiments.

$$\frac{d_s}{y_0} = 2.27\ K_s K_\theta \left[\frac{L}{y_0}\right]^{0.43} Fr_0^{0.61} + 1 \quad (10)$$

HIRE Equation

Another equation which is approved by FHWA is **HIRE**, developed from Corps of Engineers field data of scour at the end of spur in Mississippi River. This equation is applicable when the ratio of projected abutment length to the flow depth is greater than 25.

$$\frac{d_s}{y_0} = 4\ Fr_0^{0.33} \tag{11}$$

Melville (1992)

In 1992 Melville has summarized a large number of experimental results on abutment scour and has proposed a design method for maximum clear-water scour depth. He classified abutment as short ($L/y_0 < 1$) or long ($L/y_0 > 25$), and proposed that the maximum scour depth is 2L for short abutment and 10 L for the long one. For intermediate abutment lengths, the maximum scour depth is proportional to $(y_0L)^{0.5}$. Scour depth of $2(y_0L)^{0.5}$ is an envelope to nearly all data for $1 < L/y_0 < 25$) If we go back to Laursen Formula, choose 12 for r and using binomial approximation, Laursen's formula for maximum scour depth can be simplified to:

$$d_s \approx 1.93\ (y_0L)^{0.5} \tag{12}$$

This agrees with Melville's equation.

Abutment Scour in a Floodplain (1993)

In 1993, Sturm and Janjua completed their experiment for developing scour depth formula for flow in a floodplain. Here they introduced facto M as the ratio of flow in the approach section with a width equal to the opening width to the total approach flow (Q_0/Q). Their experiment resulted in the scour depth regression formulas, as follows:

$$d_s/y_0 = 8\ (Fr/M - 0.18) \tag{13}$$

This experiments was conducted under clear-water condition for standard abutment shape and alignment.

Modified Froehlich's equation for clear-water condition can also be used for this case,

$$\frac{Q_0}{q_{mc}y_0} = 2.75\frac{d_s}{y_0}\left[\left(\frac{d_s}{4.1y_0}+1\right)^{7/6} - 1\right] \tag{14}$$

where:

- q_{mc} is the unit discharge in the main channel, Q/W.

- Q and W are main channel discharge and width, respectively
- Q_0 and y_0 are discharge and flow depth in the flood palin, respectively

Example

As an example, depth scour of abutment of a bridge at Razor Creek Montana will be computed using all equations described above, and the results will be compared to the result of scour depth measurement.

The scour was due to flood larger than predicted 100 year flood used in design. This flood occurred in 1991 with the magnitude of 179.3 m^3/s. The drainage area is 44.3 km^2. The bridge has overall span of 22.9 m between abutments. Intermediate support is provided by two pile bents at 7.6 m spacing, each consisting of 7 timber piles. A layer of riprap with d_{50} of 0.40 mm was placed after flood in 1986 with a thickness of 0.61 m at the abutments. The stream bed has a sand and gravel layer, ranging in thickness from 1.2 to 4.44 m. Very densed, tan sandstone and weathered shale underline the sand and gravel to a depth of at least 10.7 m. A standard sieve analysis indicated the d_{10}, d_{50}, and d_{90} for the sand and gravel are 0.065 mm, 2 mm, and 20 mm, respectively.

Since there is not any data on the water level corresponds to the flood of 1991, the water level data was computed using Manning's formula for velocity. Manning's n value is 0.03. The results of computation can be seen in Tables 2 and 3.

Sensitivity analysis was carried out on the value of Manning's n and abutment length, since these variables have big role on the scour process. It is obvious that the larger value of Manning's n results in smaller value of scour depth. In practice, to obtain a larger value of Manning's n, riprap is used to minimize scour depth. However, increasing Manning's n value only decreases scour depth very slightly. On the other hand, decreasing abutment length has more effect on the scour depth.

Conclusion and recommendation

Scour depths calculated using different formulas vary widely. For this case, Liu's and Zaghloul's formulas give smaller values of scour depths compared to the observed scour depths. While other formulas give much larger values. Among others, Froehlich's formulas for live-bed condition gives the closest values of scour depths. This is because Froehlich's formula is developed based on more data than any other formulas.

As discussed earlier, until now the field condition has not been well modeled in the laboratory, as a result, many formulas give much larger scour depth estimation. This condition has to be solved in order to obtain better formulas. However, data seem to be the most important factor. More scour data have to be obtain from many different river conditions. With more data, regression results will be more reliable.

References

1. Local Scour at Bridge Abutment (Melville, B.W., Journal of Hydraulic Engineering, Vol. , pp.615-631, 1992)
2. Evaluating Scour at Bridge (Richardson, E.V., Hamilton, L.J., Richardson, J.R., FHWA Publication, HEC-18, 1993)
3. Flow and Scour Near an Abutment (Shen, H.W., Chan, C.T., Lai, J.S., Zhao, D., Hydraulic Engineering, Vol.1, pp.743-748, 1993)
4. The Fallacy, of Local Abutment Scour Equations (Richardson, E.V., Richardson, J.R., Hydraulic Engineering, Vol. 1, pp.749-754, 1993)
5. Scour Prediction Model at Bridge Abutments (Young, G.K., Palaviccini, M., Kilgore, R.T., Hydraulic Engineering, Vol. 1, pp.755-760, 1993)
6. Bridge Abutment Scour in a Floodplain (Sturm, T.W.,Janjua, N.S., Hydraulic Engineering, Vol. 1, pp.761-766, 1993)
7.. Bridge Scour and Change at Contracted Section, Razor Creek , Montana (Holnbeck, S.R, Parrett, C., Hydraulic Engineering, Vol. 2, pp. 2249-2255, 1993)
8. Highways in The River Environment, U.S. Department of Transportation, July 1990, pp82-102

Table 2 **Velocity distribution accross the section**

Dist (m)	Wat. Lev. (m)	Bed Length (m)	Seg. Area (m^2)	Seg. Depth (m)	Seg. P (m)	Seg. R (m)	Seg. V (m/s)	Q Seg (m^3/s)
0.00	1075.51							
1.43	1075.51	1.80	4.37	2.46	3.71	1.18	0.55	2.41
2.86	1075.51	1.55	5.75	3.31	1.55	3.71	1.19	6.83
4.46	1075.51	1.63	6.80	3.76	1.63	4.16	1.28	8.72
5.83	1075.51	1.38	6.73	3.98	1.38	4.89	1.43	9.59
7.56	1075.51	1.73	7.70	4.13	1.73	4.45	1.34	10.32
10.40	1075.51	2.84	10.28	4.26	2.84	3.61	1.17	11.99
12.00	1075.51	1.60	7.75	4.31	1.60	4.84	1.42	10.99
12.95	1075.51	1.13	6.96	4.61	1.13	6.17	1.67	11.60
13.64	1075.51	0.79	6.98	5.11	0.79	8.83	2.12	14.76
14.32	1075.51	0.85	6.61	5.06	0.85	7.82	1.95	12.91
14.73	1075.51	0.51	5.49	4.66	0.51	10.82	2.42	13.30
15.00	1075.51	0.28	5.07	4.48	0.28	18.28	3.44	17.43
16.55	1075.51	1.55	7.86	4.43	1.55	5.06	1.46	11.48
17.93	1075.51	1.38	7.44	4.41	1.38	5.40	1.52	11.34
19.48	1075.51	1.56	7.62	4.31	1.56	4.87	1.42	10.85
21.18	1075.51	1.77	7.27	3.96	1.77	4.11	1.27	9.25
22.78	1075.51	1.94	5.56	3.16	4.54	1.22	0.57	3.15
Average :			116.25	4.14	28.80	4.04	1.54	179.25
							0.24	

Table 3

Scour depth computation

Channel width : 22.9 m
Manning's n : 0.03

	L (m)		Fr		V (m/s)		Y0 (m)	
	Left	right	Left	Right	Left	Right	Left	Right
Scour Depth (m):	0.493	1.267	0.111	0.101	0.552	0.567	2.455	3.155
	1.751	2.872	1.979	2.466	2.146	3.898	2.201	3.998
	Liu's		Zaghloul's		Laursen's		Melville's	
	3.188	4.349			4.761	5.921	[illegible]	[illegible]
	Froehlich's				HIRE's		Observed	

L : abutment length projected to the flow
Fr: approach Froude Number
V : approach velocity
Y0: approach depth

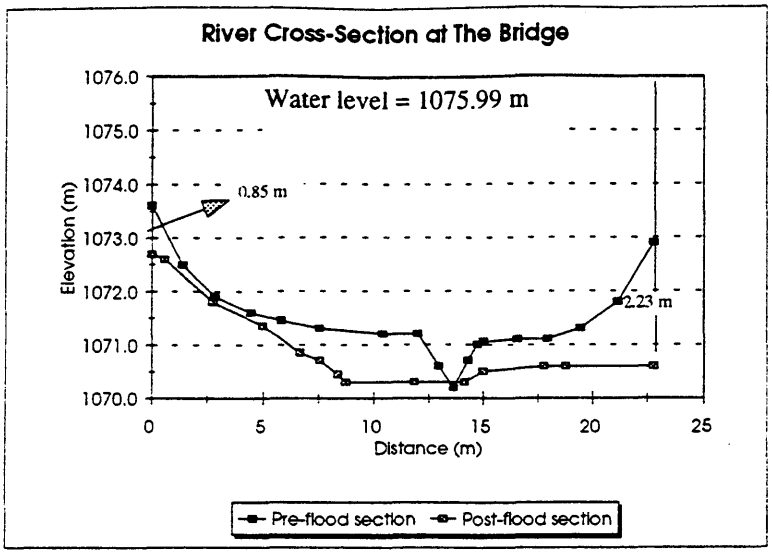
River Cross-Section at The Bridge
Water level = 1075.99 m
0.85 m
2.23 m
Elevation (m)
1076.0
1075.0
1074.0
1073.0
1072.0
1071.0
1070.0
0
5
10
15
20
25
Distance (m)
Pre-flood section
Post-flood section

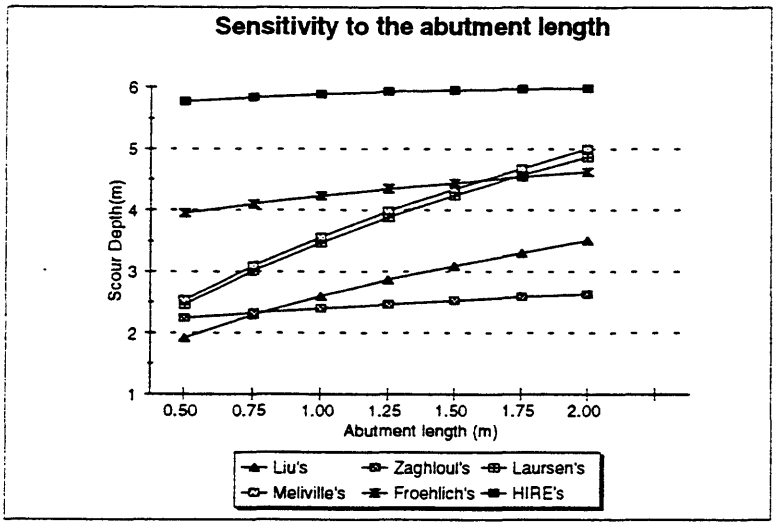
Sensitivity to the abutment length
Scour Depth(m)
6
5
4
3
2
1
0.50
0.75
1.00
1.25
1.50
1.75
2.00
Abutment length (m)
Liu's
Zaghloul's
Laursen's
Melville's
Froehlich's
HIRE's

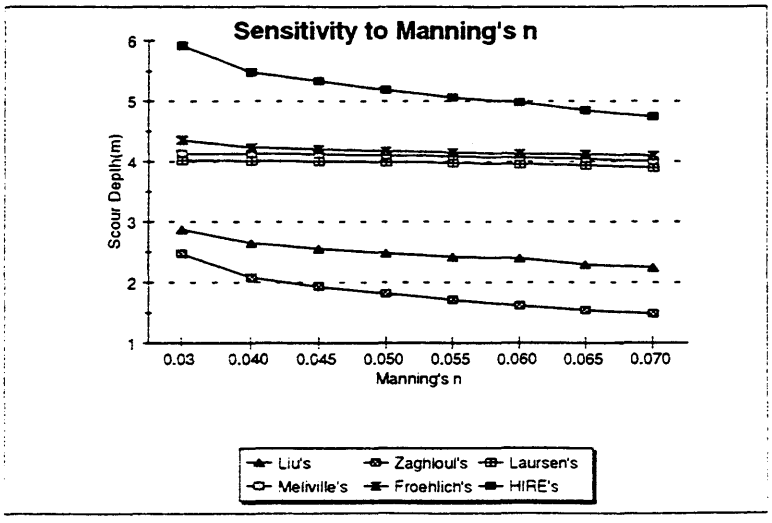
Sensitivity to Manning's n
Scour Depth(m)
6
5
4
3
2
1
0.03
0.040
0.045
0.050
0.055
0.060
0.065
0.070
Manning's n
Liu's
Zaghloul's
Laursen's
Melville's
Froehlich's
HIRE's

Performance Comparison of Dune Bedform Geometry Predictors in the Missouri and Zaire Rivers

By Todd M. Lewis

Abstract: Several different methods have been developed over the years for predicting the primary geometric properties; length and height, of dune bedforms in alluvial channels. Four of these methods; (Allen - 1963), (Yalin - 1964), (van Rijn - 1984), and (Karim - 1995) are selected and described. A performance analysis is then made using data taken from the Missouri and Zaire Rivers. Results from the analysis are then used to compare the accuracy of the methods, as well as identify the best-performing prediction method.

Introduction

The problem of predicting bedform geometry in alluvial channels is of great interest to hydraulic engineers. Knowledge of how these features develop is central in the determination of hydraulic resistance in rivers and canals, as well as being required for safe navigation of inland and coastal waterways. At this time, a quantitative description of how bed configurations develop with changing hydraulic conditions over time is still only approximately known, thus it is desirable to evaluate current prediction methodologies as to how well they perform.

Changes in bedform configuration and dimension arise from the complex interactions found between flow and bed in a natural river system. The following are currently thought of as the primary variables affecting bedform configuration and magnitude:

- The slope of the energy grade line; S_f
- Flow depth; h
- Bed sediment size; d_s
- Fall velocity of bed material; ω
  (a function of the temperature and viscosity of the fluid, as well as the size and shape of the sediment particles)

Qualitatively speaking, for sand-sized bed sediments, low discharge and velocity are associated with ripple and/or dune-covered bed configurations, while high velocity and discharge are associated with flat bed or antidune bed configurations. The following analysis will focus on prediction methods for the dune bedform configuration.

Prediction Methods

The first method considered in this paper was developed by Allen (1963) for the purpose of inferring historical hydraulic conditions (flow depth) from existing bedform topography (amplitude and wavelength). It stands to reason that if this method is accurate it should be possible to answer the converse question with the same method, i.e.: predict bedform geometry from existing hydraulic conditions. By using physical reasoning and analysis of field data, the following empirical relationship was developed by Allen:

$$\log(h) = 0.8271(\log(\Delta)) + 0.8901 \qquad (1)$$

where Δ is the predicted amplitude of the dune and h is the flow depth, both measured in meters.

With some mathematical manipulation, equation (1) can be solved directly to predict dune amplitude. Allen suggested the following relationships for wavelength, λ, measured in meters:

- For ripples $(\Delta < 0.15 \text{ m})$:

$$\log(\Delta) = 0.9508(\log(\lambda)) - 1.0867 \tag{2}$$

- For dunes $(\Delta \geq 0.15 \text{ m})$:

$$\log(\Delta) = 0.7384(\log(\lambda)) - 1.0746 \tag{3}$$

The second prediction method considered was developed by Yalin (1964). Yalin used the theory of dimensions and an analysis of the mechanical process along with two major assumptions:

- the wavelength of ripples or dunes λ are much larger than the amplitude Δ and median grain size of the bed material d_{50}
- the shear stress acting at the lowest point on the trough downstream of a ripple or dune is approximately equal to the critical shear stress

to determine that the dimensionless amplitude of a sand-wave is proportional to the dimensionless excess of tractive force:

$$\frac{\Delta}{h} = \frac{1}{6}\left(\frac{\tau_o - \tau_{cr}}{\tau_o}\right) \tag{4}$$

where τ_o and τ_{cr} are the applied and critical bed shear stresses. From dimensional considerations, Yalin proposed that the length of a sand wave is a linear function of either the flow depth or the median grain size, depending on the value of a dimensionless parameter he termed the Grain-Size Reynolds Number:

$$\overline{X} = \frac{u_* d_{50}}{\upsilon} = \sqrt{gR_h S_f}\left(\frac{d_{50}}{\upsilon}\right) \tag{5}$$

where u_* is the shear velocity, υ is the kinematic viscosity, and R_h is the hydraulic radius.

- For ripples $(\overline{X} \leq 5)$:

$$\lambda = 1000 d_{50} \tag{6}$$

- For dunes $(\overline{X} \leq 70)$:

$$\lambda = 5h \tag{7}$$

Simons and Senturk (1977) report that the first of Yalin's two assumptions is essentially accurate, while the second is flawed due to the presence of upstream velocities in the trough portion of dune bedforms.

The third prediction method considered was developed by van Rijn (1984). Van Rijn's paper outlines a new classification scheme for bed forms, a method for determining bedform dimensions, and a method for determining the effective hydraulic roughness of bedforms. The bedform prediction method is based upon an extensive analysis of more than 1500 flume and field observations. A new dimensionless parameter, dubbed the Transport Stage Parameter, is introduced as a part of the bedform prediction method. Note the similarity between the Transport Stage Parameter and Yalin's dimensionless excess tractive force:

$$T = \frac{\left(u_*'\right)^2 - \left(u_{*,cr}'\right)^2}{\left(u_{*,cr}'\right)^2} = \frac{\tau_o - \tau_{cr}}{\tau_{cr}} = \frac{\rho v^2}{\tau_{cr}\left(5.75\log\left(\frac{4R_b}{d_{90}}\right)\right)^2} - 1 \tag{8}$$

where $u_{*,cr}$ is the critical shear velocity. Once the Transport Stage Parameter is determined, the following best-fit equations can be used to predict the amplitude and wavelength of the dune bedforms:

$$\frac{\Delta}{h} = 0.11\left(\frac{d_{50}}{h}\right)^{0.3}\left(1 - e^{-0.5T}\right)(25 - T) \tag{9}$$

$$\frac{\Delta}{\lambda} = 0.015\left(\frac{d_{50}}{h}\right)^{0.3}\left(1 - e^{-0.5T}\right)(25 - T) \tag{10}$$

Once the amplitude Δ is predicted using equation (9), the following equation can be used to determine the wavelength λ instead of using equation (10):

$$\lambda = 7.333\Delta \tag{11}$$

The final prediction equation considered was developed by Karim (1995) as an independent variable to account for bedform drag in a new approach he has developed for predicting alluvial channel resistance in the framework of the Manning equation. Even though the prediction of bedform amplitude is not the end goal of Karim's work, I found that it was an interesting addition to the methods considered because it employs all four of the 'primary' variables in its methodology: flow depth, friction slope, median grain size, and fall velocity. The relations were developed empirically from both laboratory and flume data. Karim's prediction algorithm is as follows:

a) calculate $\frac{u_*}{\omega} = \frac{1}{\omega}\sqrt{ghS_f}$

b) calculate $F_r = \frac{v}{\sqrt{gh}}$, $F_t = 2.716\left(\frac{h}{d_{50}}\right)^{-0.25}$, and $F_u = 4.785\left(\frac{h}{d_{50}}\right)^{-0.27}$

c) if $(F_r < F_t)$ and $\left(0.15 < \frac{u_*}{\omega} < 3.64\right)$, then:

$$\frac{\Delta}{h} = -0.04 + 0.294\left(\frac{u_*}{\omega}\right) + 0.00316\left(\frac{u_*}{\omega}\right)^2 - 0.0319\left(\frac{u_*}{\omega}\right)^3 + 0.00272\left(\frac{u_*}{\omega}\right)^4 \quad (12)$$

d) if $(F_r < F_t)$ and $\left(\frac{u_*}{\omega} < 0.15\right)$, or if $(F_r < F_t)$ and $\left(\frac{u_*}{\omega} > 3.64\right)$, or if $(F_r > F_u)$ then:

$$\frac{\Delta}{h} = 0 \quad (13)$$

e) if $(F_t \le F_r \le F_u)$, then $\frac{\Delta}{h}$ is the minimum between equation (12) and the following:

$$\frac{\Delta}{h} = 0.20\left(\frac{F_u - F_r}{F_u - F_t}\right) \quad (14)$$

Comparison of Methods

To evaluate the accuracy of the four prediction methods, and compare them against one another, an independent database was chosen so as not to introduce any bias towards a method that was developed for a specific set of data. The selected database consists of information taken from a published study by Julien (1992), regarding bedform geometry in large rivers. Specifically, data from 15 cross sections were chosen from two large rivers; the Missouri River and the Zaire River. This database is shown in Table 1. The following information provides some insight into the rivers the data was taken from:

- The Missouri River is the longest river in the United State of America. It flows 4,368 km (2,714 mi) through a drainage basin covering about 1,371,100 km^2 (529,400 mi^2). The natural vegetation along the river is grass. Mean annual temperatures range from 4° to 10° C (40° to 50° F) in the north to 10° to 15° C (50° to 60° F) at Saint Louis. Annual precipitation in the Missouri River basin ranges from 510 to 1015 mm (20 to 40 in).

- The Zaire (or Congo) River is the second longest river in Africa. It flows 4,660 km (2,900 mi) through a drainage basin covering over 3,458,000 km^2 (1,335,000 mi^2). The river basin can be divided into three sections; open grasslands with scattered trees in the northern and southern regions, and tropical rain forest in the central region. Mean annual temperatures range from 21° to 27° C (70° to 80° F). Annual precipitation in the Zaire River basin varies in each of the three aforementioned regions; 200 to 400 mm (8 to 16 in) in the northern region, 1,675 mm (66 in) in the central region, and 1,200 mm (47 in) in the southern region.

Table 1 - bedform data taken from Julien, (1992)

Sample Number	River	Discharge Q (m^3 / s)	Bedslope So (-)	Flow Depth h (m)	Mean Velocity v (m / s)	Froude Number Fr (-)	Chezy Coeff. C (m^1/2 / s)	Grain Chezy Coeff. C' (m^1/2 / s)	Bed Hydraulic Radius Rb (m)	50% Grain Dia. d50 (m)	90% Grain Dia. d90 (m)	Water Temperature t (deg. C)	Kinematic Viscosity ν (m^2 / s)	Fluid Density ρ (kg / m^3)	Dynamic Viscosity μ (N * s / m^2)	Fall Velocity w (m / s)	Measured Dune Height H (m)	Measured Dune Length L (m)
1	Missouri	2980	0.0001550	3.08	1.37	0.25	62.9	83.4	36.883	0.000199	0.000286	22	9.57E-07	997.6	9.547E-04	0.0250	1.01	64.00
2	Missouri	3050	0.0001610	3.15	1.37	0.25	61.1	82.4	37.787	0.000208	0.000333	23	9.76E-07	997.4	9.735E-04	0.0265	0.88	62.00
3	Missouri	2930	0.0001440	3.00	1.40	0.26	67.1	82.9	36.170	0.000193	0.000299	18	1.078E-06	998.4	1.076E-03	0.0220	1.01	107.00
4	Missouri	2970	0.0001460	3.04	1.40	0.26	66.2	83.1	36.487	0.000207	0.000294	18	1.078E-06	998.4	1.076E-03	0.0245	1.04	102.00
5	Missouri	2950	0.0001520	2.92	1.44	0.27	68.1	82.9	34.839	0.000209	0.000288	14	1.161E-06	999.2	1.160E-03	0.0236	0.79	128.00
6	Missouri	3060	0.0001470	2.83	1.52	0.29	74.6	82.5	33.906	0.000209	0.000295	16	1.240E-06	998.8	1.239E-03	0.0241	0.85	113.00
7	Missouri	3270	0.0001540	2.85	1.63	0.31	78.5	82.3	34.058	0.000223	0.000304	9	1.329E-06	1000.0	1.329E-03	0.0237	0.82	137.00
8	Missouri	3070	0.0001480	2.78	1.56	0.30	76.9	82.4	33.475	0.000222	0.000295	10	1.310E-06	1000.0	1.310E-03	0.0238	0.76	120.00
9	Missouri	3080	0.0001470	2.81	1.56	0.30	76.8	82.5	33.561	0.000209	0.000292	7	1.440E-06	1000.0	1.440E-03	0.0203	0.73	174.00
10	Missouri	3170	0.0001450	3.09	1.40	0.25	66.0	83.1	36.983	0.000204	0.000298	22	1.003E-06	997.6	1.001E-03	0.0252	1.16	76.00
11	Missouri	3190	0.0001530	2.91	1.58	0.30	74.6	83.0	34.920	0.000199	0.000285	17	1.078E-06	998.6	1.076E-03	0.0230	1.43	113.00
12	Missouri	3030	0.0001570	3.00	1.53	0.28	70.3	81.5	36.105	0.000210	0.000357	13	1.208E-06	999.4	1.207E-03	0.0231	1.16	96.00
13	Missouri	3080	0.0001600	2.77	1.67	0.32	79.7	82.1	33.416	0.000224	0.000306	5	1.524E-06	1000.0	1.524E-03	0.0217	0.58	58.00
14	Missouri	2920	0.0001250	3.09	1.38	0.25	70.5	83.4	37.269	0.000200	0.000289	19	1.041E-06	998.2	1.039E-03	0.0238	0.98	70.00
15	Missouri	3110	0.0001520	2.94	1.63	0.30	76.8	83.0	35.410	0.000222	0.000289	13	1.180E-06	999.4	1.179E-03	0.0256	0.85	96.00
16	Zaire	19950	0.0000504	14.50	1.37	0.11	50.7	90.5	174.299	0.000345	0.000545	28	8.35E-07	996.4	8.320E-04	0.0551	1.50	150.00
17	Zaire	23680	0.0000560	14.50	1.46	0.12	51.2	90.5	174.299	0.000345	0.000545	29	8.16E-07	996.2	8.129E-04	0.0557	1.60	170.00
18	Zaire	28490	0.0000634	15.50	1.52	0.12	48.5	91.0	185.812	0.000345	0.000545	29	8.16E-07	996.2	8.129E-04	0.0557	1.50	160.00
19	Zaire	27700	0.0000622	17.00	1.51	0.12	46.4	91.7	203.218	0.000345	0.000545	29	8.16E-07	996.2	8.129E-04	0.0557	1.40	200.00
20	Zaire	24040	0.0000566	17.00	1.48	0.11	47.7	91.7	203.218	0.000345	0.000545	29	8.16E-07	996.2	8.129E-04	0.0557	1.20	220.00
21	Zaire	21100	0.0000522	16.50	1.40	0.11	47.7	91.5	198.085	0.000345	0.000545	28	8.35E-07	996.4	8.320E-04	0.0551	1.20	120.00
22	Zaire	24830	0.0000578	17.00	1.48	0.11	47.2	91.7	203.218	0.000345	0.000545	27	8.53E-07	996.6	8.501E-04	0.0546	1.40	130.00
23	Zaire	19950	0.0000504	10.50	1.25	0.12	54.3	88.0	126.592	0.000345	0.000545	28	8.35E-07	996.4	8.320E-04	0.0551	1.60	95.00
24	Zaire	23680	0.0000560	10.00	1.38	0.14	58.3	87.6	120.278	0.000345	0.000545	29	8.16E-07	996.2	8.129E-04	0.0557	1.30	90.00
25	Zaire	19950	0.0000504	14.00	1.37	0.12	51.6	90.2	167.737	0.000345	0.000545	28	8.35E-07	996.4	8.320E-04	0.0551	1.90	125.00
26	Zaire	23680	0.0000560	13.50	1.50	0.13	54.6	89.9	161.422	0.000345	0.000545	29	8.16E-07	996.2	8.129E-04	0.0557	1.80	140.00
27	Zaire	28490	0.0000634	15.00	1.55	0.13	50.3	90.8	181.118	0.000345	0.000545	29	8.16E-07	996.2	8.129E-04	0.0557	1.50	280.00
28	Zaire	27700	0.0000622	15.00	1.55	0.13	50.7	90.8	181.118	0.000345	0.000545	29	8.16E-07	996.2	8.129E-04	0.0557	1.30	370.00
29	Zaire	24040	0.0000566	14.50	1.50	0.13	52.4	90.5	174.299	0.000345	0.000545	29	8.16E-07	996.2	8.129E-04	0.0557	1.50	370.00
30	Zaire	21100	0.0000522	14.50	1.43	0.12	52.0	90.5	174.299	0.000345	0.000545	28	8.35E-07	996.4	8.320E-04	0.0551	1.90	225.00

Table 2 - predicted bedform geometry calculated from the information in Table 1

		van Rijn's Method					Allen's Method		Yalin's Method			Karim's Method			
Sample Number	River	Critical Mobility Factor Tau*c (-)	Mobility Factor Tau* (-)	Transport Parameter T (-)	Predicted Dune Height Δ (m)	Predicted Dune Length λ (m)	Predicted Dune Height Δ (m)	Predicted Dune Length λ (m)	Grain Size Reynolds # X (-)	Predicted Dune Height Δ (m)	Predicted Dune Length λ (m)	Bed Shear Velocity U* (m / s)	Transition Froude # Ft (-)	Upper Regime Froude # Fu (-)	Predicted Dune Height Δ (m)
1	Missouri	0.049	1.45	15.8	0.17	22.59	0.33	6.28	14.186	0.50	15.40	0.0682	0.24	0.35	0.58
2	Missouri	0.048	1.48	15.8	0.18	23.10	0.34	6.51	14.967	0.51	15.75	0.0702	0.24	0.36	0.60
3	Missouri	0.052	1.36	16.2	0.16	22.00	0.32	6.01	11.700	0.48	15.00	0.0653	0.24	0.35	0.51
4	Missouri	0.050	1.30	15.6	0.18	22.29	0.32	6.15	12.719	0.49	15.20	0.0662	0.25	0.36	0.54
5	Missouri	0.051	1.29	16.1	0.16	21.41	0.31	5.75	11.922	0.47	14.60	0.0662	0.25	0.36	0.48
6	Missouri	0.051	1.21	18.3	0.12	20.75	0.30	5.47	10.756	0.45	14.15	0.0638	0.25	0.37	0.38
7	Missouri	0.052	1.19	19.5	0.10	20.90	0.30	5.53	10.913	0.45	14.25	0.0650	0.26	0.37	0.30
8	Missouri	0.052	1.12	17.8	0.13	20.39	0.29	5.31	10.767	0.44	13.90	0.0635	0.26	0.37	0.35
9	Missouri	0.056	1.20	17.5	0.13	20.61	0.29	5.40	9.234	0.45	14.05	0.0636	0.25	0.37	0.33
10	Missouri	0.049	1.33	16.2	0.17	22.66	0.33	6.31	13.513	0.50	15.45	0.0664	0.24	0.36	0.59
11	Missouri	0.051	1.36	20.6	0.08	21.34	0.31	5.72	12.246	0.47	14.55	0.0663	0.25	0.36	0.31
12	Missouri	0.052	1.36	18.6	0.12	22.00	0.32	6.01	11.850	0.48	15.00	0.0682	0.25	0.36	0.43
13	Missouri	0.055	1.20	19.4	0.10	20.31	0.29	5.28	9.646	0.44	13.85	0.0656	0.26	0.38	0.26
14	Missouri	0.050	1.17	15.6	0.18	22.66	0.33	6.31	11.779	0.49	15.45	0.0613	0.24	0.35	0.58
15	Missouri	0.050	1.22	20.1	0.09	21.56	0.31	5.82	12.506	0.47	14.70	0.0665	0.25	0.37	0.35
16	Zaire	0.032	1.28	11.4	0.89	106.33	2.13	79.34	34.969	2.36	72.50	0.0846	0.19	0.27	4.62
17	Zaire	0.032	1.43	13.2	0.77	106.33	2.13	79.34	37.761	2.36	72.50	0.0893	0.19	0.27	4.73
18	Zaire	0.032	1.73	14.3	0.73	113.67	2.31	88.49	41.502	2.54	77.50	0.0982	0.19	0.27	5.26
19	Zaire	0.032	1.86	13.8	0.82	124.67	2.58	102.94	43.095	2.78	85.00	0.1019	0.18	0.26	5.84
20	Zaire	0.032	1.69	13.2	0.86	124.67	2.58	102.94	41.087	2.78	85.00	0.0972	0.18	0.26	5.75
21	Zaire	0.032	1.51	11.7	0.95	121.00	2.49	98.03	37.982	2.69	82.50	0.0919	0.18	0.26	5.48
22	Zaire	0.033	1.73	13.0	0.88	124.67	2.58	102.94	39.721	2.78	85.00	0.0982	0.18	0.26	5.81
23	Zaire	0.032	0.93	10.0	0.78	77.00	1.44	46.77	29.790	1.69	52.50	0.0721	0.21	0.29	3.01
24	Zaire	0.032	0.98	12.6	0.62	73.33	1.36	43.18	31.345	1.61	50.00	0.0741	0.21	0.30	2.90
25	Zaire	0.032	1.24	11.5	0.86	102.67	2.04	74.91	34.359	2.27	70.00	0.0832	0.19	0.27	4.42
26	Zaire	0.032	1.33	14.2	0.67	99.00	1.95	70.58	36.380	2.20	67.50	0.0860	0.19	0.28	4.31
27	Zaire	0.032	1.67	15.0	0.67	110.00	2.22	83.87	40.806	2.45	75.00	0.0965	0.19	0.27	5.06
28	Zaire	0.032	1.64	15.0	0.67	110.00	2.22	83.87	40.484	2.45	75.00	0.0958	0.19	0.27	5.05
29	Zaire	0.032	1.44	14.0	0.72	106.33	2.13	79.34	37.907	2.36	72.50	0.0897	0.19	0.27	4.74
30	Zaire	0.032	1.33	12.5	0.82	106.33	2.13	79.34	35.588	2.36	72.50	0.0861	0.19	0.27	4.66

1) I assume that the channels analyzed are wide, i.e.; (Rh = h)
2) The friction slope was computed using the Chezy equation (Sf = (V/C)^2 * (h)^-1)

With the selected database, each of the four prediction methods were used to calculate the predicted dune geometric properties; dune amplitude Δ and dune wavelength λ (with Karim's method, only the dune amplitude was calculated.) These values are shown in Table 2. Dimensionless ratios were then formed to compare predicted vs. measured values for both the amplitude $\left(\text{Height Ratio} = \frac{\Delta}{H}\right)$, and the wavelength $\left(\text{Length Ratio} = \frac{\lambda}{L}\right)$ of the bedforms along the selected cross sections of the Missouri and Zaire Rivers.

Graphs were then constructed by plotting the sample number vs. the selected dimensionless ratio. These graphs, Figure 1 (amplitude comparison) and Figure 2 (wavelength comparison), illustrate the performance of the four different methods in predicting the actual measured bedform geometrical property. It is noted that values of 1 for the dimensionless ratios correspond to an exact agreement between predicted and measured values. Values greater than 1 denote an over-prediction of the measured bedform geometrical property while values less than 1 denote under-prediction.

Results

From Figure 1, the predicted vs. measured dune amplitude graph, average values of the dimensionless amplitude ratio were obtained for both rivers with all of the different prediction methods. These values were then used to determine the following:

For the Missouri River:

1) Allen's method under predicts dune amplitude by 76%
2) Yalin's method under predicts dune amplitude by 48%
3) van Rijn's method under predicts dune amplitude by 85%
4) Karim's method under predicts dune amplitude by 52%

For the Zaire River:

1) Allen's method over predicts dune amplitude by 47%
2) Yalin's method over predicts dune amplitude by 62%
3) van Rijn's method under predicts dune amplitude by 47%
4) Karim's method over predicts dune amplitude by 226%

From Figure 2, the predicted vs. measured dune wavelength graph, average values of the dimensionless wavelength ratio were obtained for both rivers with all of the different prediction methods. These values were then used to determine the following:

For the Missouri River:

1) Allen's method under predicts dune wavelength by 94%
2) Yalin's method under predicts dune wavelength by 84%
3) van Rijn's method under predicts dune wavelength by 76%

For the Zaire River:

1) Allen's method under predicts dune wavelength by 51%
2) Yalin's method under predicts dune wavelength by 55%
3) van Rijn's method under predicts dune wavelength by 35%

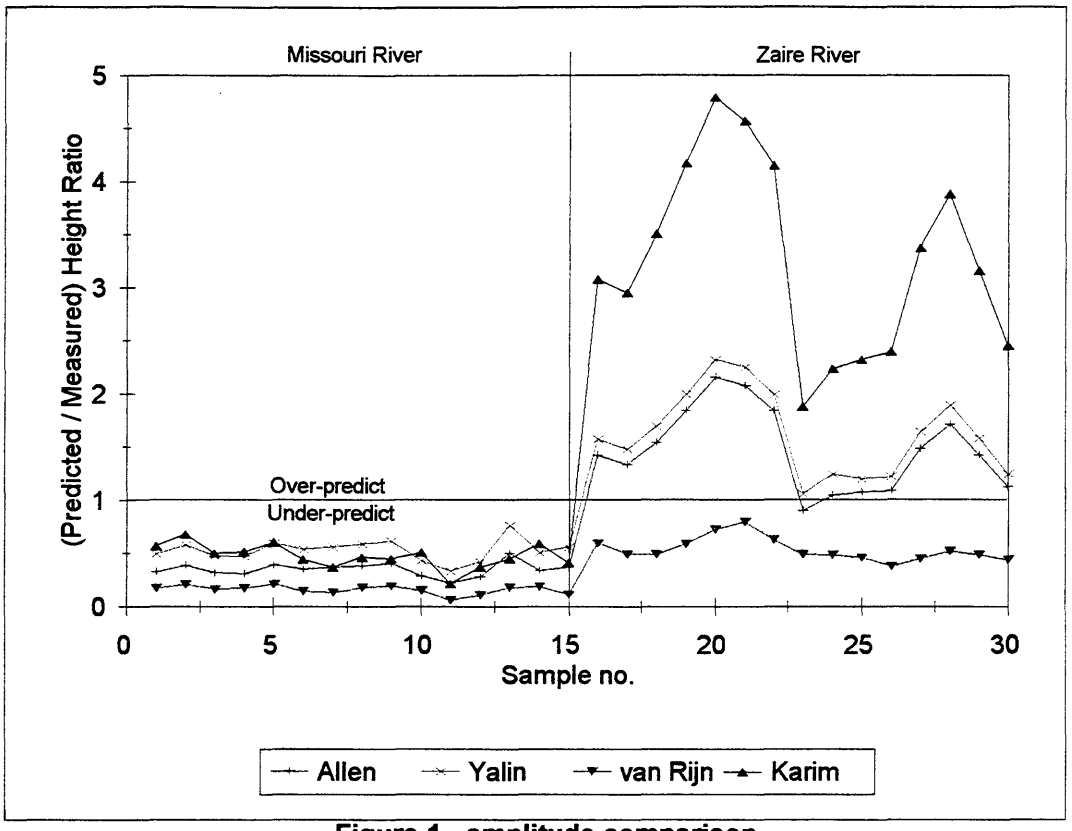

Figure 1 - amplitude comparison

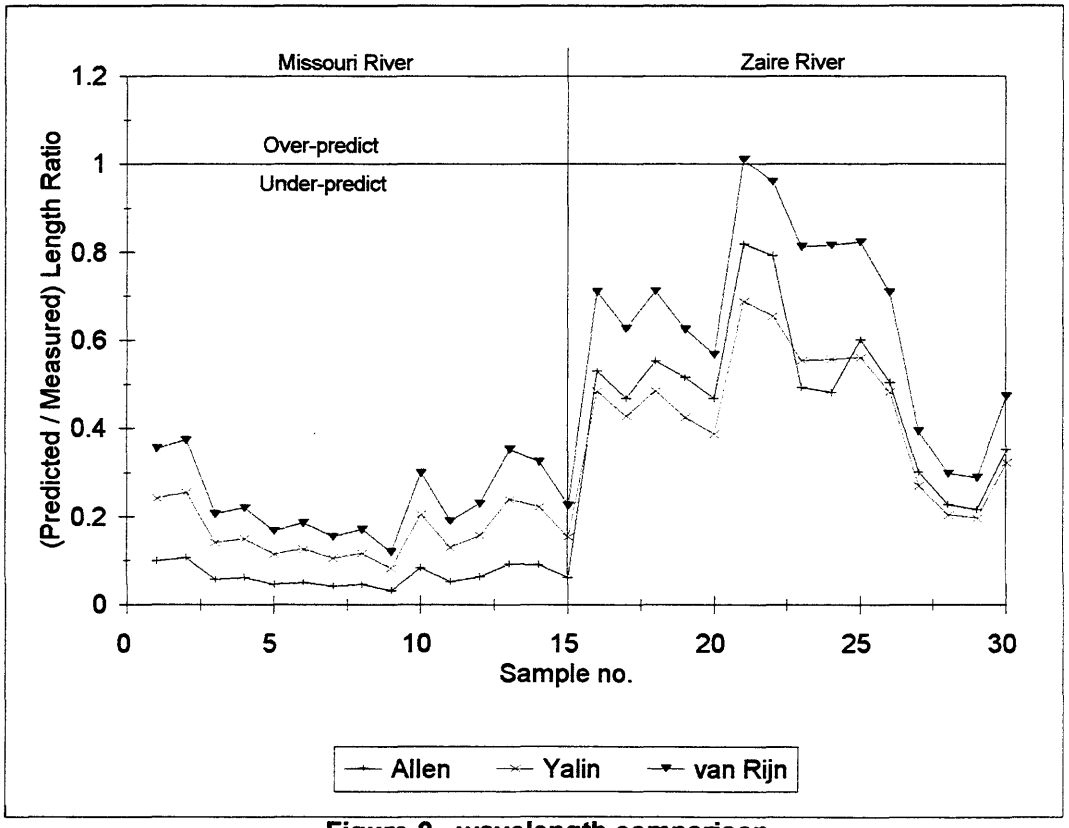

Figure 2 - wavelength comparison

In general, all of the methods surveyed under predicted dune length for both of the rivers studied, however the degree to which this under-prediction extended varied between the two rivers. The three methods as a group were off by about 80% in the Missouri River, but only by 40% in the Zaire River.

More variability was observed in dune height prediction; all four prediction methods under predicted dune amplitude in the Missouri River, while van Rijn's technique was the only method to under predict dune amplitude in the Zaire River. Karim's prediction technique seems to be highly site specific, as the dramatic jump in the dimensionless amplitude ratio in Figure 1 shows.

Conclusions

Four different methods developed to predict dune geometry were investigated and compared. A brief description of the development and application of each of the methods was presented. An independent data set was then used to compare the four different prediction methods; dimensionless ratios of predicted to measured bedform geometric characteristics were computed and then plotted to illustrate how the various methods over or under predicted the desired dune characteristic.

Even though all of the surveyed prediction techniques under predict dune wavelength, progress in predicting dune wavelength does seem to have been made. The method proposed by van Rijn performed significantly better than the earlier efforts of Yalin and Allen for both rivers considered. In fact, an examination of Figure 2 shows a chronological improvement in prediction ability, starting with Allen's method, then moving to Yalin's, and most recently to van Rijn's. A possible reason for this improvement is the inclusion of additional hydraulic parameters in the later techniques. Allen's method is essentially a function of flow depth h alone. Yalin's method incorporates an additional term, the friction slope S_f. Yalin's technique is primarily a function of shear stress τ_o, which in turn is a function of flow depth and friction slope: $\tau_o \approx \gamma h S_f$. Van Rijn's method adds another parameter to those used previously: median grain size d_{50}. It seems reasonable that the inclusion of the additional terms provides for more accuracy in predicting dune wavelength.

While progress seems to have been made in predicting dune wavelength, it would seem that the opposite is occurring with the prediction of dune amplitude. No clear cut picture presents itself from this analysis as to which prediction technique is the "best". It is interesting, however, to note the similarity between the results of Allen's and Yalin's methods. They consistently follow each other for both of the rivers considered with an amplitude prediction from Yalin's method being about 17% greater than Allen's for all data considered. It also seems that the inclusion of fall velocity ω does not seem to have helped Karim's method in the Zaire River. The dramatic over-prediction seen in Karim's method could be the end result of a greater proportion of non-alluvial materials present in the Zaire River than in the Missouri, but this is speculation on my part.

References

Allen, J. R. L. (1963). "Asymmetrical ripple marks and the origin of water-laid closets of cross-strata." *Liverpool and Manchester Geological Journal*, Vol. 3

Allen, J. R. L. (1970). *Physical Processes of Sedimentation*, Elsevier Press

Julien, Pierre Y. (1992). "Study of bedform geometry in large rivers." Rotterdamseweg : Delft Hydraulics

Karim, Fazle (1995). "Bed Configuration and Hydraulic Resistance In Alluvial-Channel Flows." *Journal of Hydraulic Engineering, ASCE*, Vol. 121, No. 1

Simons, D.B., and Senturk, F. (1977). *Sediment Transport Technology*, Chapters 5 & 6, Water Resources Publications

van Rijn, L. C. (1984). "Sediment transport, Part III: bedforms and alluvial roughness." *Journal of Hydraulic Engineering, ASCE*, Vol. 110, No. 12

Yalin, M. S. (1964). "Geometrical Properties of Sand Waves." *Journal of Hydraulics Division, ASCE*, Vol. 90, No. HY5

COMPARISON OF BEDLOAD PREDICTION FUNCTIONS TO FIELD DATA FROM THE COLORADO RIVER IN GRAND CANYON

By Brian L. Cluer

ABSTRACT: The literature abounds with functions for predicting bed sediment discharge of non-cohesive material. In this paper, four functions are compared against bedload measurements made on the Colorado River in Grand Canyon by sequential dune migration tracking. The function of Meyer-Peter Muller, as modified by Chien, was found to closely approximate the field data regression.

INTRODUCTION

Sand is an important resource of the regulated Colorado River downstream of Glen Canyon Dam. It is important because deposits along the banks provide a foot hold for riparian vegetation, which is the essential component of the whole riverine habitat and ecosystem. Deposits of sand in this bedrock river channel also have characteristic geomorphologies that create areas of backwater used by some endangered native fishes as feeding and rearing habitat. Sand deposits on channel margins are formed by recirculating eddies that exist in lateral flow separation zones. Flow separation is typically caused by channel constrictions that are the result of coarse debris accumulations at the mouths of tributaries.

Managing the sand resource has become important since Glen Canyon Dam and Lake Powell behind it efficiently trap the average annual sediment load of approximately $100(10^6)$ tons. Pre-dam sediment in channel and bank storage and the relatively small inputs of a few ephemeral tributaries now make up the sediment resources. Management tries to minimize the downstream transport of sediment through controls on the operations of the dam.

The part of sediment that moves in contact with the channel bed is called the bedload. This is but one definition for the coarse fraction of sediment transported through a river channel, but it is adequate for this paper. The bedload of the Colorado River in Grand Canyon consists of sand and coarser materials. The finer materials are transported as suspended load.

Sand transported as bedload in the form of dunes migrating along the channel bed was measured during channel surveys in the Summer 1993. These data were analyzed and the bedload discharge volume per unit time is reported. Directly measuring bedload is problematic because direct sampling apparatus introduce disturbances to the local flow pattern and sediment transport rate, and sand-sized particles come into suspension in and around samplers and thus escape entrapment. Many investigators have developed equations to predict bedload from hydraulic parameters. It is the goal of this paper to compare three of the better known predictive bedload equations to the field data collected at one site on the Colorado River in Grand Canyon 300 km downstream of Glen Canyon Dam.

METHODS

Bedload Measurements A series of hourly channel topography surveys that lasted for 24 hours included a profile of the channel thalweg. Dune bedforms existed in the portion of the channel between the pool and riffle and hourly sonar profiles showed a systematic progression of the bedforms in the downstream direction. Consequently, the bedforms were determined to be

dunes, not antidunes, and they could therefore be used as indirect measures of bedload. Bedload analysis was conducted on a 20 meter section of the thalweg where bedforms were persistent and the flow depth was approximately uniform.

The thalweg was profiled repeatedly at hourly intervals with an InnerSpace 448 echo sounder and navigation was provided by a Super Hydro positioning system that also recorded the ship position in Cartesian coordinates as well as the water and bed surface elevations.

Post processing involved digitizing a 20 meter long section of the thalweg sonar profiles that included the dune bedforms so that the x-axis could be scaled in proportion to the z-axis of the sonar charts. The analog sonar charts were selected for this purpose because the outline of the bedforms was superior to the digital data, due primarily to the increased density of points on the sonar charts. Plots of the scaled bedforms were then used to determine the geometry and downstream velocity of dunes. Dune height, length, and dune crest x-axis position were recorded for each hourly thalweg survey. Three dunes were selected for tracking positions and the average migration distance was used to determine migration velocity. The average dune height and migration distance were used to determine the unit volume of bed sediment transported along the thalweg in hourly increments.

Other information obtained during the hourly surveys included the average flow depth over the 20 meter section. In addition an RDI Instruments board acoustic doppler current profiler measured water discharge, velocity distribution and water temperature. The energy slope or friction slope (S_f) was calculated using the Manning equation assuming an n value of 0.035. This method was used because measuring the water surface over a short interval is very unreliable even with modern electronic surveying equipment. This is especially true for larger rivers and unsteady flow conditions.

The bed sediment was sampled with a clam shell dredge in the eddy deposit adjacent to the pool approximately 75 meters upstream of the dune tracking location. Sediment size distribution was determined by sieve analysis of a 1 kg split from the 10 kg sample. The relevance of this sample is discussed later.

Bedload Calculations Many formulas have appeared in the literature since DuBoys (1879) presented his tractive force relation. Three bedload prediction equations were selected for this study in order to gain a historical perspective on bedload calculation. The equations selected were; DuBoys (1879), Meyer-Peter Muller (1948), and the Einstein Bed Load Function (1950).

One of the earliest attempts to generalize bedload processes was by DuBoys who began with the premise that shear stress per unit area of the bed (τ_o) is the product of the unit weight of water (γ), depth of flow (D), and gradient (S). DuBoys reasoned that the amount of bedload transported depended on velocity shear at the base of the flow, the difference between the velocity of flow at the bed and the maximum velocity of flow in the water. He assumed that the sediment deep in the bed was stationary and that the overlying sediment moved in sheets at increasing velocities until the maximum velocity section of the flow moved the particles at the same velocity as the water. He suggested that particle motion began at that point at which shear stress was great enough to overcome some critical value. The resulting fundamental equation by DuBoys became

$$q_s = \chi\, \tau_o\, (\tau_o - \tau_c) \qquad (1)$$

where q_s is bedload sediment discharge (ft^2/s), χ is a characteristic sediment coefficient related to the thickness of the layers of sediment expressed as

$$\chi = 0.173/d_s^{(3/4)} \quad (2)$$

where d_s is a representative grain size. The expression

$$\tau_o (\tau_o - \tau_c) \quad (3)$$

has become known as the excess shear relation where a critical shear stress value must be exceeded to initiate sediment motion. The critical shear stress value τ_c in the DuBoys function is determined from the equation

$$\tau_c = 0.0125 + 0.019\, d_s \quad (4)$$

The DuBoys equation results in estimating the volume of bed material per unit width and time.

The simplicity of the approach and the sometimes close agreement with flume and field data apparently explain the popularity of the DuBoys function: it has been the most widely used model (Graf 1986). Schoklitsch (1926) and Donat (1929) improved the DuBoys function and generated an entire family of transport functions that relied on the concept of excess power or excess shear in one form or another.

Meyer-Peter and Muller (1948) proposed further modification of the Schoklitsch approach after more than a decade and a half of experimentation. This complex function includes accountings for grain resistance and bedform resistance and relies in part on the difference between the unit weights of water and sediment. Chien (1954) simplified and reduced the original formulation to

$$q_{bv} = \left(\frac{12.9}{\gamma_s \sqrt{\rho}}\right)(\tau - \tau_c)^{3/2} \quad (5)$$

in which q_{bv} is unit bedload volume per second, γ_s is the specific weight of sediment and ρ is the density of water. τ is the shear stress and τ_c the critical shear stress as defined by the Shields (1936) diagram. The equation is dimensionally homogeneous so that any consistent units can be used.

The US Bureau of Reclamation (USBR 1960) also modified the Meyer-Peter Muller function for units commonly used in the United States. This function is

$$q_b = 1.606\left[3.306\left(\frac{Q_b}{Q}\right)\left(\frac{D_{90}^{1/6}}{n_b}\right)^{3/2} y_o S_f - 0.627 D_m\right]^{3/2} \quad (6$$

in which q_b is in tons per day per foot width, y_o is flow depth, S_f is friction slope, n_b is a roughness coefficient for the total stream. The term Q_b/Q reduces to 1 for wide channels. Both formulations of the Meyer-Peter Muller functions are compared in this paper.

Einstein (1950) approached the bedload transport problem from a statistical perspective. His guiding principles were the following experimental results regarding bedload (Graf 1971, p. 140):

(1) A steady and intensive exchange of particles exists between bedload and the channel.

(2) Bedload moves slowly downstream, while the movement of individual particles is by quick steps with long intermediate stops.

(3) The average step made by a particle is always the same and appears to be independent of flow condition, transport rate, and bed composition.

(4) Different transport rates result from different average time between steps and different thicknesses of the moving layer.

From these precepts Einstein (1950) developed complex probabilistic functions to describe the motion of average particles. The mean transport conditions then combine in a forecast of total transport rates. Einstein's method estimates the total bed sediment discharge in the sum of the contact load and the suspended load. This division is certainly a continuum in nature, but the demarcation is justified in that there is a difference in behavior of the two loads particularly in downstream velocity. The contact load function, or Einstein's Bed Load function, gives the rate of transport for individual particles that make up the bed material. The Einstein Bed Load function was used to calculate bedload for the materials sampled at the Grand Canyon field site. The equations, definitions and graphs necessary to calculate bedload from the Einstein function require approximately 5-6 pages and therefore are not reproduced here. Simons and Senturk (1977, p. 610-615) provided an extensive worked example which was reprinted by Richardson et al. 1990.

For this investigation the Einstein B.L. function was calculated for four particle sizes representative of the field sample gradation. Partial bedload discharges for each of the size classes were then summed for a total discharge estimate. The Einstein and USBR modified Meyer-Peter Muller equations predict bedload in tons/day-foot. These results were converted to volumetric discharge in m^2/hr using standard specific weight and void ratio values for fine sand, widely published in the literature.

RESULTS AND DISCUSSION

Field Measurements The field measurements obtained that were pertinent to the calculation and comparison of bedload using the equations described previously are summarized in table 1.

Discharge during the sampling period was unsteady as the Glen Canyon Dam peak load hydroelectric facility responded to midday demand. The daily 'tide' pattern shown in figure 1 is typical, with discharge ranging from 404 to 689 m^3/s over the 24 hour period. The damping

effect of distance is not strong enough to significantly reduce the flow fluctuation even at the distance of 300 km downstream. Discharge at the dam ranged between 280 and 570 m^3/s by operational agreement for this period of time. It appears that maximum discharge actually exceeded the dam release at this distance downstream.

Bedload discharge was also unsteady during the sampling period, ranging from 0.46 to 2.69 m^2/hr (figure 1). A loop rating effect is evident in that bedload for a given water discharge is greater during descending discharge than it is during ascending discharge (figure 2). The peak bedload occurred several hours after the peak discharge. There was a tendency for bedload to reach a relative maximum and then diminish while water discharge was increasing. Sediment transport in waves or pulses was described in an early paper by Ehrenberger (1931) who found that bedload at a measurement station in the Danube River moved as a series of highly irregular waves with an almost constant period of 20 minutes but with a highly variable amplitude. Many other similar occurrences have been reported subsequently, including laboratory examples from newly forming drainage network channels in an artificial landscape (i.e. Parker 1976).

Table 1. Field data.

Observation	Qw (m^3/s)	Flow Depth (m)	Measured q_{bv} (m^2/hr)	Manning Slope (n=0.035)
1	450	6.35	0.92	0.000107
2	442	6.35	1.01	0.000103
3	468	6.40	0.57	0.000112
4	533	6.70	0.46	0.000125
5	544	6.65	0.90	0.000134
6	585	6.85	1.63	0.000140
7	565	6.80	1.05	0.000134
8	577	6.85	1.57	0.000136
9	549	6.85	2.18	0.000123
10	689	7.05	2.10	0.000176
11	565	6.95	1.85	0.000124
12	562	6.85	1.99	0.000129
13	640	6.85	1.47	0.000168
14	566	6.90	0.77	0.000128
15	517	6.80	1.56	0.000112
16	575	6.70	1.37	0.000146
17	491	6.70	2.69	0.000106
18	516	6.60	1.66	0.000123
19	522	6.35	1.08	0.000143
20	471	6.40	1.33	0.000114
21	443	6.35	0.61	0.000103
22	404	6.30	0.84	0.000088
23	412	6.25	0.50	0.000092

Two days prior to taking the bedload measurements an event that caused the rapid erosion of the eddy deposit upstream of the sampling site resulted in introducing approximately 12,000 m^3 of fine sand to the channel. Gradual deposition of a new eddy bar was evident in sonar traces within a few days. This newly forming eddy bar was sampled with a clam-shell dredge and the sample was sieved for size analysis (table 2). The bed material making up the dunes that were tracked in this investigation is assumed to have consisted of the same size materials that replaced

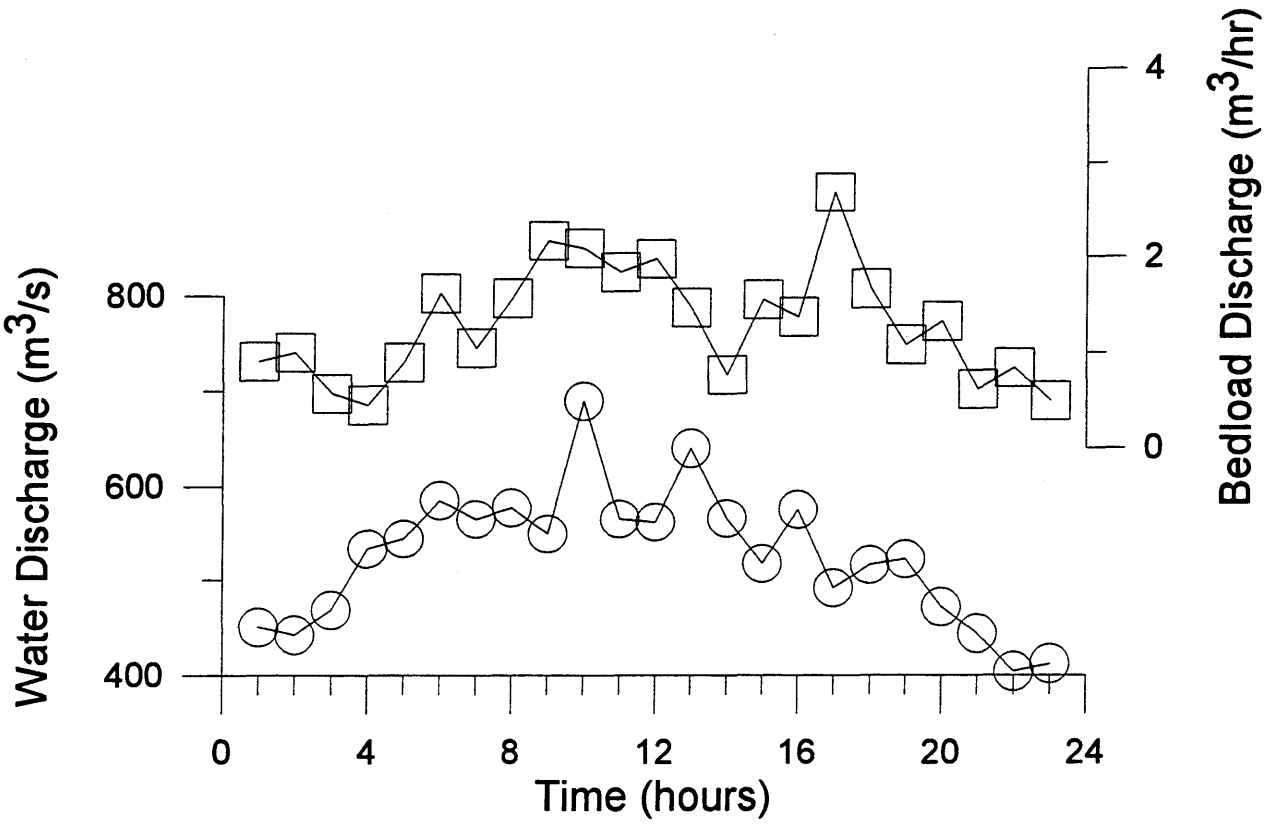

Figure 1. Time-series plots of water and bedload discharge.

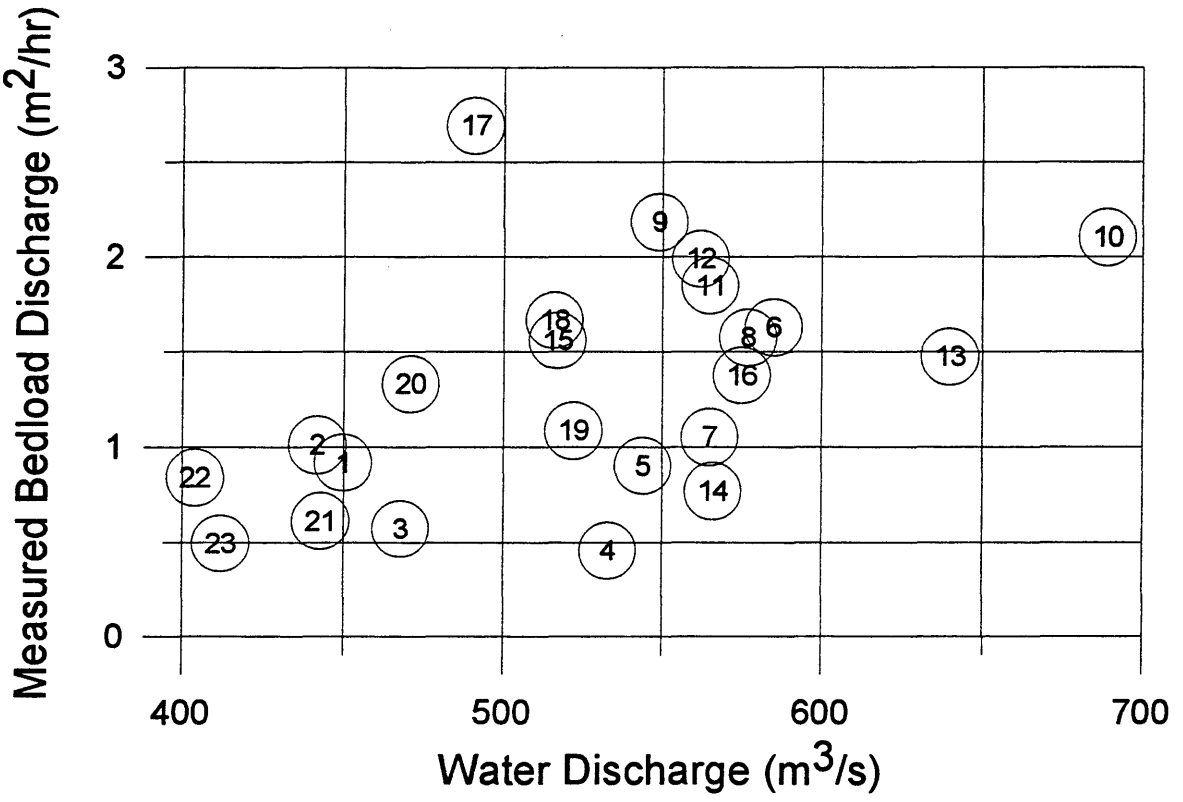

Figure 2. Time sequence plot of water discharge and measured bedload discharge. Numbers in circles show the hour that measurements were made.

the eddy bar. This assumption is supported by remote photographic observations that show the eddy bar had been eroded and deposited 12 times in a 2.5 year period including the time when the channel measurements were made (Cluer 1995).

Table 2. Particle size analysis.

Size Class	Diameter (mm)
d_{10}	0.11
d_{16}	0.11
d_{35}	0.12
d_{50}	0.14
d_{65}	0.17
d_{84}	0.21
d_{90}	0.24

Bedload Predictions The equations described previously were applied using the field data to predict bedload in order to compare the results with the field data and to the other predictive equations. The results are presented in figure 3 which is a plot of unit water discharge per second versus unit bedload discharge per hour. Each equation performed uniquely, but generally all estimated bedload within the range of the field data (table 3).

Table 3. Summary statistics of measured and predicted bedload.

	Measured	*DuBoys*	*Chien, MPM*	*USBR, MPM*	*Einstein*
Mean	1.31	2.12	1.33	1.06	2.10
Minimum	0.465	0.87	0.72	0.21	1.50
Maximum	2.69	4.70	2.40	3.59	2.93
Variance	0.36	0.82	0.16	0.64	0.12
24-Hour Total	30.10	48.85	30.63	24.34	48.32

The DuBoys equation predicted bedload very closely to measured load for the lower discharges. In the intermediate discharges, DuBoys' function tended toward the maximum measurements and at the highest discharges it began to overestimate bedload by a factor of 2.

The two modified Meyer-Peter Muller equations performed differently, in fact almost as differently as any two equations tested. The Chien formulation predicts bedload very closely to the regression line plotted through the measured load data. It slightly under predicts at the lower discharges and slightly over predicts at the higher discharges. Overall, the Chien formulation agreed very favorably with the field data.

The USBR modified Meyer-Peter Muller equation severely under estimated bedload at the lower discharges by factors of 2-3 but performed better at the higher discharges where it tended toward the high end of the measured load range. This function and the DuBoys function both drop off asymptotically toward zero discharge at the lower end of the data range. These two functions have strikingly similar shapes that parallel throughout the data range. However, the DuBoys predictions are within the data at the lower discharge range where the USBR modified Meyer-Peter Muller equation drops off toward zero well within the data range.

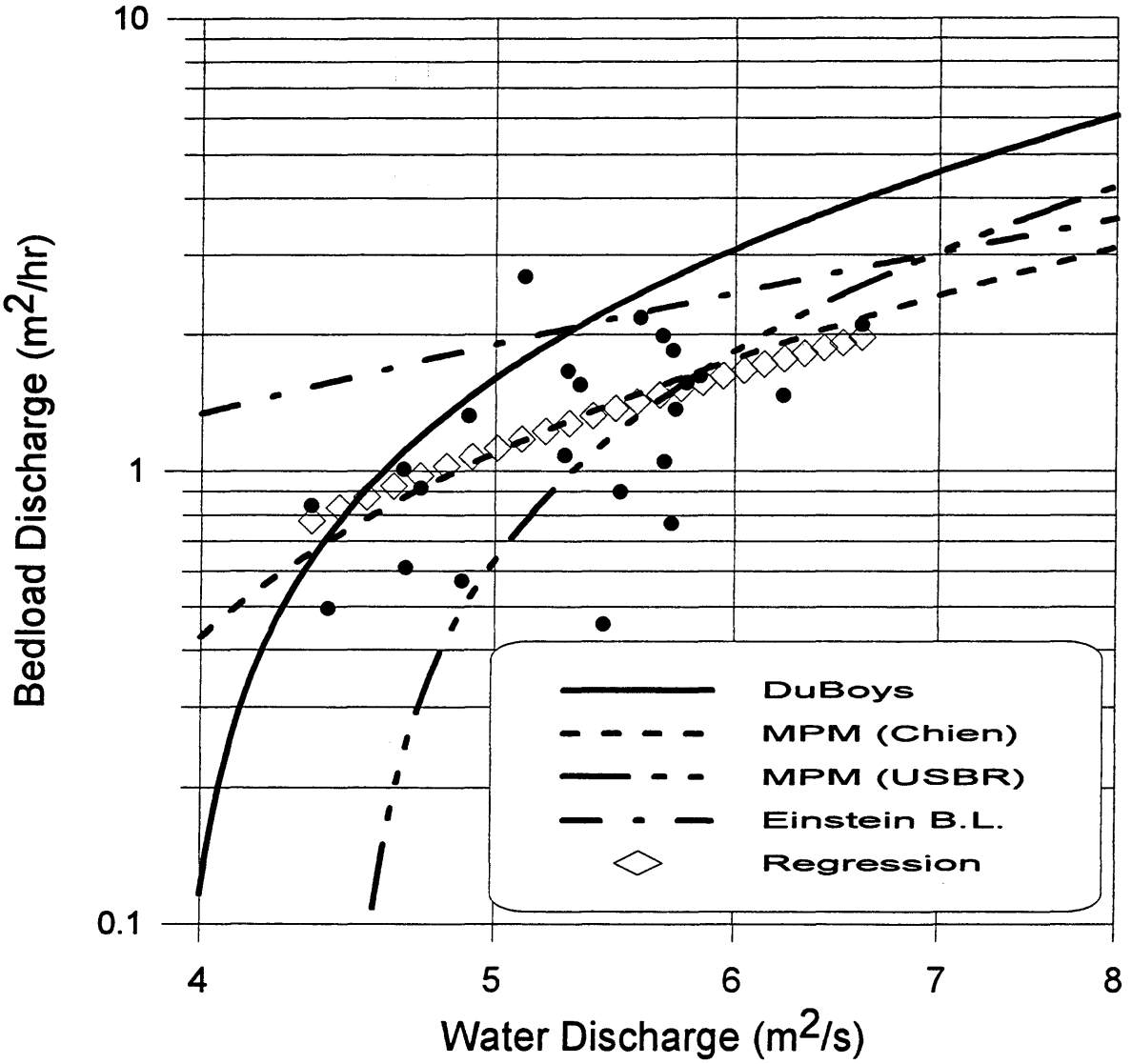

Figure 3. Plot of unit water discharge and unit bedload, comparing the field data (dots) with four prediction equations. The diamonds are the regression line of the field data. See legend for line styles corresponding to bedload functions.

The Einstein Bed Load function significantly over estimated bedload for the lower discharges, by factors of 2-3. In the middle of the data range and at the higher discharges it predicted very closely to the higher measurements but well in excess of the regression line for the data. The Einstein Bed Load function had the lowest slope and displayed no tendency to drop off toward zero at the lower discharge range.

The total unit bedload discharge measured over the 24 hour sampling period, 30.10 m^2, was most closely predicted by the Chien modified Meyer-Peter Muller equation, 30.63 m^2 (table 3). The other equations under predicted or over predicted the total unit bedload discharge.

Results of the predictive equations are strongly correlated with each other, but only weakly correlated with the measured bedload (table 4). This is not surprising as the prediction functions all use very similar inputs, and the measured bedload displayed a loop rating behavior which is difficult to predict.

Table 4. Correlation of measured and predicted bedload results.

	Measured	*DuBoys*	*Chien MPM*	*USBR MPM*	*Einstein*
Measured	1				
DuBoys	0.390	1			
Chien, MPM	0.397	0.998	1		
USBR, MPM	0.339	0.983	0.968	1	
Einstein	0.413	0.982	0.987	0.952	1

Applying the prediction equations in this investigation revealed some nuances worth discussing. The DuBoys equation was very easy to apply and the relatively small number of simple terms resulted in little doubt or question about the inputs and the predicted outcome. The same was generally true of the Chien modified Meyer-Peter Muller equation which was straight forward and easy to apply. However, the USBR modified Meyer-Peter Muller equation, which is more similar to the original function, was more difficult to apply and more uncertainty existed in the process and results. In particular, the chosen n-value has a large effect. For example, bedload prediction is increased by a factor of two by simply selecting n=0.038 instead of 0.035 as used in this investigation. Because n-value selection is subjective and varies with individual practitioners, this sensitivity likely leads to poor predictions using this form of the equation. The Einstein Bed Load equation, while difficult and cumbersome to apply, leaves little uncertainty in the results. But many terms in the equation have only very small effects, leading one to speculate that perhaps these terms could be combined and simplified while still obtaining satisfactory results. Perhaps this why the Einstein function has not been as widely used as the Meyer-Peter Muller function.

CONCLUSION

This investigation compared four of the more familiar bedload functions to field data from the Colorado River in Grand Canyon. The field bedload data were obtained by analyzing migrating dune bedforms observed in hourly sonar charts during a 24 hour channel survey session in Summer 1993. Discharge was unsteady during the survey since the river is regulated for peak demand hydropower. Bedload was unsteady also, exhibiting a loop rating effect.

Predicting bedload from numerical functions spanning eight decades of research shows that the functions have progressively become more complicated and difficult to apply while not substantially increasing in accuracy. The Meyer-Peter Muller function as modified by Chien

predicted bedload in good agreement with the measured load regression line and also closely predicted the total load over 24 hours. However, a sediment management approach may be better served by a function that predicts the time averaged mean bedload discharge. The Colorado River in Grand Canyon is a supply limited river and the measurements presented in this paper were obtained immediately following a local introduction of sandy sediment. Consequently, once this sediment source was depleted, the bedload would have been dramatically reduced and all of the predictive functions would over predict sediment transport.

APPENDIX. REFERENCES

Chien, N. (1954). "The present status of research on sediment transport." *Proceedings,* ASCE, V. 80.

Cluer, B. L. (1995). "Cyclic fluvial processes and bias in environmental monitoring, Colorado River in Grand Canyon." *Journal of Geology,* July 1995.

Donat, J. (1929). "Uber sohlangriff und geshiebetrieb." *Wasserwirtschaft,* 26(27).

DuBoys, M. P. (1879). "Etudes du regime et l'action exercee par les eaux sur un lit a fond de Graviers indefiniment affouilable." *Annales de Ponts et Chausses.* 5(18), 141-195.

Ehrenberger, R. (1931). "Direkte geshiebemessungen an der Donau bie Wein und deren bisherige Ergebnisse." *Wasserwirtschaft,* 34(33-45).

Einstein, H. A. (1950). "The bed load function for sediment transportation in open channels." *Technical Bulletin 1026,* U.S. Dept. of Agric., Soil Conservation Service, Washington, D.C.

Graf, W. H. (1971). *Hydraulics of sediment transport.* McGraw-Hill Book Co., Inc., New York, N.Y.

Graf, W. L. (1988). *Fluvial processes in dryland rivers.* Springer-Verlag, New York, N.Y.

Meyer-Peter, E., and Muller, R. (1948). "Formulas for bed-load transport." *Proceedings,* 3rd Meeting, Intern. Assoc. Hydraulic Res., Stockholm, 39-46.

Parker, R. S. (1976). "Experimental study of drainage evolution." Dissertation, Colorado State University.

Richardson, E. V., Simons, D. B., and Julien, P. Y. (1990). "Highways in the river environment." U.S. Dept. Trans.

Schoklitsch, A. (1926). "Die geschiebebewgung an flussen und an stauwerken." Springer, Wien.

Shields, A. (1936). "Anwendung der ahnlichkeitsmechanik und der turbulenzforschung auf die geschiebebewegung." Calif. Inst. Tech. Pub. 167.

Simons, D. B., and Senturk, F. (1977). *Sediment transport technology.* Water Resources Publications, Ft. Collins, CO.

U.S. Bureau of Reclamation (1960). "Investigation of Meyer-Peter, Muller bedload formulas." Sed. Sec., Hyd. Branch, Denver, CO

A REVIEW OF EQUATIONS USED TO MODEL TRANSPORT VELOCITIES OF SINGLE BED-LOAD PARTICLES

Prepared for: CE 717 River Mechanics
Prof. Pierre Y. Julien
Spring Semester, 1995

Claudio I. Meier

Fort Collins, April 1995.

1. Introduction

Bed-material movement has been extensively studied because of the important role it plays in enginering, geological and environmental problems. Engineers need to understand bed-material sediment behaviour, in order to model and then alterate the river environment (e.g., for flood prevention, to create habitat, or to facilitate navigation), design artificial watercourses and related hydraulic structures, and to estimate reservoir life. Geologists and geomorphologists, on the other hand, use this knowledge to reconstruct the past by interpreting present environments, for example, through the analysis of hydraulically-sorted deposits.

The detailed nature of bed-material transport, which depends on complex interactions between flow and sediment grains, involving a multitude of variables, remains elusive. In particular, sediment transport rates, which are required for many practical applications, are not well understood yet. It is common for estimates by different methods, to differ by orders of magnitude when calculated for real river flows situations. Two main approaches have been followed to attempt to solve the problem:

1. An empirical approach, based on measuring solid rates and corresponding flow conditions, and then correlating the results on the basis of statistical assumptions. The results of many of these experiments, expressed as equations that are mainly empirical in character, give conflicting estimates when applied to river flows.

2. Physically-based, theoretical approaches, that attempt to describe the internal mechanics of sediment transport. Efforts to test these rational theories are hindered by the lack of knowledge about individual grain behaviour, due in part to the inherent difficulty in making observations at the boundary of a completely mobile bed .

Evaluations of selected sediment transport rate models have been carried out, helping in selecting the adequate equation for specific cases. Nonetheless, these have not addressed the reasons that lie behind the relative success or failure of a particular model; their "bulk measurement" approach does not allow to conclude whether discrepancies between predictions and measurements are caused by deficiencies in the theoretical framework or in the experimental data originally used to derive the equation.

The most basic physical way to express bed load transport is as the product of the mass (or weight, or volume) of grains moving at any instant over a unit area of bed by the mean speed of the moving grains. Differential transport velocities of single particles are also the major

factor in sediment sorting. Nonetheless, experimental research has overwhelmingly emphasized the determination of threshold conditions for initiation of particle motion, instead of paying attention to the motion of individual sediment grains.

This paper reviews the differents models that have been proposed for the transport velocity of single bed-load grains. This corresponds to the mechanisms of rolling and sliding, in continuous contact with the bed, and saltation. Even though saltating particles are not touching the bed for most of the time, their trajectories are low enough for the motion to be considered as bed-load. Suspended particles travel basically at the surrounding fluid speed and will not be treated here.

Only a few - a dozen or so- attempts have been made at experimentally determining the transport velocity of grains carried as bed-load. Of course, as already mentioned, the difficulty in identifying and following one particular grain immersed in a completely mobile bed layer forces one to adopt a simplified approach. The main simplification in all experiments is that only the motion of single particles over a fixed bed has been studied, either by glueing particles to the flume bottom or by using hydraulic conditions such that bed particles were not entrained.

Objections can be made regarding the use of this "single-grain over fixed bed" technique to gain knowledge about a process involving multiple grains flowing on a mobile bed. The most important relates to the fact that the presence of other moving grains must affect the motion of any individual particle through collisions. This would invalidate the use of the present models for situations with high transport rates. On the other hand, for low sediment fluxes the number of collisions is so reduced that simplifications should apply. Another objection regards the use of a glued, fixed bed. Even though there are indeed strong differences between a fixed and a mobile bed, there are conditions in which sediment grains move on top of flat, loose, stable beds, without disturbing their stability. This phenomenon was called "particle overpassing" by Everts (1973), who defined through flume experiments the conditions under which it would happen. Allen (1983) and Carling (1990) give clear examples of this process occurring in natural (river) environments.

Readers are referred to Gómez (1991) for a complete review on bedload transport processes, with emphasis on predicting and estimating bedload discharge, and to Bridge and Dominic (1984) for a review on bed load grain velocity studies. To my knowledge, there exists no review of the types of equations that have been proposed to model grain transport velocity.

2. Equations for Grain Transport Velocity

The different models that have been proposed in order to estimate transport velocities of single particles are reviewed in chronological order. Even though experimental conditions will be also mentioned (when applicable), the main focus will be on the form of the different equations that have been proposed.

Krumbein (1942)

The first study on the subject is due to Krumbein (1942). He was mainly interested in analysing the effects of particle shape in sediment transportation, and to that end made experiments in flumes. He also related the observed behaviour to the settling velocities of particles. His experiments were confined to the bed movement of single particles of different shapes over a hydraulically smooth bed, for turbulent flow conditions. By performing dimensional analysis, the experiment was reduced to determining how the ratio of particle velocity to mean flow velocity, Up / U, varies with sphericity, as the Froude number, Fr, changes. Krumbein noticed that the curves followed an exponential type of equation, and proposed:

$$U_p / U = (U_p / U)_o \ (1 - \exp (-a F_r)) \qquad (1)$$

where a is a constant, but he overlooked the fact, noticed by Kalinske (1942) in a discussion to his paper, that all his experiments were made at a constant flow depth, h, of 13.1 cm, which allows to write the Froude number as a function of mean flow velocity:

$$F_r = U / \sqrt{(gh)} \Rightarrow F_r = U / \sqrt{(9.81 \times 0.131)} \Rightarrow F_r = 0.879\ U$$

For the case of spheres, (1) can then be written as:

$$Up / U = 0.88 \ (1 - \exp (- 1.85\ U)) \qquad (2)$$

Thus, Krumbein's equation is not more than a plot of Up / U against U. He did not make any attempts neither to correlate against other variables than Fr, nor to find a physical basis for his empirical equation. Moreover, the nominal diameter of all particles tested was kept constant, so that size effects were not taken into account. Finally,even though flow was turbulent, all experiments were done over a smooth bed, thus having little or no applicability to the real world situation.

Kalinske (1942)

In the already mentioned discussion to Krumbein's (1942) paper, Kalinske asserted that the Froude number has no physical significance in regard to the movement of particles on the bed. He proposed that "physical analysis indicates that the particle velocity, Up, should be equal, or at least proportional, to (U' - Uc) , where U' is the velocity of the fluid acting on the particle and Uc is the critical velocity for that particle". As U' must be proportional to U, the mean flow velocity, he obtained the following expression, where b is a constant:

$$U_p = b(U - U_c) \qquad (3)$$

Kalinske applied his model to Krumbein's data and found the best agreement for b ranging from 0.9 to 1.0. No mention is made regarding how to obtain the critical velocity for a given particle.

Ippen and Verma (1955)

They analyzed in flume experiments the motion of small spheres over beds of different roughness, for turbulent flow conditions. Upon plotting the ratio U / Up against the Reynolds number, Re, they found that, after a transition of variable length (proportional to grain density), U / Up reached an ultimate value that remained constant over a wide range of Re. They also noticed that particle velocity increased directly with size, and attributed this to the fact that larger particles protrude into higher velocities than smaller ones. Assuming that the ultimate, nearly constant ratio U / Up is governed by the following variables: (G-1), k/d, and 1/S, where G is the specific gravity of grains; d, their diameter; k, the roughness size; and S the energy grade slope (equal to bed slope because of uniform flow), they obtained the following equation as a best fit to the data:

$$U / U_p = 1 + 1/12 \ (G - 1) \ (k / d) \ (1 / \sqrt{S}) \qquad (4)$$

This equation is explicitly dependent on the particle size, d, and does show an increase in particle velocity with size. From the definitions of shear velocity and mean bed shear stress:

$$U_* = \sqrt{(T_o / \rho)} \qquad (5) \qquad \text{and} \qquad T_o = \gamma S h \qquad (6)$$

one obtains:

$$S = U_*^2 / (g h) \qquad (7)$$

and replacing this result, (7), in equation (4) leads to:

$$U / U_p = 1 + c\ (k / d)\ (1 / U_*) \qquad (8)$$

where $c = 1/12\ (G-1)\ \sqrt{(gh)}$, a constant for a given flow depth. Ippen and Verma's equation written in this form clearly shows that particle velocity is directly related to both particle size and shear velocity, whilst inversely related to roughness size.

Meland and Norrman (1966)

This experimental study, together with one from Francis (1973), represents the best and most complete attempt to date to generate information about single grains transport velocities. In fact, most recent theoretical papers on sediment transport rates rely heavily on these two for data in order to calibrate their models. Meland and Norrman investigated the interacting effect of water velocity, bed roughness and particle size on the transport rate of single particles over rough beds by turbulent flows, keeping particle shape, density and bed packing constant. They used glass beads only, rolling atop a bed made out of the same beads.

Upon analyzing their results, in which particle velocity is plotted against particle size for different values of shear velocity, it can be clearly seen that for a given bed roughness and shear velocity, large particles move faster than small ones, as concluded by Ippen and Verma (1955). Meland and Norrman give two main reasons to this behaviour: the fact that larger particles ride higher off the bed, being thus exposed to greater velocities; and the decrease in rolling resistance when the ratio of particle size to roughness size is increased. They also found that the influence of size upon transport velocity decreases with increasing shear velocity and with decreasing bed roughness size. In other words, at high shear velocities and small bed roughnesses particle speed tends to be constant with size.

They proposed two models: regression equations based on their data, and a highly convoluted (and intractable) semi-empirical formula derived from Bagnold's (1973) bed-load equation. We will limit our discussion to the regression equation for the higher (continuous motion) transport stage, which reads as follows:

$$U_p / k^m = 7.05\ U_*\ d^n / k\ -\ 5.1 \qquad (9)$$

where:

$$m = 0.75 \qquad \text{and} \qquad n = (0.014\ k / U_*)^{0.26}$$

Of course, this empirical equation applies only to Meland and Norrman's experiments; the constants appearing in the equation are of no particular importance. What matters is the arrangement of the variables, which indicates again that U_p is directly related to U_* and d, and inversely related to k. Another way of saying the latter point, with more physical insight, is that Up is directly related to the ratio (d / k) of particle size to roughness size, i.e., larger particles roll easier than smaller ones over a given bed, or a given particle rolls more easily over a smooth than a rough bed.

Meland and Norrman also observed that transport velocities were lower in beds of loosely packed glass beads than in corresponding fixed, solid beds. This effect was most noticeable at high transport stages, and decreased, or was even reversed for low shear velocities.

Parsons (1972)

Parsons reported measurements on the rates of travel of several sizes of sand grains and glass beads in laminar sheet flow (i.e., overland flow) at differing discharges and slopes, over a smooth bed. He found that particles moving in contact with the bed (i.e., rolling and sliding motion) travelled at speeds approximately half that of the velocity of water in unobstructed flow, at a distance from the bed equal to the radius of a sphere of equal volume. Interestingly enough, for some tests with a large number of grains thrown at the same time, Parsons did not fing any significant difference in speed.

For glass beads he found a quite good agreement with the following equation:

$$U_p = T_o \, d / (4 \mu) \; (1 - T_o' / T_o) \qquad (10)$$

where μ is the fluid viscosity, and T_o' is an apparent minimum, or critical, bed shear stress required for the glass beads to roll (obtained from extrapolating the behaviour of a plot of $(U_p \mu) / d$ against T_o, up to finding the intersect of the curve with the axis for T_o). Using equation (5), the definition of shear velocity, one can express T_o and T_o' as:

$$T_o = \rho U_*^2 \qquad (11) \qquad \text{and} \qquad T_o' = \rho U_*'^2 \qquad (12)$$

Replacing these into (10), and calling $\rho / (4 \mu)$ a constant c, results in:

$$U_p = c \, d \, (U_*^2 - U_*'^2) \qquad (13)$$

This is an interesting equation, not only because U_p is shown to depend directly on d, but also due to its form, expressing U_p as proportional to a difference between a velocity and a critical velocity. In this case, it is shear velocities squared, whilst Kalinske's equation (3) was based on the difference between actual flow velocities.

Ikeda (1971)

Ikeda made a theoretical analysis of the mechanics of the motion af a single spherical grain rolling on the bed, by considering the four main forces acting on the particle: drag, lift, gravity and friction with the bed. The resulting equation is as follows:

$$U_p / U_* = U_1 / U_* - \left[4/3\ \mu\ (G - 1) / (\mu\ C_L + C_D)\ g\ d / U_*^2 \right]^{1/2} \qquad (14)$$

where U_1 is the fluid velocity at the center of the spherical grain, and C_D and C_L are the drag and lift coefficients, respectively. Of course, no mention is made regarding how do the latter two vary during grain transport. Assuming a logarithmic velocity profile, U_1 can be related to U through a constant: $U_1 = a\ U$. In order to be able to simplify equation (14) we will have to make some weak assumptions regarding C_D and C_L: that we are in the range of Re for which C_D is approximately constant ($C_D \approx$ 0.4 to 0.6) and that the particle is not rolling (of course the spherical grains do roll, which further weakens the first assumption); finally, that C_L is proportional to C_D, and thus also constant. By doing so one obtains:

$$U_p = a\ U - b \sqrt{d} \qquad (15)$$

where a and b are constants that depend on particle size. A summary look at (15) might give the impression that U_p decreases with size, but this is not true. In effect, the constant a, that relates fluid speed at particle center height with mean flow velocity, is an increasing function of grain speed. In other words, (a U) will be larger for larger grains.

Francis (1973)

Francis made an exhaustive study on the motion of solitary grains along the bed of a flume. His investigation was limited to particles moving over a fixed, plane bed made out of particles of the same sort, i.e., he did not consider the effects of grain size relative to roughness size.

Francis found a satisfactory correlation between Up, and the particle settling velocity, Vg . He found considerable differences in Up for grains of different shapes, with angular particles always travelling more slowly than rounded ones. The effect of grain size on Up was always

accounted for by using the regression with Vg, but shape effects could not be reduced. Francis also did experiments with spherical particles travelling over a bed consisting of perpendicularly laid cylinders of the same diameter as the grains. In this case particles travelled faster than any natural grains. Finally, he observed marked grains moving in the company of many other grains, in order to test the applicability of results derived from single grain experiments. In this case, speed was reduced 5 % on average below that corresponding to solitary grains. This effect was most noticeable for low transport stages, and disappeared altogether for very high shear velocities.

Only in a later paper (Abbott and Francis, 1977), reviewed below, did Francis propose an equation for Up on the basis of his experiments.

Fernández Luque and van Beek (1976)

Fernández Luque and van Beek used a different approach than the one in previous studies, by using a loose bed for all their experiments. They measured particle velocities as a function of bed shear stress in a closed flow rectangular flume. The measured grains were scoured from the bed and then rolled on top of it. These experiments on loose beds, with low bed-load rates, correspond to the "overpassing" process (Everts, 1973), as defined in the introduction.

The average transport velocity of particles (which were saltating, or even under suspension, for most of the time) was found to be equal to the average fluid velocity for turbulent flow without bed load at about three particle diameters above bed surface, minus a constant proportional to the critical shear velocity at Shield's condition for entrainment, U_{*_c}. The equation, valid over a wide range of slope, is:

$$U_p = 11.5 \left(U_* - 0.7\, U_{*_c} \right) \qquad (16)$$

The form of this equation is quite misleading, since it would seem that U_p would decrease with size (because U_{*_c} is higher for larger particles), but this is not the case because the points through which the equation was plotted correspond all to different experiments. Thus, in (16), U_* is also a function of size, because in experiments with larger particles, larger shear velocities were required not only to entrain grains, but also to keep them moving. As in Francis (1973), the particles were rolling atop a bed made out of the same material, so that the effect of size can not be described.

Romanovskiy (1977)

Not only does Romanovskiy show his own experimental results, he also discusses previous

approaches to the problem of modelling grain transport velocity. In particular, he presents Goncharov's (1938) equation, which is based on experiments:

$$U_p = U_1 - U_{1c} \qquad (17)$$

Here, as in Ikeda's equation (14), U_1 is the flow velocity at the height of the particle center; U_{1c} is the critical value, at the threshold of motion, for U_1. Assuming a logarithmic velocity profile, it is again possible to relate U_1 to the mean flow velocity U trough a constant, so that one obtains:

$$U_p = a (U - U_c) \qquad (18)$$

This is identical to Kalinske's equation (3). In this case it was not only experimentally derived but it was derived earlier, too. Of course, if one considers the definition of shear velocity:

$$U_* = \sqrt{(f/8)}\ U \qquad (19)$$

where f is the Darcy-Weisbach coefficient (a weak function of flow depth, that we will assume constant here), one can obtain equations (3) and (18) in terms of shear velocities:

$$U_p = c (U_* - U_{*c}) \qquad (20)$$

where c is a new constant that takes into account $\sqrt{(f/8)}$, which is assumed constant. The latter equation is quite similar in form to Fernández-Luque and van Beek's, (16).

Romanovskiy made a simplified analysis of the forced acting on a rolling grain and proposed:

$$U_p = a (U - U_c \sqrt{(\tan \alpha / \mu)}) \qquad (21)$$

where $\tan \alpha$ is the dynamic friction coefficient, whilst μ is the static friction coefficient. For a particle at repose, $\tan \alpha = \mu$, and if U is allowed to increase slowly from zero, at a certain velocity $U = U_c$ the particle will be entrained. From his experimental work he concluded that the form of equation (21) adequately represents the data.

Abbot and Francis (1977)

This paper continued the investigations reported by Francis (1973). More experiments were carried out and the following equation was found to represent all data sets with very low

scatter:

$$U_p = b\ (\ U_* - U_{*c}\ ) \qquad (22)$$

It must be noted that, aware of the fact that a particle riding on top of the bed has a far lower threshold of motion than one inserted into it, Abbott and Francis obtained U_{*c} based on actual measurements of overriding grains. Thus, instead of using Shield's criterion, the critical shear velocity was derived assuming a Shields parameter value of $\theta_o = 0.02$. Of course, it should be noticed that (22) is identical to (20) and most similar to (16).

Mantz (1980)

In a laboratory experiment aimed at simulating "overpassing" conditions, Mantz studied low transport rates of disc shaped particles over flat beds composed of the same discs. The resulting data fit extremely well ($r = 0.996$, $n = 15$ data points) the following regression:

$$U_p = 9.2\ U_* - 9.4 \qquad (23)$$

which looks similar to Ikeda's equation (15). By using Bagnold's (1973) concept of a "retarding force" and then applying dimensional analysis, Mantz came up with the following model:

$$U_p = a\ U_* - b\ U_* / \sqrt{\theta} \qquad (24)$$

where a is a constant, $b = (\ 2 \tan\alpha / c\ )^{0.5}$, c is a fluid drag coefficient, proportional to U_p^2, and θ is the dimensionless shear stress $\theta = T / (\rho'\ g\ d)$, with ρ' = density of submerged particles. Mantz applied this equation to Francis (1973) and to his own data, obtaining excellent results.

Bridge and Dominic (1984)

Bridge and Dominic made an exhaustive analysis of bed-load grain transport velocity data, in order to calibrate their proposed physically-based model to estimate sediment transport rates. On theoretical grounds (by following two different approaches) they showed that :

$$U_p = a\ (\ U_* - U_{*c}\ ) \qquad (25)$$

where a $U_{*c} = V_g \sqrt{\tan\alpha}$, in which V_g is the settling velocity of particles and $\tan\alpha$, the dynamic coefficient of friction, is defined at the threshold of motion. Bridge and Dominic present a list of authors who have derived expressions similar to (25), that includes Kalinske,

Bagnold, Ikeda, Francis, Fernández-Luque and van Beek, Engelund and Fredsoe, Abbott and Francis, Romanovskiy, Mantz and Naden. The value of the coefficient a, varies among these authors between 6 and 14.3 , with a mean value of a = 10.7. Application of this model to almost all existing data sets on single grain transport velocities yielded excellent results.

Bridge and Hanes (1985) in a correction to the 1984 paper proposed revising eq. (25) as follows:

$$U_p = a \left[U_* - U_{*c} (\tan\alpha / \tan\alpha_c)^{0.5} \right] \qquad (26)$$

where $\tan\alpha_c$ is the value of $\tan\alpha$ at the threshold of motion. This correction allows the second term in the right-hand side of (26) to go towards zero when the point of true suspension is approached. In its original form, eq. (25) predicted that grain velocity was always less than fluid velocity by the amount $a U_{*c}$, which is clearly not the case when the particle is taken into suspension. Anyhow, the effect of this modification is very slight, because at low transport stages $\tan\alpha \approx \tan\alpha_c$, and at high stages U_* is much larger than $U_{*c} (\tan\alpha / \tan\alpha_c)^{0.5}$.

van Rijn (1984)

For developing his sediment transport model, van Rijn uses Bagnold's (1973) expression, expressed as:

$$U_p / U_* = \alpha_1 - \alpha_2 \sqrt{(\theta_c / \theta)} \qquad (27)$$

in which $\alpha 1$ and $\alpha 2$ are coefficients, and θc is obtained from Shields criterion. Of course, this equation can easily be reduced to:

$$U_p = \alpha_1 U_* - \alpha_2 U_{*c} \qquad (28)$$

if one applies the definition of the dimensionless shear stress, θ. Van Rijn applied these equations to Fernández-Luque and van Beek's, as well as to some of Francis data. The agreement was not as good as in the original papers.

Naden (1987)

In her derivation of a simple model of gravel-bed topography, from sediment transport, Naden proposes an equation of the following form, obtained through a simplified analysis of forces:

$$U_p = U_1 - V_g \sqrt{(\tan\alpha)} \qquad (29)$$

Analyzing experimental data by Meland and Norrman (1966) and Francis (1973), the following semi-empirical equation is proposed:

$$U_p = 11.8\ U_* - V_g \sqrt{(\tan\alpha)} \qquad (30)$$

This equation gave an excellent fit when applied to the above-mentioned data sets. The values of the dynamic friction angle α depend on the ratio of moving grain to bed grain diameter, according to the following: for d/k = 1:2, $\alpha = 27°$; for d/k = 1:1, $\alpha = 11°$; for d/k = 2:1, $\alpha = 5°$.

Wiberg (1987)

In her derivation of a physically-based model of bed-load sediment transport, Wiberg used Francis (1973), Fernández-Luque and van Beek (1976) and Abbott and Francis's (1977) data sets to derive the following semi-empirical equation:

$$U_p / U_* = 4.2\ [(T - T_c) / T_c\ ]^{1.2} / (T / T_c) + 2.4 \qquad (31)$$

This equation can be reduced if the regression exponent 1.2 is made 1.0. In such a case:

$$U_p / U_* = 4.2\ (1 - T_c / T) + 2.4 \qquad (31)$$

3. Conclusions

The best equations to model the transport velocity of single grains in bed-load motion seem to be those that are semi-empirical in character, i.e., whose general form is obtained from simplified physical analysis of the mechanics behind the motion of particles, but whose coefficients need to be adjusted in light of experimental data.

Theoretical developments are usually intractable, and do not allow the calculation of actual transport velocities on a practical basis.

Most equations that have been proposed are based on the difference between an actual flow condition (velocity, shear stress, shear velocity) and the same condition at the threshold of entrainment.

It is clear that, if it were not for the friction with the bed, particles would tend to have the same velocity as the surrounding fluid. Thus, particle velocities can be thought of as lagging behind the flow velocity, due to friction. This friction does depend on the relative size of the particle, compared to the size of the bed grains. This can be expressed in many different ways: simply by introducing the ratio (d/k) in the equation, or by using the dynamic friction angle α, or the dynamic friction coefficient $\tan\alpha$.

The main problem in using the available models remains the quantification of this retarding force due to friction with the bed.

4. Notation

a,b,c	constants
C_D, C_L	coefficients of drag and lift, respectively
d	particle nominal diameter
f	Darcy-Weisbach resistance coefficient
Fr	Froude number of flow
g	gravitational acceleration
G	specific gravity of particles
h	flow depth
m,n	coefficients in Meland and Norrman's equation
Re	Reynolds number of flow
S	slope of the energy grade line
U	mean flow velocity
U_c	U at threshold of motion
U_p	grain transport velocity
U'	velocity of the fluid acting on particle
U_*	flow shear velocity
U_*', U_{*c}	U_* at threshold of motion
U_1	fluid velocity at particle center
U_{1c}	U_1 at threshold of motion
V_g	settling velocity of particle
α	dynamic angle of friction
α_1, α_2	coefficients in van Rijn equation
γ	specific weight of fluid
μ	fluid viscosity, or static coefficient of friction
ρ, ρ_f	density of fluid
ρ_s	density of grains
ρ'	submerged density of grains
$\tan\alpha$	dynamic coefficient of friction
θ	dimensionless shear stress
θ_o, θ_c	θ at threshold of motion
T, T_o	mean bed shear stress
T', T_c	shear stress at threshold of motion

5. References

Abbott J.E. and J.R.D. Francis. 1977. Saltation and suspension trajectories of solid grains in a water stream. Philos. Trans. Roy. Soc. London. 284 (1321): 225-254.

Allen J.R.L. 1983 Gravel overpassing on humpback bars supplied with mixed sediment. Sedimentology 30: 285-294.

Bagnold R.A. 1973. The nature of saltation and of bed-load transport in water. Proc. Roy. Soc. London Ser. A 332: 473-504.

Bridge J.S. and D.F. Dominic. 1984. Bed load grain velocities and sediment transport rates. Water Resources Research. 20(4): 476-490.

Bridge J.S. and D.M. Hanes. 1985. Correction to "Bed load grain velocities and sediment transport rates". Water Resources Research 21(5): 775.

Carling P.A. 1990. Particle overpassing on depth-limited gravel bars. Sedimentology 37: 345-355.

Everts C.H. 1973. Particle overpassing on flat granular boundaries. J.Waterways Harbors Coast. Div. Am. Soc. Civ. Eng. 99(WW4): 425-437.

Fernández-Luque R. and R, van Beek. 1976. Erosion and transport of bed-load sediment. J. Hydraulic Research 14(2):127-144.

Francis J.R.D. 1973. Experiments on the motion of solitary grains along the bed of a water stream. Proc. Roy. Soc. London A 332:443-471.

Gómez B. 1991. Bedload transport. Earth-Science Rev. 31(2): 89-132.

Goncharov V.N. 1938. Movement of Sediments. ONTI, Leningrad-Moscow. 312 p.

Ikeda S. 1971. Some studies on the mechanics of bedload transport.Proc.Jpn.Soc.Civ.Eng. 185: 61-69.

Ippen A.T. and R.P. Verma. 1955. Motion of particles on bed of a turbulent stream. Trans. Am.Soc. Civ. Eng. 1955 . p.921-938.

Kalinske A.A. 1942. Discussion of "Settling velocity and flume behaviour of non-spherical particles" by W.C. Krumbein. EOS Trans. AGU 23:632-633.

Krumbein W.C. 1942. Settling velocity and flume behaviour of non-spherical particles. EOS Trans. AGU 23:621-632.

Mantz P.A. 1980. Low sediment transport rates over flat beds. J. Hydraulics Div. Am. Soc. Civ. Eng. 106(HY7): 1173-1190.

Meland N. and J.O. Norrman. 1966. Transport velocities of single particles in bed-load motion. Geografiska Annaler 48 A (4):165-182.

Naden P. 1987. Modelling gravel-bed topography from sediment transport. Earth Surf. Proc. 12:353-367.

Parsons D.A. 1972. The speed of sand grains in laminar flow over a smooth bed. In: Shen H.W. (Ed). Sedimentation-Symposium to honor H.A. Einstein.

Rijn, van L.C. 1984. Sediment transport, part 1: bed load transport. J.Hydraul.Eng. 110(10):1431-56.

Romanovskiy V.V. 1977. Investigation of the speed of bed load movement. Soviet Hydrol. 16(2):108-112

Wiberg P.L. 1987. Mechanics of Bedload Sediment Transport. Dissertation submitted in partial fulfillment for the requirements for the degree of Ph.D. University of Washington, Seattle.

STRUCTURAL MEASURES AGAINST RAINFALL INDUCED DISASTERS IN QUEBRADA AREAS

by J.KUROIWA [1], Associate Member.

Abstract

Peru with a population of 22'000,000 inhabitants and 1'285,216 km^2 has concentrated 1/3 of its population in the Capital (Lima) and surrounding areas. The Rimac River basin (3, 230 km ^{2}), where Lima is located, runs from the Andes to the Pacific Ocean. Ground elevation ranges from sea level to 5,650 m with the middle upper area of the basin being surrounded by the Andes mountains beginning at about 4,000 m. The very steep topography becomes one of the main causes of the various disasters.

Since snow melt is minimum, the runoff of the Rimac River is mainly dominated by the rainfall pattern in the upstream area. When El Nino phenomenon (a southern shift of tropical sea water along the coast of Ecuador and Peru) hits the Peruvian coast, extra warming produces more rainfall. Sometimes unexpected rainfall occurs in zones that are usually dry. The lack of vegetation in those areas makes the soil very erodible, so when rainfall occurs, soil and large particles are rapidly removed and transported to lower zones. If the lower zones are populated, a disaster occurs.

Very interesting information was found in a report generated by Japanese International Cooperation Agency (JICA) regarding debris flows generated in the "Quebradas" (very steep creeks in mountainous zones). These are connected to the Rimac river which was the original focus of the study. A further problem is the incidence of slope failures with similar results to the debris flows. However, these failures are not as prevalent . Different approaches have been found in the review of literature in order to analyze the flow in the quebradas based on the occurrence of debris flows in March of 1987. Furthermore, several mitigation measures are summarized and discussed. The main parameters that have been found in defining mitigation measures in Quebrada areas are: physical characteristics of Quebradas, spatial distribution and type of properties to be protected, materials availability and labor availability. Among other parameters, the social environment is also addressed in the choice of the method to mitigate flashfloods. A debris basin together with biotechnical slope protection and erosion control are preferred, since the use of intensive labor is not significantly costly and can generate jobs in the area. In the upper reaches of the mini basin under study native vegetation was found, so that drought-resistant trees can be planted.
Inundation also occurs in the areas close to the river, but this is not the focus of the study.

Introduction:

The analyses presented in this report are based on a series of rainfall induced disasters in the Rimac river basin in the country of Peru (see Fig. 1) . These disasters include inundation, debris flows and slope failures and occur regularly. However, the disasters that recently occurred in the 1980's have been much more severe both in terms of loss of life as well as property damage. Severe debris flows in quebradas also occurred in 1925 that coincided also with high discharges in the Rimac River. Along with structural damage, there is also interruption of traffic along the main road and railroad that connect the capital with important mining concerns as well as main cities in central Peru. The disasters that have occurred have resulted in the studies by the Japanese International Cooperation Agency (JICA) that will be presented in this report as well as the elucidation of the need to address these disasters in the Rimac river basin.(JICA, 1988).

1. Department of Civil Engineering, Colorado State University. Fort Collins, CO 80523.

One of the main goals of urban and regional planning is to protect the population and their properties against natural and human hazards. A set of tools developed to achieve this goal is microzonation which is the delineation of different areas prone to hazards of different kinds and intensities. The maximum benefit may be obtained from the microzonation studies, if the area to be developed is used without any other restrictions than those dictated by the site natural conditions. In any case the, the area of interest is divided in sectors of differing hazards, considering all possible natural calamities that threaten that area. (Kuroiwa,1986)

Land strips close to water bodies having a high probability of flooding, have to be designated for recreational purposes and other water related activities. In the next strip, which only floods on extraordinary occasions, only construction permitted are those that do not gather large number of people. The safest sectors are then appointed to the most important urban components such as the high density residential areas and to the activities on which the community depends. (Kuroiwa, 1986).

In the case of the Quebradas the debris flows have already occurred so that microzonation will be more the study of the areas already subjected to different amounts of damages. Here microzonation can identify post disaster damages and possibly suggest the covers the rest of the basin area corresponding to the northern part of Huarochiri.

Description of project area

The Rimac river basin runs from the Andes mountains to the Pacific Ocean. The climate is generally complex due to the nature of the steep topography and the phenomenon known as "El Niño"which is a southern shift of tropical sea water along the coast of Ecuador and Peru. Ground elevation ranges from sea level to 5,650 m with the middle upper area of the basin being surrounded by the Andes mountains beginning at about 4,000 m. This description therefore implies a very steep topography which consequently becomes one of the main causes of the various natural disasters.

The basin's climate can be described as arid to semiarid and there is sparse natural vegetation as a consequence. Due to the lack of vegetation there is remarkable weathering of the rocks especially in the middle lower reaches of the basin which produces many unconsolidated deposits of weathered granite providing potential material for debris flows. Within the area of interest (Quebrada Pegregal) vegetation was found in the upper reaches by the author and reported in a thesis by Carhuayal(1992). Deforestation has taken place since the Spanish invaded Peru. Timber was used for mining operations and also introduced goats in the Valley, devastating native species. Eucalyptus imported from Australia were introduced successfully, but reforestation using native species has not a major endeavor in the area.

Total annual rainfall ranges from 10 mm/year in the coastal area to around a 1,000 mm/year in the mountainous area (see Figure 2). This range is due to the influence of cold sea water near the coastal areas which keeps precipitation to a minimum but this effect is considerably weakened in the vicinity of the Andes. Therefore, the runoff of the Rimac River is mainly dominated by the rainfall pattern in the upstream area. The annual average runoff at the town Chosica where the catchment area is nearly 70 % of the total area of the basin, is 32 m^3/s as calculated for the period from 1969-1987. Sixty five percent of annual runoff volume occurs in the 4 months between January and April and it discharges into the Pacific Ocean. The maximum runoff volume that has ever been recorded was 500 m^3/s on March 19th, 1925 at Chosica. The probable flood discharge was estimated using a conventional unit hydrograph method .The 100-year flood was estimated at 660 m3/s, and the 500 year flood at 820 m3/s.

Sutton (Carhuayal, 1992) established that rainfall below 250 mm/year would not produce runoff. Below that isohyet the basin is supposed to be arid and semiarid above that.

The Rimac River basin contains not only the Rimac river but also the Santa Eulalia which is the main tributary to the Rimac. There are also other minor tributaries that empty directly into the Rimac. These can be seen in the general map of the basin. The area ratio of each land use category in the Rimac River basin is approximately measured as follows: town and villages occupy 4.6% o the total area, farms in flat land 1.7%, farms in mountain slopes 7.1% , mountain areas without vegetation 30.0%, mountain areas with vegetation 34.6%, swamps 0.8%, glaciers 0.9% and lakes 0.3%(See fig 3). So, about 70% of the basin is mountainous. The flat plain is developed only in the lower reaches which include the Lima-Callao metropolitan district.

Disasters in the Rimac Valley

According to the records and information, disasters caused by debris flow, inundation, slope failure, etc. occurred almost every year in the Rimac river basin. However, it was found that the disasters that occurred in 1983 and 1987 were remarkably serious. They will be briefly described in the following paragraphs.

1983 Disaster

In 1983, disasters were remarkable not only in the Rimac river basin , but also in other parts of the continent. According to the National Civil Defense Committee, the total toll in provinces of Huarochiri and Lima was 285 consisting of 22 dead and 233 injured for the period of January through June. Most of these occurred in the Rimac river basin. The precipitation from January to March increased noticeably due to intense rainfall caused by El Nino event. Monthly rainfall records indicate 62.8 mm of February and 189.2 mm of March in Matucana. As a result, intensive damages were inflicted on settlement areas in the middle reaches, and Central Highway of Route 20 and railway connecting Metropolitan Lima and mountainous area. The traffic system was interrupted for long time.

Disaster in 1987

A large scale disaster due to debris flow, inundation and slope failure happened on and around March 9, 1987.

Disasters were classified into the following three categories:

a) Debris flows happened in five quebradas located in Chosica district. Houses were damaged by impact of boulders as well as sediment deposits (See Figures 4 and 5)

b) Inundations occurred in Campoy/ Zarate district located in the lower reaches on the right bank area along the Rimac river. The cause was the overflow from Quebrada Jicamarca, the major tributary located in the lower reaches of the Rimac River

c) Other disasters such as debris flows in Quebrada La Cantuta, slope failure at Santa Rosa de Palle, Bajo Village and inundations from the Rimac river in Huachipa area. The damage of this disaster was comparatively small.

Floods in the Rimac valley are events that occur usually further down the Rimac river than around the township of Chosica where the main natural disasters are the previously mentioned debris flows. However, the debris flows can cause floods by blocking part of the natural watercourse.

Structural measures for disaster prevention and mitigation in Quebrada Areas

In order to prevent and mitigate future rainfall produced disaster structural measures are necessary . The report by JICA covers measures that both enhance present structures as well as ones

that need to be constructed in areas where hazards have been identified but are lacking any preventive structural measures. These include debris flow, inundation and slope failure prevention. The focus of this study is debris flows and mitigation measures, so it will be outlined in the following section. For inundation measures the reader can refer to the JICA report.

Analysis of quebrada characteristics and needed structural measures

A different type of flood occurs in the Rimac Valley that may be classified as alluvial fan flow. Alluvial fans are defined as "a triangular or fan shaped deposits of boulders, gravel, sand and fine sediment at the base of desert mountain slopes deposited by intermittent streams as they debouch onto the valley floor" (Stone, 1967)

For the present study the areas delineated were based on disasters that occurred in the Quebradas surrounding Chosica. Since no software was found to run "typical floods" in Quebradas (whose behavior change when they become an alluvial fan type of flow), they were made based on surveys made after they occurred. (JICA, 1988)

Features of Quebrada areas

The quebrada area is a tributary which is connected to the main river. The highest portion of each Quebrada Area is remarkably elevated so that most have a peak portion higher than 2,000 meters. The elevation difference of each area is also remarkable with a difference of more than 1,000 m. The slopes of tributaries within the quebradas themselves are generally very steep with an average slope steeper than 10 degrees. In fact, tributaries with slopes of 30 degrees or more are not exceptional.

Features of slope areas

Slope areas are surrounded by the quebrada areas and also lead to the main river The length of the slope area generally ranges from 1 km to 10 km with a horizontal length generally ranging from 1 km to 4 km. Slope height is higher than 500 m. Most of them are lower than 2,000 m. Average slope gradient of the slope areas is steeper than 15 degrees and about a quarter of the slopes are steeper than 30 degrees.

Classification of divided areas

Areas were divided into three groups in accordance with the degree of danger and protective properties as follows:

Group A: Group A has the highest degree of danger and protective properties, also having the actual experience of disaster. It is ranked in the highest priority level. Then, the countermeasure for debris flow disaster prevention is individually established in each area through a detailed study.

Group B: Group B has a relatively less degree of danger and protective properties compared with the above Group A

Group C: Group C has little danger or protective properties. The counter-measure is not examined.

Structural Plans for group "A" areas

The deposit volume of a long-term scale debris flow with about 100-year return period is considered for the structural plan for debris flow disaster prevention in accordance with usual practice.

The estimate of the long-term deposit volume at each quebrada is based on the deposit volume experienced in a large scale in Qda. Pedregal in March, 1987, considering that the past records show that the similar scale of deposit volume occurs at a long term of 60 to 100 years. See Figure

Furthermore, the deposit volume is considered to be proportional to the drainage area of each quebrada. Besides that, it is considered that the situation of vegetation will predominantly effect on the probable deposit volume. Consequently, the long term deposit volume at each quebrada is based on the following equation:

$$V = \frac{V_p}{C_p} \times C \times 1.2 \times F$$

where:

V = the long-term deposit at each quebrada

V_p = the deposit volume occurred in Qda Pedregal in march, 1987 (157,200 m^3)

C_p = the catchment area of Qda Pedregal (10.6 km^2)

C = the catchment area of each Quebrada

1.2 = the safety factor which is usually applied in consideration of the accuracy of the measurements.

F = the reduction factor to be determined in accordance with the situation of vegetation in each quebrada. (1= no vegetation; 0.8 = vegetation covers 10 - 30% of the basin; 0.6= vegetation covers 30% -60% of the basin; 0.4 = vegetation covers 60%-90% of the basin; 0.2 vegetation covers more than 90%)

Type A:

It is required to check the debris/mud flow as much as possible and control the excessive flow confining in the channel since the residential houses are already settled densely along the quebrada channel on the fan. This is further divided in: (See Figure 6a,b,c and e)

A: There is a suitable site for check dam (See fig 7)

A: There is not suitable site for check dam.

Then the structural plan is made as follows:

a) Channel works for erosion control of fans and fixing of channel route (type A and A). (See fig 6a).

b) A series of dam at the upstream stretch of channel works for debris/mud checking and erosion control (Type A) . See Fig 6b

c) Sand arresting works at the upstream side of channel works as there is no appropriate dam site for checking sufficient volume of debris/mud (Type A) . See Fig 6c

Type B:

It is not considered reasonable to check the flow by a check dam in the case that residential houses are thinly located along the quebrada. This is further divided in the following types: (See Fig 6d)

B1: There is none or very few houses on the fan area

B2: There are a few houses on the fan. It is therefore required to control the direction of the flow as much as possible at the top of fan. (See Fig 6-e)

The structural plan is made as follows:

a) Training dikes and excavation of channel for regulating the course of flow (Type B1 and B2)

b) Protection of public structures such as road and railway and/or improvement of existing protection structures (type B1 and B2)

c) Low dam for arresting and erosion control at the top of the fan (Type B2)

d) Plantation for sand arresting at the top of fan or energy dissipation on banks

Type C:

It is required to check the debris/mud flow as much as possible and convey the excessive flow smoothly to the main river, in order to avoid blocking the main river channel since the densely populated residential areas and/or important public structures located on the opposite side of the confluence or in the downstream stretch will be affected.

The structural plan is made as follows:

a) Dam for checking the debris/mud erosion control and stabilizing hillside base

b) Low dam(s) for energy dissipation, flow direction control and erosion control at the downstream stretch of check dam.

c) Excavation at the outlet of quebrada channel for smooth inflow to the main river

d) Construction of dikes on the opposite bank of main river located opposite side of the quebrada outlet for preventing flooding from the main river and encroachment of debris flow onto properties on the opposite side.

Structural plans for group "B" areas

It is considered that the scale of debris flow in the slope areas is generally small since the scale of associated quebradas is small. Therefore structural measures are implemented on a smaller scale. For the debris flow/rockfall/slope failure, the following structures are considered:

a) Bridges (in gullies/quebradas)

b) Rockshed tunnel (in gullies/quebradas)

c) Retaining wall (on slopes)

Alternative Techniques

Two different approaches to analyze floods in alluvial fans were found in the review of literature. Abdelbary (1982) modeled an existing alluvial fan: Embudo Canyon Fan, Alburquerque, New Mexico. Originally the continuity, momentum, and resistance equations were used. Subsequently a sediment transport equation developed after the runs was utilized for the final analysis. Relations between flow rate, alluvial fan geometry and sediment size were found and multiple and entrenched braided channel zones were identified. The assumption made by Abdelbary is that flow in an alluvial fan resembles a jet flow so that velocity is proportional to the square of the distance from the apex; since in alluvial fan flow expands laterally, and depth and velocity decrease in the downstream direction. Another assumption is that alluvial fans reach a condition of equilibrium in which the velocity, depth, width of flow and the bed slope adjust such that the energy is just sufficient to transport the sediment delivered to it. So Abdelbary's theory can not be applied in the following cases:

1. Unsteadiness due to lagging between water and sediment hydrographs.
2. Nonuniform soil distribution.
3. Geological and topographical controls such as humps and depressions.
4.Excessive seepage loss.

The following relationship was proposed:

Where:

$$D = D_o \exp\frac{Q}{D_o W_o \sqrt{g d_s}}\left(\sqrt{\frac{\beta}{\frac{x}{W_o}+\beta}-1}\right)$$

D_o= Depth at the apex

D= Depth at distance x from the apex

W_o= Canyon width (Width at the apex)

x = Distance measured from the apex

Q = Discharge

β = an empirical constant = 60.0

This equation together with the equations mentioned before allows prediction of the behavior of flow in the entrenched reach.

Abdelbary analyzed three potential mitigation measures : the use of a debris basin, leveed channel and channelization. He found that in general there is no advantage in using one or another, and it essentially depends on the alluvial fan characteristics and the cost of their implementation.

Debris Basin:

The purpose of a debris basin is to provide a reservoir or stilling-type basins that reduce flow velocity sufficiently to allow large rocks, sediment, and debris to be deposited. The effect of a debris basin is on the one hand to retard the flow which results in a smaller peak discharge and to reduce the sediment flow on the other hand. Flow width is expected to decrease resulting in smaller flooded areas. The disadvantage of the debris basins is that after a series of floods, they become filled with incoming material and they become very ineffective unless the debris is removed. The continual maintenance of debris basins could be very expensive. This approach is preferred if the sediment load in the watershed is very heavy or the fan surface is very irregular.

System of Sediment Basins: a case study

Bednar and Fluke (1980) reported that sedimentation ponds were built in Eastern Kentucky to control sedimentation downstream a mine. The pond system consisted of instream ponds where a bulldozer was used to excavate a portion of the stream channel, using the excavated material to form the downstream embankment. The principal spillway was usually a corrugated metal pipe, with the open emergency spillway located at a slightly higher elevation on the opposite side of the embankment. Once the ponds were constructed, they were not maintained. Clogging of outflow pipes by floating debris and accumulated sediment caused excess use and rapid deterioration of the emergency spillway and embankment and short circuiting of the ponds. So, maintenance is very important when sediment ponds are used.

Leveed Channel:

Five equations were used by Abdelbary to obtain flow width, depth, velocity, and be and energy slopes. Omitting one of the equations allows one degree of freedom. Since in the experiments the flow was free to cut the banks or adjust the slope the previous equation is not valid when the flow is restricted. So either width or bed slope can be specified. If width is specified, bed slope has to be modified, according to the calculated bed slope. This could be very expensive. On the other hand, if bed slope is specified width of the channel has to be modified. The disadvantage of using this latter approach is that the design channel may encroach on inhabitated areas. The former approach could be used for the reach downstream whereas the second approach could be used for the reach upstream, where housing density is supposed to be lower. This would be the best choice if a large portion of the fan has been used for urban development.

Channelization:

The cross section is modified to carry a higher discharge, a higher sediment load or both. Enlarging the cross section and stabilizing the bed and the banks by using riprap or concrete linings is one way of channelization to carry larger discharges. This has the disadvantage of possible aggradation for lower discharges with high sediment load.

Another way of channelization is accomplished by using dikes to narrow the channel width. A narrower channel produces deeper flow for the same discharge . Since relative roughness decreases higher velocities are expected, resulting in a larger transport capacity. This could be very expensive. Furthermore, it may take several flood events before the channelized cross section is established.

In the review of literature, information related to the behavior of alluvial fan in the lower reaches was also found. Rachocki (1981) focused on the "network" formed by the braided channels and developed a random walk model. He used an actual alluvial fan to carry out a set of experiments. He concluded that the fundamental agent shaping the fan is the distribution of discharge in the braided channel system. Grain size distribution was found to be of secondary importance and a main channel could also be identified.

Pircas

Techniques used by the Incas to control debris flows are addressed in a professional thesis (Carhuayal, 1992). One of the main components of the terraces is the pirca or retaining wall made out of rocky masonry. It has a weir by which water flows through. A succession of these walls can be installed within a small creek in order to retain sediments that otherwise would flow downstream.(See figure 8)

Azudes

In order to control "trenching" small dams are suggested to be built within the gully in order to reduce erosion. Some of them are done with timber and rocks; others are done with just rocks and cement mortar. The latter is more effective since timber is a rather scarce resource in the area. They look like terraces.

Biotechnical Slope protection and Erosion Control.

This technique combines the perspectives and techniques of engineering and horticulture to achieve the retention of earth masses and the prevention of soil slopes from slopes.

Since background in soil mechanics is expected, the effect of herbaceous and to a lesser extent woody vegetation in controlling erosion are introduced:

1. Interception: foliage and plant residues absorb rainfall energy and prevent soil compaction from raindrops.
2. Restraint: root system physically binds or restrains soil particles while above-ground residues filter sediment out of runoff.
3. Retardation: above ground residues increase surface roughness and slow velocity of runoff.
4. Infiltration: roots and plant residues help maintain soil porosity and permeability.
5. Transpiration: depletion of soil moisture by plants delays onset of saturation and runoff.

Woody vegetation might also affect the balance of a slope. Roots mechanically reinforce a soil by transferring shears stress to the roots. Surcharge can also occur since the weight of vegetation exerts both a downslope stress and a stress component perpendicular to the slope which ten to increase the tendency to sliding. (Gray and Leiser, 1982).

Major factors in selecting the species to be used include: Climate (principally rainfalls, minimum and maximums temperatures and constancy of these parameters); topography; site soils (soil type, pH, salinity), adjacent vegetation, and of course availability. Length of growing season is also a major factor.

All these factors were taken into account in order to select a species, and three species are preferred: Huarango (Acacia Macracantha), Molle (Schinus Molle), and Aloe (Aloe Succotrina). The first two are trees whose maximum height fluctuates between 6 to 10 meters with a coverage of 8 to 12 meters of diameter. The third species is a bush whose maximum height is 1.50 m and is planned to be used in conjunction with the other two species in the upper reaches of the mini basin Pedregal. Three of the species are drought resistant and do not require major care. An interesting factor is that Huarango and Molle can be reproduced by seeds, so transportation to the upper reaches by personnel would not be a problem. (The upper reaches are almost inaccessible by car). (Fig 9)

Resources availability:

Local geology is encased within the Rimac River Basin where volcanic and intrusive rocks are abundant. Granite and granodiorite are found to be significantly fractured and weathered in the surface. Colluvial deposits of this material in varying sizes (ranging from silty-sandy soil to 4m boulders) are noticeable.

The bottom if the creek is filled with colluvial and alluvial deposits. Local material can therefore be used for building stabilization structures in the upper reaches and also in the lower reaches.

Labor availability:

The following excerpt has been selected from Rubio (1988):"In general one of the main problems is that just 35% of the workers have a job with a good salary; 54% receive a rather low salary and 11% of them is inactive. Due to this reasons the country is saturated of supply of labor and salaries are still low despite inflation and the permanent incorporation of young people to the working population".

So, choosing an method for protecting human settlements that involves extensive labor is not a bad idea, at least in Peru.

Recommendations

Upper reaches can be stabilized by using ancient techniques, and introducing native species, drought resistant trees and bushes, since native vegetation has been reported in those areas . In the lower reaches, the Master Plan introduced by JICA is to be developed. Where plantations are suggested by JICA, the previously mentioned species were found to be the best for the area.

Materials for any type of construction (Inca modified and the ones proposed by JICA) are available in the area and appropriate techniques should be applied for their use. A modification can be introduced in pircas to convert them to self forming terraces by providing adequate downstream protection.

In upper reaches of the Rimac Valley, between 2,500 m above sea level and 3,500 m above sea level, true biotechnical erosion control techniques could be more effective.

REFERENCES:

1.Abdelbary, Mohamed Rafeek. Alluvial fan hydraulics and flood hazard mitigation measures. Dissertation. Department of Civil Engineering. Colorado State University. 1982

2. Bednar R.E and Fluke D.J. Demonstration of Debris Basin Efectiveness in Sediment Control. Project Summary U.S. Environmental Protection Agency. EPA 600/PS-7-80-154. Sept 1980.

3. Carhuayal, Raul.Estudio del Metodo de Correcion de Drenaje para evitar los huaycos y su aplicacion en la Quebrada Pedregal . Professional Thesis. Universidad Nacional de Ingenieria. Lima, Peru.1992.

4. Garcia, Kerry T. Effect of Erosion- Control Structures on Sediments and Nutrients Transport, Edgewood Creek Drainage, Lake Tahoe Basin, Nevada, 1981-83. U.S. Geological Service Water Resources Investigative report 87-4072. 1988.

5. Gray, Donald H. and Leiser, Andrew T. Biotechnical Slope Protection and Erosion Control. Van Nostrand Reinhold Company.1982

6. JICA. (Japan International Cooperation Agency). Final report for the master plan study on the disaster prevention project in the Rimac River Basin. March, 1988. Tokyo, Japan.

7. Kuroiwa J. Physical planning for multi-hazard mitigation. Proceedings of the International Symposium held at Rimouski. Quebec, Canada, 3-9 August 1986.

8 Rachocki, Andrzek. Alluvial fans. John Wiley and Sons. 1981.

9. Rubio, Patricio. Peru. Ediciones Anaya, S.A. 1988. Madrid, Spain.

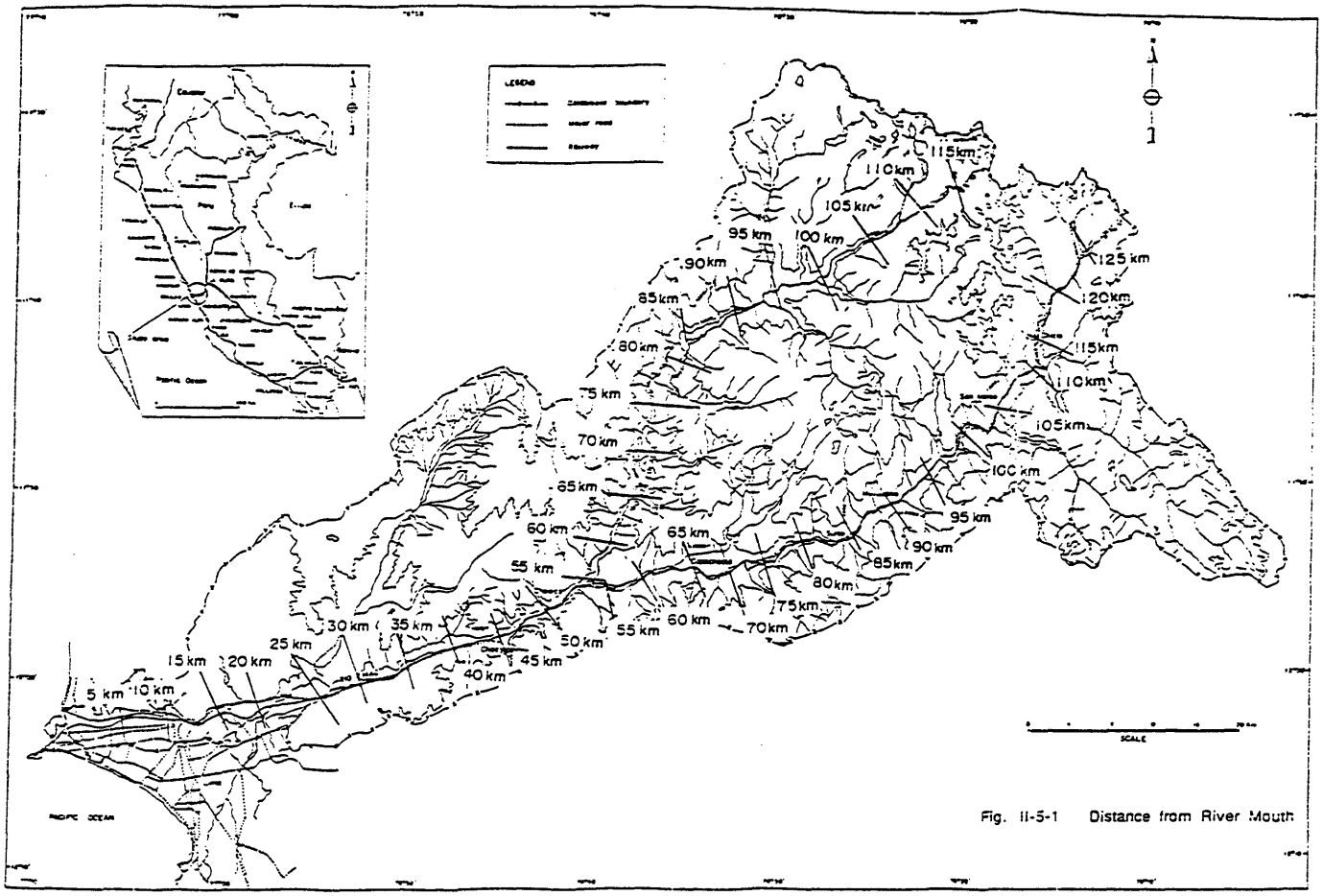

Figure 1 General location of the area under study

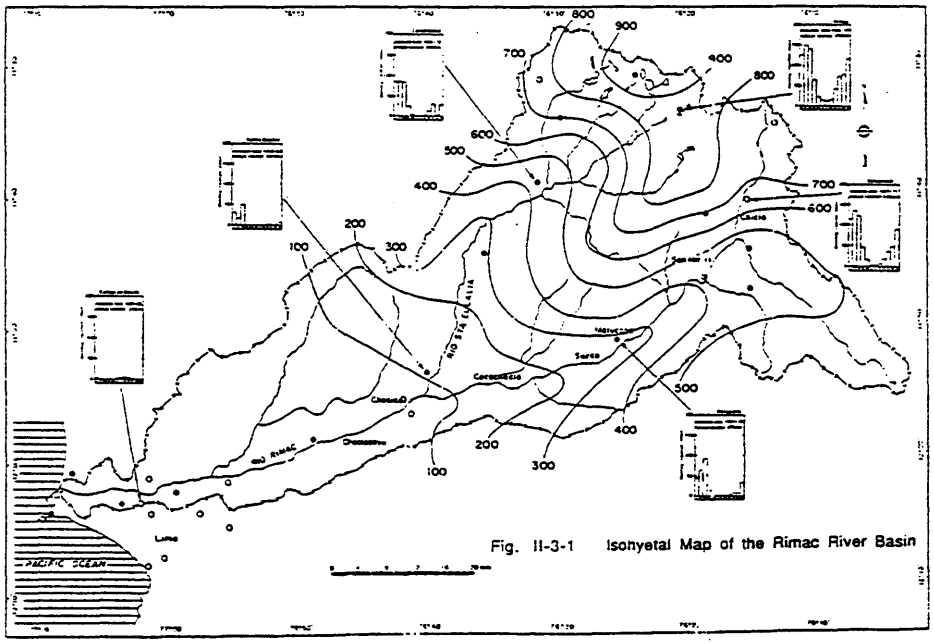

Figure 2 Isohyetal map of the Rimac River basin

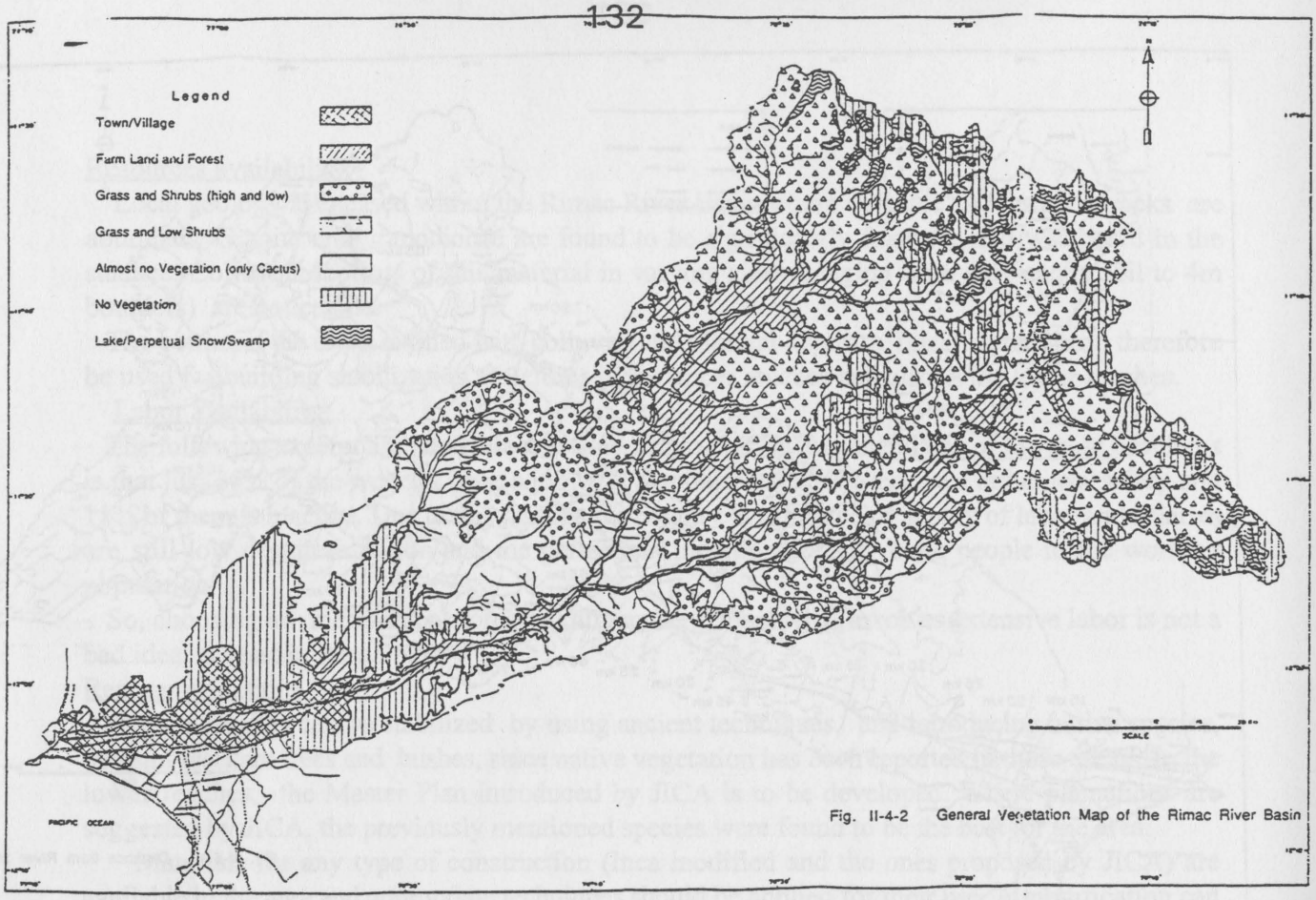

Figure 3: Vegetation and land use of the Rimac River basin

Figure 4: View of Quebrada Pedregal. Notice the steepness of the mountains and the lack of vegetation.

Figure 5. General view of Qda Pedregal Houses in the center have been filled with debris

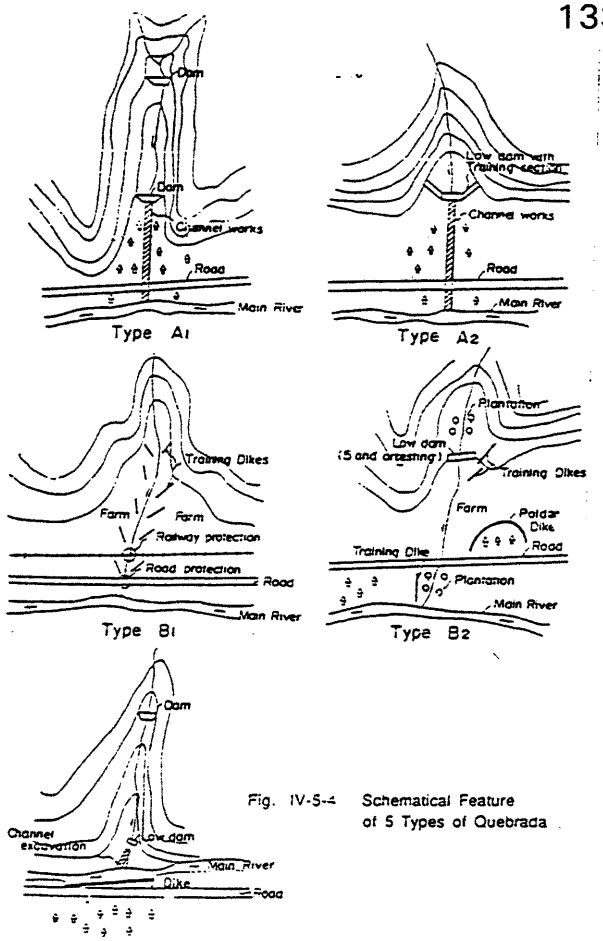

Fig. IV-5-4 Schematical Feature of 5 Types of Quebrada

Figure 6: Different types of structural measures.

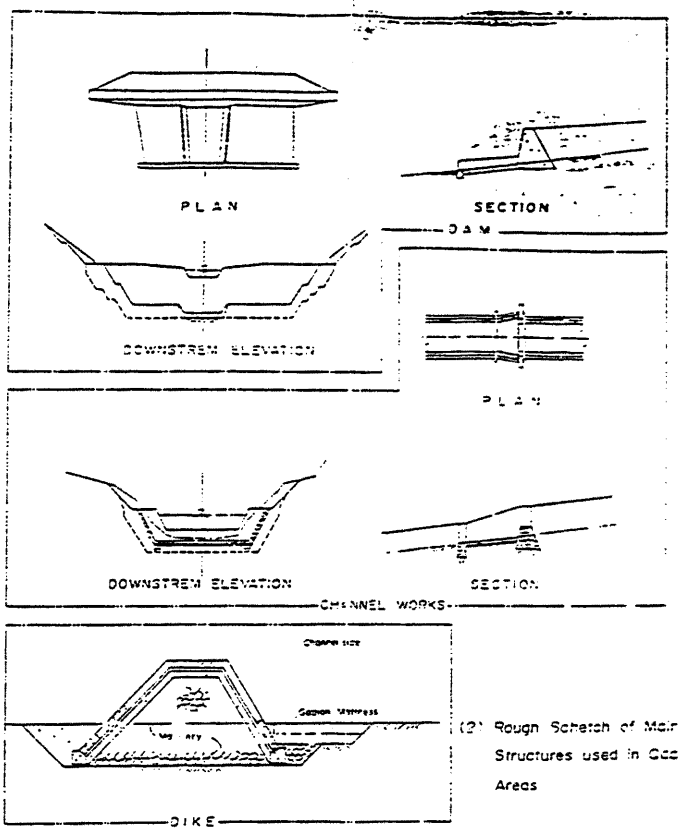

(2) Rough Sketch of Main Structures used in Geo Areas

Figure 7: Dam proposed dam by JICA for debris basin

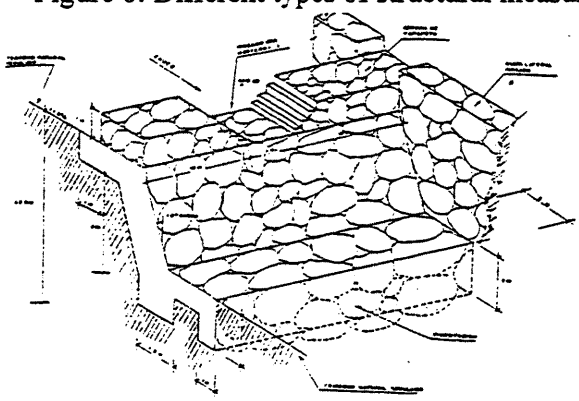

Fig. 3.7 Pirca, dique vertedor

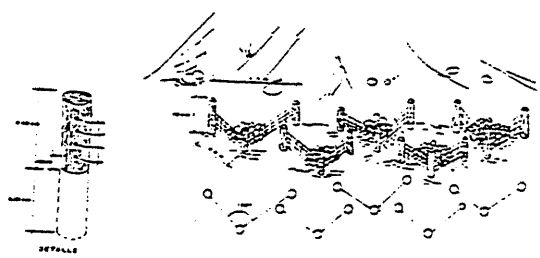

Figure 8: Pirca and Contention mesh

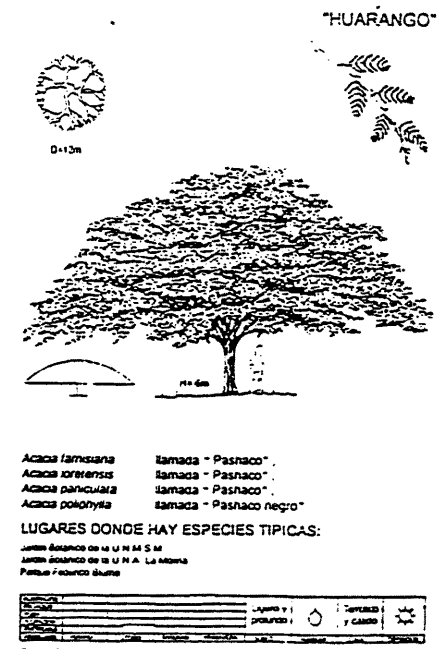

Figure 9: Native tree proposed for forestation

Fluvial processes and habitat critical to endangered fishes of the Green River, Utah

By Edmund J. Wick

ABSTRACT: The Green River remains the most promising riverine habitat for maintaining self sustaining populations of endangered fishes on the Colorado River System. Native fishes evolved unique adaptations to local geology, highly variable flows, and sediment laden waters of the historical river system. Habitat change due to extensive water development has threatened fluvial processes critical to early life history stages of the endangered Colorado squawfish and razorback sucker. Changes in flow and sediment supply have resulted in loss of connectivity to most of the floodplain throughout the basin. Restoration of flow seasonality and duration are important for providing system productivity, critical nursery habitat, and maintenance of spawning areas. Levees which isolate prime wetland nursery areas from the river are being modified to allow access to naturally spawned razorback sucker larvae in hopes of improving recruitment.

INTRODUCTION

The Green River forms a major northwest stem of the Colorado River Basin (Fig 1) which occupies approximately eight percent of the continental land mass of the United States. The Basin is one of the most highly developed river systems in the world (Carlson and Muth, 1989). It is an example of a dryland river system with ever increasing population pressure and competitive demand for its water resources which has resulted in stress on native biota and natural river function (Davies et al. 1994). Because the river basin was isolated from other river basins for millions of years 74% of its fish fauna are endemic, unique to rivers in the Colorado River Basin (Behnke and Benson, 1983). Extreme flow variability, turbidity and temperature created a harsh aquatic ecosystem in which only 13 species coevolved.

Of the 13 native fish species, four are endangered and two have become candidate species which may require future listing. The four big river endangered fishes include the Colorado squawfish (Ptychocheilus lucius), a giant predacious minnow (reaching five in length and 60-80lbs), the razorback sucker (Xyrauchen texanus), a sucker adapted to filter feeding on zooplankton in floodplain environments. The humpback chub (Gila cypha) is specially adapted to deep turbulent canyon reaches and the bonytail chub (Gila elegans) was found in a variety large river environments. Candidate species now include the roundtail chub (Gila robusta) which is a omnivore most commonly found midsize tributary rivers and the flannelmouth sucker (Catostomas latippinus) a detritavore which inhabits both tributary streams and larger river environments.

These fish developed unique adaptations to local fluvial geomorphology. Specialized adaptations to highly variable environments turned into competitive disadvantages following regulation of flows, modification of habitat, alteration of sediment supply and temperature and introduction of nonnative species.

System instability and habitat change

Prior to the extensive dam building on the Colorado River System during the 1960's, altered sediment balances, introduced vegetation, and varied climatic and flow cycles worked in concert to cause river channels to respond in complex ways (Schumm and Gellis 1989). During the late 1800's and early 1900's a period of increased flows and sediment production occurred (Fig. 2). This was followed by a period of moderate flows and appearance of more persistent, introduced riparian vegetation (salt cedar) in the lower Colorado River system (Fig. 3). Salt cedar progressively colonized banks in an upstream direction at a rate of about 20 km/yr (Graf, 1978). Graf showed a consistent rate of spread from the Colorado River near Lee's Ferry, Arizona in 1910 to Browns Park on the Green River upstream of Dinosaur National Monument by 1950.

Endangered Fish Coordinator, National Park Service, 1201 Oakridge Drive, Suite 250, Fort Collins, CO. 80525.

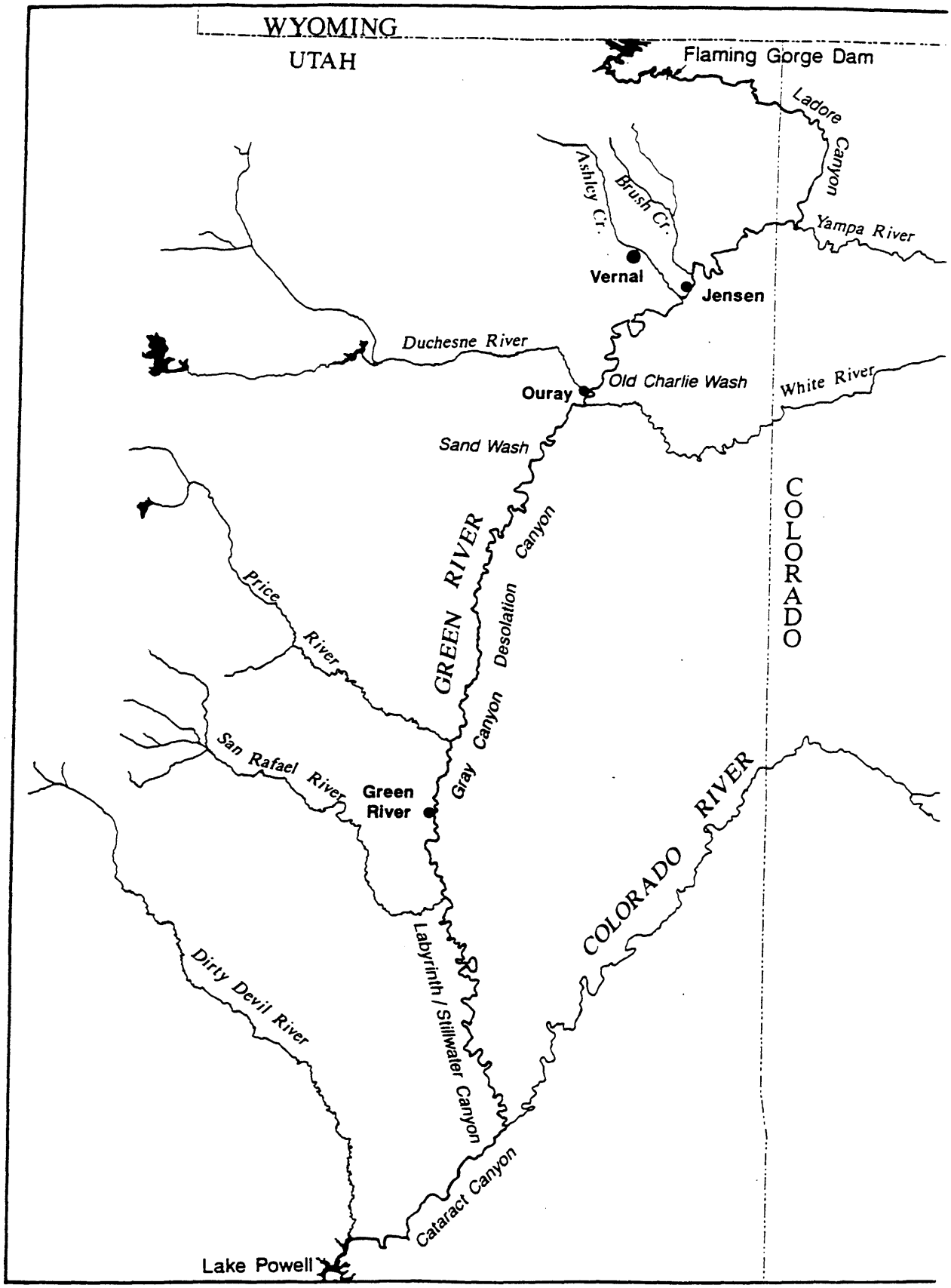

Fig. 1. Green River Basin, Study Area

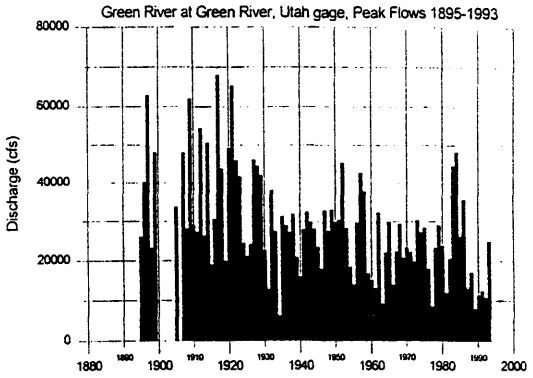

Fig. 2. Historical peak flow discharge records for lower Green River, Green River, Utah. 1895-1993. From; Green River Endangered Species Habitat Investigations. Resource Consultants & Engineers, INC.

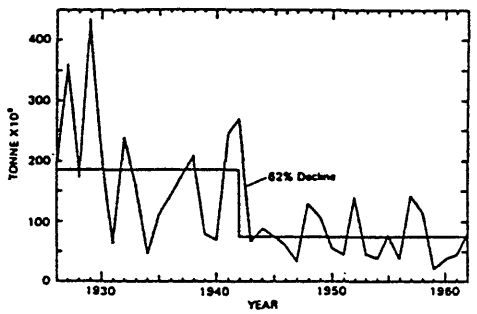

Fig. 3. Annual sediment discharge on the Colorado River at Grand Canyon. Abrupt decline in median sediment loads suggested by Schumm and Gellis (1989) for the periods 1926-1941 and 1942-1962, prior to closing Glen Canyon Dam

Sediment deposits, without high flows to scour them, were quickly stabilized by vegetation and natural levees developed (Graf 1978, 1985). Flooding frequency temporarily increased as even moderate flows filled narrowed, vegetation encroached river margins. Sediment deposited in low velocity vegetated surfaces on top of river bank margins and mid-channel islands raising surface elevations from 1 m to 3.5 m above low water level in the Canyonlands reach of the Green River. River widths in this reach were reduced on average 27% (range 13-55%).

Continued water depletions coupled with increased bank height eventually reduced flooded overbank frequency. Agricultural and urban development along rivers resulted in additional levee construction compounding the effects of natural levee formation. Dam construction in the 1960's further reduced seasonal variability, sediment supply, and resulted in channel incision. Loss of floodplain connectivity was prevalent through the entire upper basin except during extremely high flow events resulting in decreased organic particulate supply (productivity) in the river system. Access to productive low velocity habitat to native fishes occurred only when flows exceeded 20,000 cfs at the Jensen gage on the Green River.

Complex cumulative impacts on native fishes

Without access to low velocity floodplain, larvae and young-of-year native fishes are transported or displaced downstream greater distances, with many being carried by main channel currents into downstream reservoirs where predation pressure by introduced fishes is high. Introductions of nonnative fishes associated with altered riverine and reservoir environments cause predatory and competitive pressures on native fishes. Dams and diversion structures blocked migratory routes, diverted young and adults fishes from the main river into canal and irrigation systems. Water quality declined as a result of leached salts, minerals and agricultural chemicals. When large flood events passed through channelized areas on the Colorado River, channels beds degraded, or rivers broke through levees, causing damage to developed areas on the floodplain. Former spawning and nursery habitats utilized by fish where severely disrupted causing fish displacement, emigration and recruitment failure.

It is a challenge is to work through these complex impacts to the Colorado River System and identify trends or cycles in channel evolution in space and time so that habitat restoration efforts are effective (Schumm and Gellis, 1989) Fluvial process and flow patterns responsible for creating and maintaining habitat that fish need at critical times to complete their life cycles require identification. There are no easy cookbook approaches to guide research efforts on large complex river systems.

When recovery efforts for endangered fishes began in the late 1970's and early 1980's, the Instream Flow Incremental Methodology (IFIM) was considered a possible tool to determine the needed flows to provide spawning habitat and other important life history requirements. This methodology was commonly applied on trout species in smaller river systems where data is often gathered visually and more is known about the life history of the fish and habitat dynamics. Early attempts to apply IFIM on the Colorado River System were unsuccessful because the model required large quantities of accurate data. There remained much uncertainty regarding habitat requirements of the endangered fish. The physical processes maintaining the habitats used were not as yet understood and little interdisciplinary communication was occurring between biologists, geomorphologists and hydrologists. Evolution of this methodology may provide opportunity for application in the future (Stalnaker, 1993)

METHODS AND RESULTS

Interdisciplinary approaches; a needed methodology for understanding biological system response to physical process

Colorado Squawfish's unique life history adaptations to flow regime

In 1991, an interdisciplinary team of hydrologists, geomorphologists, and fish biologists were assembled to study Colorado squawfish spawning bars on the Yampa River. This effort identified recessional-flow bar dissection as a primary process of spawning substrate preparation (Harvey et al. 1993). This study was conducted because questions arose concerning reported annual flushing flows requirements of 30,000+ cfs for spawning habitat maintenance of this endangered species. Because squawfish successfully produce young larvae at various peak flows from 6,000-30,000 cfs, it was suspected that a spawning substrate maintenance process occurred other than high flushing flows which mobilize the entire river bed.

Colorado squawfish spawn during lower third of the recessional limb of the annual snowmelt hydrograph on the Yampa River at mid-channel bars located 16.5 and 18.5 miles upstream from the confluence with the Green River within Dinosaur National Monument. This is one of two confirmed spawning locations for this species in the Upper Colorado River Basin. The other is located near Three Fords Rapid in Desolation Canyon on the Green River (154 river miles from the Colorado River Confluence). The long distance migratory spawning behavior of Colorado squawfish was documented by radiotelemetry studies conducted simultaneously on three different rivers. The movement of squawfish to specific spawning locations in Yampa and Desolation canyons suggested that suitable spawning habitat in the basin may be limited to unique geomorphological locations and that special imprinting (chemoreceptive) mechanisms similar to salmon are likely involved enabling Colorado squawfish to return to specific natal spawning sites (Wick et al . 1983; Tyus 1986; Harvey et al. 1993) Results of geomorphology and HEC-2 analysis of the Yampa River spawning area indicates that the bars were deposited because of reduced hydraulic slope due to backwater effect at peak discharges during high flow years because of channel constrictions downstream. The cleansing and reworking of spawning cobbles occurred during the recessional limb of hydrograph as ponding above the primary bars increased local hydraulic slope and resulted in recessional-flow bar dissection. Shear stress increased over the bar deposits at lower discharge enabling motion of the bed and redistribution of spawning cobbles into secondary and tertiary bars.

The spawning areas are unique in that they occur in geologic transitions from harder to softer rock types (Morgan to Weber at Yampa Site) in confined canyon reaches. Less erosional resistance results in slope reductions from .3 to .1 and increases in sinuosity from relatively straight channel reaches to highly meandering with well developed riffle- pool sequences. The required combination of geologic and flow conditions resulting in quality spawning sites are not common on the Green-Yampa system. This spawning adaptation to rare and unique geological conditions tends to congregate Colorado squawfish in large numbers and makes populations of developed around these sites vulnerable to severe decline if physical process or access to the sites are disrupted. The need for high energy spawning locations also suggests that they evolved under highly variable flow and sediment conditions. Sufficient energy is maintained at the spawning sites for several years following high flow events to entrain cobbles on the recessionary limb. However, high flows sufficient to develop backwater conditions and deposit cobble entrained from upstream are required periodically to rebuild bar elevations. The amount of time it takes to degrade the bars to a point where sufficient motion of the bed no longer occurs has not been determined. Critical questions remain as to whether sufficient flow will be available in the future, at

sufficient frequency, to rebuild and maintain the spawning habitats in the face of continued pressures to develop more water.

Other critical components of maintaining squawfish reproduction involve maintenance of proper temperature cues to which fish have adapted and insuring that adequate nursery habitat is available downstream of spawning sites.

Spatial distribution patterns and nursery habitat availability

Nursery habitat for squawfish is formed as recessional flows decline to base flow. At this time sand deposits emerge forming embayments and slackwaters. If flow regulation increases discharge significantly above base flow levels these low-velocity habitats do not emerge and remain inundated. Young fishes are transported downstream greater distances. Displacement downstream is especially problematic when reservoirs are present downstream increasing risk of predation. An important component of squawfish habitat is the space requirement for completion of all life history phases. Adults will travel two hundred miles to spawn and young-of year may be displaced over 300 miles on the Green River before they begin to return upstream. This spatial component is important because habitat conditions vary with phase of channel evolution and channel type downstream. Suitability of nursery sites change over time and space. Therefore, trends in channel aggradation and degradation and effects on habitat need to be understood.

The major management action taken to date to manage habitat for Colorado squawfish on the Green River System has been to reduce post runoff releases and limit daily fluctuation to maximize backwater nursery habitat quantity and quality during base flow. This Green River nursery habitat extends from the Yampa River confluence downstream to the Colorado River inflow to Lake Powell a distance over 400 river miles.

Aerial videography methods were used to identify backwaters throughout the key nursery habitat areas. Prime nursery areas for annually produced yearclass are 120 river miles below key spawning sites. Fish surveys are being conducted annually to compare habitat availability with actual fish use.

Razorback suckers opportunistic spawners

Razorback sucker spawn in both lake and river environments (Minckley, 1983). In 1994, at Lake Mohave's Nevada Bay I observed several razorback adults spawning on lake shore cobble deposits in four to five feet of water. This bay was windy subject to wave action. Razorback larvae were clearly visible in a shallow shoreline bay and were collected by dipnet. However, small sunfish were present at the entrance to the habitat and were likely preying upon the razorback larvae as they drifted in from the spawning sites.

Razorback females worked the bottom substrate at the Lake Mohave site with their anal and tail fins. Sometimes noticeable depressions are formed. I have also noticed this behavior in small holding ponds at Ouray National Wildlife Refuge. I have collected razorback females with anal fins almost completely worn off from river spawning sites indicating they work bottom substrates in river spawning sites also.

In main river environments, razorback sucker congregate at the spawning bars just prior to peak flows on the Green River about 10 river miles upstream of Jensen, Utah and on the lower 2 miles of the Yampa River above its confluence with the Green River (Tyus and Carp 1990). It was assumed that suitable gravel spawning substrates are annually maintained by high spring flushing flows. However, this species often initiates spawning prior to spring peak flows as temperatures approach 14 degrees centigrade. Since sand deposition has been noted over the main spawning areas on the Green River during the post runoff period, concern was raised by fish biologists regarding possible effects on spawning success. A channel monitoring study was initiated to determine the dynamics of sediment movement at the spawning sites. Experimental re-regulation of flows from Flaming Gorge were available if needed to maintain the conditions there.

The razorback spawning site on the Green River is similar to sites used by squawfish because it is associated with an island and has a downstream constriction which creates a backwater effect at high flow (Fig. 5). Seven transects were placed through the bar reach and they were sampled on four occasions; April 93, June 93, August 93 and April 94 (Fig. 6) Specific spawning areas used by the fish were identified by electrofishing running-ripe females over the bar and radiotelemetry studies of migratory behavior.

In late April and May, with flows less than 7,000 cfs the spawning cobbles at cross section E-4 were free of sand. In June, just after peak flows ranging between 17,000-20,000 cfs considerable sand deposition was noted in the spawning reach. In August, at base flow levels of 1,400 cfs sand deposition was reduced, indicating

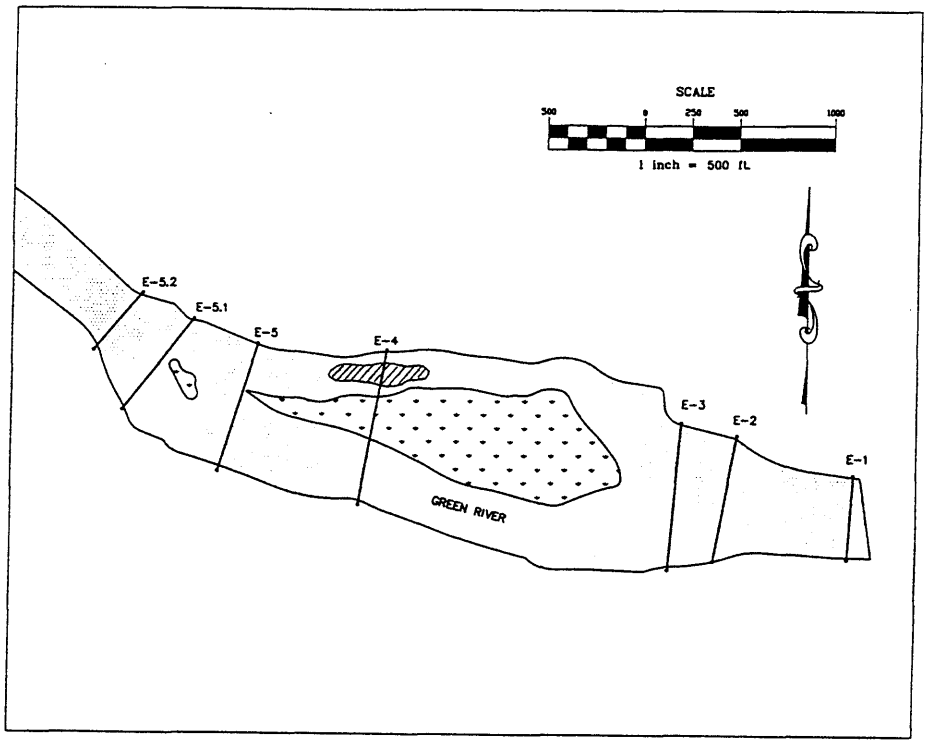

Fig. 4. Cross section placement at razorback sucker spawning bar, on Green River. River mile 311 above Colorado River Confluence. Spawning site is hatched area in the right channel.

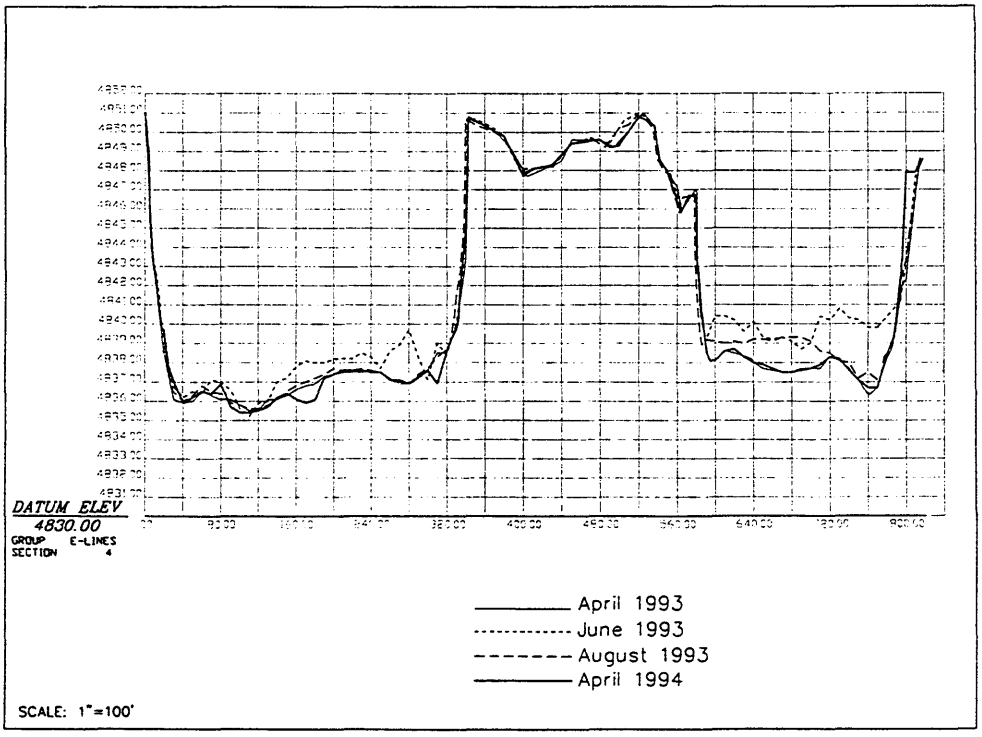

Fig. 5 Cross section profiles of E-4 through spawning site.

movement of sand out of the reach. By April, 1994, at flows around 2,200 cfs, the spawning reach was again clean of sand and similar in cross sectional form to the transect taken a year earlier (Fig. 6). Patterns of deposition and scour were reversed at the constriction (cross section E-5.2) indication velocity reversal between expansion and constriction zones. Recessional flows over higher energy bar deposits are an important physical process in maintaining razorback spawning sites similar to the maintenance of Colorado squawfish bars. However, razorback spawn and larvae hatch from the bar prior to the deposition of sediment at peak flows.

Running ripe congregations of razorback and radiotagged fish have also been located on shoreline cobble deposits at another site five river miles downstream indicating that other process involving secondary currents may also produce suitable substrate for spawning.

Light trap sampling technique developed for razorback larvae

Results of newly developed light trap sampling programs for razorback larvae in 1993 and 1994 on the Green River indicate that razorback young are produced in surprisingly abundant numbers. Several hundred larvae were collected in only two weeks of effort in 1993. In 1994, increased sampling resulted in the capture of over 1200 larvae indicating that it is likely that millions of larvae are produced. Razorback larvae were distributed from just below the spawning bars in Dinosaur National Monument, down through Canyonlands National Park, and into Lake Powell. The size and developmental phases of these larvae based on capture date and location indicate that the source could have been from the upstream spawning sites (personal communication, Darrel Snyder, Larval Fish Laboratory, Colorado State University). No other confirmed spawning locations have been identified.

Based on results of these larval collections suitable spawning habitat appears not to be the limiting factor responsible for recruitment failure. Limited recruitment is likely related to altered river flows which affect feeding and nursery habitat, growth rate of larvae, and associated predation pressure. Recently developed methods using individual-based modeling approaches have been successful in predicting recruitment success of early life stages of fish (Crowder et al. 1992) We plan to utilize this type of modelling approach to assist in developing better understanding of what is required for razorback sucker to successfully recruit.

Evolutionary process and local adaptation

Basin wide examination of historical patterns of adult razorback spawning concentration and associated geomorphological features infer relationships between unconfined floodplain reaches and razorback reproduction and recruitment. All known spawning aggregations in the Upper Basin were upstream of unconfined river reaches (Delta on the Gunnison, Rifle, Grand Valley and Moab on the Colorado River and Jensen and Ouray on the Green River. This observation suggests that survival was dependant or tied to unconfined river reaches which are usually associated with wetland and floodplain terraces potentially a rich in food source for both young and adult fish.

Habitat succession during early life phase

Razorback young emerge from spawning cobbles at or near peak flows and either passively drift or actively seek flooded areas which contain adequate food (zooplankton densities) to survive. Papoulus and Minckley (1990, 1992) conducted experiments on razorback larval food requirements and determined that 20 organisms/liter (zooplankton) were required for survival of young. Floodplain habitats near Ouray, Utah were examined and were found to contain 200-300 organisms/liter. Historically, depending on magnitude and duration of runoff, razorback larvae could have spent up to six weeks in floodplain wetlands (Fig. 7)

Due to reduced flows and other factors resulting in loss of connectivity, habitat use is presently restricted to flooded tributary stream mouths and flooded cut off side channels except during exceptionally high flow years (exceeding 20,000 cfs at Jensen, Utah) These habitats usually contain between 20-30 zooplanktors/liter offering a secondary or marginal type habitat for the razorback larvae. Flooded tributary mouths are considered marginal habitat because of reduced food levels. However, if these habitats are used in succession or in conjunction with restored connectivity with highly productive floodplain wetlands, they may provide habitat for young razorback to grow to a size which increases their chances to survive.

Flow duration identified as potential limiting factor

A likely factor contributing to recruitment failure is that flow durations have been shortened. Razorback larvae have insufficient growing time prior to being drawn back into river environments by declining flows before they are ready morphologically to cope with different food types and predation pressures. Hilrew (1994) indicated that predation on mobile and patchily distributed prey can be intense overall whilst remaining elusive in patch scale experiments. He further indicated that predator impact may be limited to those hydraulic conditions that favor the predators. In 1994, we observed that razorback larvae reached 17 millimeters in length in flooded tributary backwater habitats when these habitats began receding under present flow release patterns and became no longer usable.

When razorback larvae hatch and swim up out of the cobble they are between 8 and 10 mm long. At this size and until they reach about 24 mm they have terminal mouths best adapted for feeding on zooplankton. When razorback larvae are forced back into the river under present flow recessional regimes, in-channel river slackwaters are few in number, relatively devoid of food and cover, and heavily utilized by potential predators. Since razorback are the first species to spawn on an annual basis their larvae are especially vulnerable as a food item to predators. In-channel river slackwater habitats have very low zooplankton densities of only one organism/liter (Grabowski and Hiebert, 1989).

It is hypothesized that predation pressure on razorback larvae by nonnatives (particularly the red shiner) in natural flooded backwater environments will be reduced because of more abundant food alternatives. Experiments conducted by the Larval Fish Laboratory, Colorado State University showed that predation by red shiner (the most abundant nonnative on the upper Green River) on razorback larvae was reduced significantly when an alternate food source was available (Robert Muth, Larval Fish Laboratory, Colorado State University, personal communication.)

Razorback larvae grow about 0.3 - 0.4mm/day. At this rate it would take about 45 days for their mouth to become subterminal - thus better adapted for feeding on the bottom. Also, fins are fully developed by the time larvae reach 20mm. If razorback larvae could reach a these larger sizes they could more effectively exploit benthic food resources (chironomids) available in the river, better avoid predators and hold position in higher velocity currents.

Physical constraints on Green River releases at Flaming Gorge

Maintenance of seasonality of flows was not considered when designs for turbines and power production were implemented at Flaming Gorge Dam. Flow releases greater than 4600 cfs exceed the power producing capacity through the turbines. Although releases of up to 8000 cfs can be achieved by using jet tube by-pass-flows, this only occurs during extremely high years to avoid overtopping the spillway. Reluctance to release water exceeding power production capability makes floodplain restoration difficult to implement. It is likely that jet tube flows will be needed to achieve needed duration and magnitude to maintain historic connectivity patterns between the river and floodplain. Historically, flows would exceed 12,000 cfs on the upper Green River above the Yampa River confluence during wet years. Average flow volume was slightly less but similar in magnitude to the Yampa River (Fig. 7).

Contrast of historical and present flow duration patterns

Historically, the offset timing of peak flows from the Green River would commonly provide flow duration of 45 days (Fig. 7). The Yampa River peaks between 13,000 to 15,000 cfs during wet cycles and usually two weeks earlier than the Green River. In order to achieve the historical floodplain duration during wet years it may be necessary to bring the Green River release up into the 6000 to 8000 range as the Yampa recedes off of its wet year peak from 15,000 to 12000 cfs. This level of combined river flow would be need to match the observed floodplain connectivity which occurred in 1993 between peak flows of 20,000 to 21,000 cfs at the Ouray, Utah wetlands area.

Fig. 8 shows the flow pattern released from Flaming Gorge Dam in 1994 which matches the timing of the Yampa River peak. This release pattern which is presently recommended under the Biological Opinion for Flaming Gorge resulted in a rapid loss of secondary nursery habitat (flooded tributary mouths) and insufficient growing time.

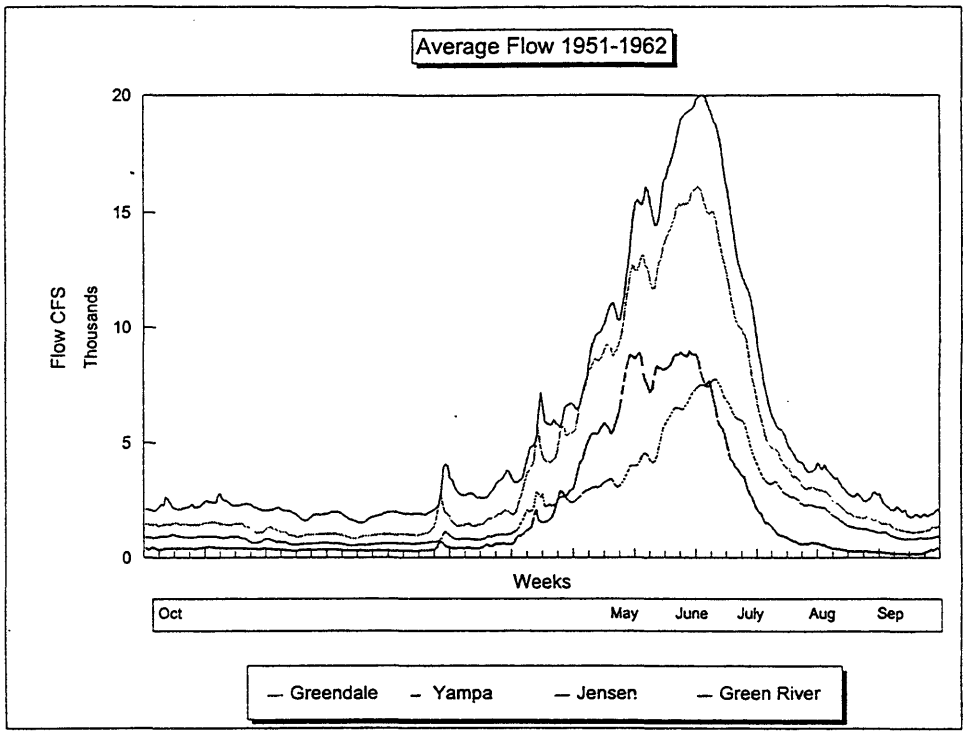

Fig. 6. Pre Flaming Gorge flows. Greendale gage is the flow release from Flaming Gorge Dam.

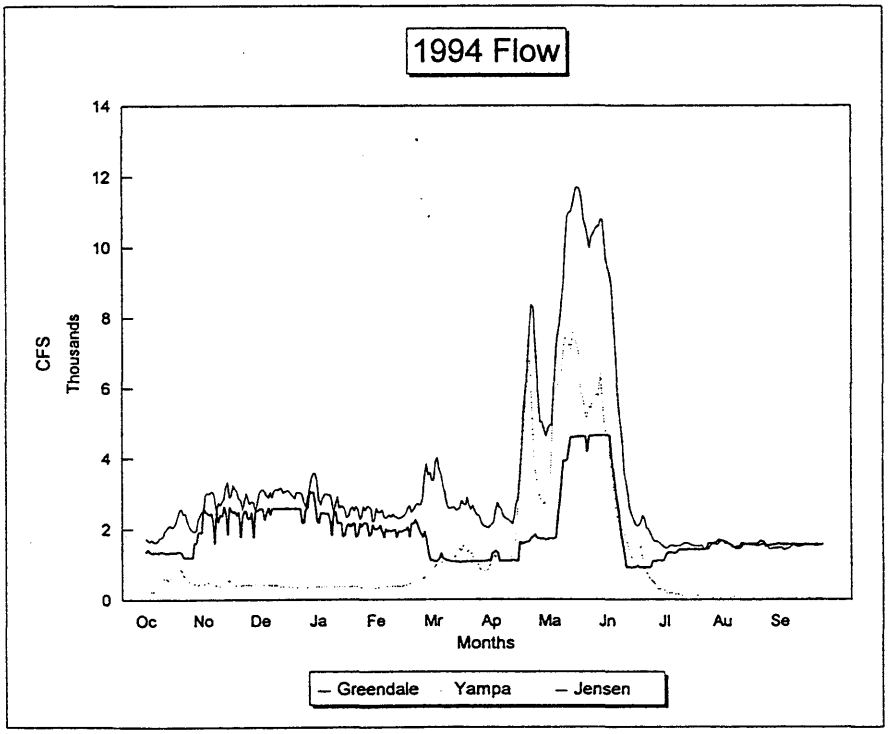

Fig. 7. Actual 1994 flows. Greendale gage is the flow release from Flaming Gorge Dam.

Proposed flow management changes and evaluation

In 1995, I have requested an increase in flow duration to more closely match the historical offset pattern of Yampa-Green river flows. Larval sampling programs using light traps and controlled experiments will be conducted to determine if there is improved growth and survival of razorback larvae. The increased duration of food availability, and growing time should result in greater survival of larvae.

Computer-Assisted Floodplain Hydrology and Hydraulics (HEC-2) is being used in both unconfined reaches and other flooded tributary areas where razorback larvae are present to determine flow magnitude needed to provide access and adequate areas of cover. Transects are placed at base flow and will be calibrated by measuring bed profile and water surface elevation again at peak flows. Staff gages are being placed in key nursery habitat areas and photographed daily by remote automatic camera to establish relationships of water elevation with the nearest USGS gaging stations.

Political and economic constraints on flow re-regulation

Natural functioning river ecosystem values have not yet replaced the old ingrained ways of water management in the West. Presently the Bureau of Reclamation (BOR) considers it illegal to release flows beyond power plant capacity, in spite of the Endangered Species Act. The potential value to be gained by retro-fitting turbines in the jet tubes is being evaluated by the BOR but results have not been reported (personal communication Larry Crist). A recent Economic Assessment evaluated enhanced flow options and concluded a positive economic effect of endangered fish recovery (Brookshire et al. 1993). Power revenues downstream would be increased as extra water moves through the system. Significant economic value may result from reductions in salinity levels, increased cash crop production, and improved urban water supplies of the lower basin states. If out of state water sale was allowed, the benefits of recovery actions would increase for the upper basin states. However, it is presently considered illegal to sell water out state.

Institutional Constraints and Contradictions in Water Allocation

Constraints on allowing free market forces to more efficiently allocate water to both instream and downstream uses include: 1) Colorado River Compact; 2) Arizona v. California; 3) Upper Basin Agreement; 4) State water laws; and 5) Bureau of Reclamation contracts tying water to certain project areas. Most western states like Colorado employ the prior appropriation doctrine which allows only the consumptive use portion of a water right to be transferred. Therefore it is difficult to transfer water which has no former history of consumptive use. This constraint requiring prior water development in order to effect a transfer is inefficient and restrictive on allowing economic benefit to be derived from water originating in a state and sold out of state.

This institutional constraint was challenged in the Sporase decision which ruled that water is an article of interstate commerce (Commerce Clause [102 S. Ct. 613, 1982). This decision allowed judicial invalidation of any legislation or regulation which poses an "impermissible burden" on interstate commerce.

This ruling offers some encouragement that the present water laws can be changed to allow more flexibility in water allocation to aid in recovery efforts and meet economic assessment requirements of the Endangered Species Act (ESA). I seriously doubt that increased flow releases will be allowed without demonstrating the economic benefits of doing so. I believe the rational economic benefit approach of appealing to the head instead of the heart (Ridley and Low, 1993), stands the best chance of gaining public support.

DISCUSSION

New Instream Flow Approach Approved In The Upper Basin

Restoration of seasonality in flow patterns was recommended by Stanford (1993) in his review of instream flow needs to assist in the Recovery Implementation Program for Endangered Fishes of the Upper Colorado River System (RIP). Stanford (1993) cautioned that five additional recommendations would have to accompany restoration of seasonal patterns to complete his recommended approach: 2) provide a common understanding of water availability; 3) add a community ecology perspective; 4) understand biological adaptations to physical processes; 5) implement a priori peer review process;
and 6) implement adaptive management

Stanford was generally impressed with the amount of information gathered to date by the Recovery Program and encouraged moving forward with management strategies. His approach if applied as a package will have a good chance of success because it calls for direct confrontation of critical uncertainties which could take years to adequately answer given the present conservative research approach. However, as mentioned earlier constraints placed on the magnitude of releases from Flaming Gorge are thwarting evaluation of long term recovery strategies. If only portions of these recommendations are implemented and community ecology studies are applied extensively basin wide, huge research budgets will be consumed without leading to practical management applications. This must be avoided.

Engineering vs. natural approaches

Presently the Recovery Implementation Program is very cautious regarding wide scale habitat restoration involving flood flow strategies. Small projects which involving only portions of diked wetlands have been designed as demonstration projects. Sections of former levees are to be lowered and reinforced and fish capture kettles installed. These small scale projects will assist the learning process and give insights as to potential level of recruitment to expect, however they are to expensive and labor intensive to apply long term. The cost of restoring one tenth of one wetland was estimated at $500,000.00.

Once larval survival is better understood in relation to the myriad of potential limiting factors and restoration of natural flow patterns are determined feasible, then dikes can be removed from unconfined river reaches and natural bank contours restored. Self sustaining populations can be maintained primarily with flow management alone provided present flow restrictions are removed.

Another important factor to consider is that of adult habitat. Adult razorback have been collected in flooded wetland areas primarily after the spawning period in fatter condition compared to those caught in the river. Adults are specially adapted filter feeders, utilizing their fine gill rakers and unique dorsal hump as a stabilizer. Access to wetlands may be important in conditioning the adults after spawning for the upcoming year. Heavy seasonal feeding after spawning is common in many fish species. Floodplain dependent species often rely on heavy feeding during the flood period to sustain them through the rest of the year and this provides the majority of their annual growth (Welcome, 1979). Small scale intensive efforts directed at only the early life history stage may not be sufficient to also provide enough adult feeding habitat, especially if adult populations are augmented.

Other controversial engineering solutions involve increasing water surface elevations by constricting channels with wing dams or rock reinforcements. These types of solutions may cause local bed instability and require long term maintenance costs. These unnatural structures may be used by introduced species such as smallmouth bass and walleye placing additional pressure on native species.

Another approach would be build riverside hatcheries or grow-out facilities and stock fish into the present river system. However, lower basin attempts at stocking millions of razorback sucker young into river environments failed to establish any viable populations. Raising fish to adult size would be expensive and the core problems would not be solved. Program goals of establishing self sustaining wild populations place caution to this approach. Evaluation of management actions become more difficult when fish are introduced at the same time habitat restoration efforts are undertaken. If reproducing populations are present, rectification of habitat deficiencies should be examined first. Stocking hatchery reared fish should be a last resort.

REFERENCES

Behnke, R. J., and D. E. Benson. 1983. Endangered and threatened fishes of the Upper Colorado River Basin. Colorado State University Cooperative Extension Service Bulletin. 503A:38p.

Brookshire, D. S., M. McKee and G. Watts. 1993. Draft economic analysis of proposed critical habitat designation in the Colorado River Basin for the razorback sucker, humpback chub, Colorado squawfish, and bonytail 535 pp

Carlson, C. A., and R. T Muth. 1989. Lifeline of the American Southwest. Pages 220-239 in D. P. Dodge, editor Proceedings of the International Large Rivers Symposium. Canadian Special Publications of Fisheries and Aquatic Sciences 106.

Crowder, L. B., J. A. Rice, T. J. Miller, and E. A. Marschall. 1992. Empirical and theoretical approaches to size-based interactions and recruitment variability in fishes. in D. L. DeAngelis and L. G. Gross Eds. Individual-based models and approaches in ecology: Populations, communities and ecosystems. Chapman and Hall, New York

Davies, B. R., M. C. Thoms, K. F. Walker, J. H. O'Keeffe and J. A. Gore. 1994. Dryland rivers: their ecology, conservation and management. in. The rivers handbook. Hydrological and ecological principles. eds. P. Calow and G. E. Petts Volume 2. Blackwell Scientific Publications. London.

Graf, W. L. 1985. The Colorado River: instability and river basin management. Association of American Geographers, Washington D. C. 86 pp.

Graf, W. L. 1978. Fluvial adjustments to the spread of tamarisk on the Colorado Plateau region. Bulletin of the Geographical Society of America 89: 1491-1501.

Grabowski, S. J. and S. D. Hiebert. 1989 Some aspects of tropic interactions in selected backwaters and the main channel of the Green River, Utah: 1987- 1988 U. S. Bureau of Reclamation, Research and Laboratory Services Division, Environmental Services Section, Denver Colorado. 130pp

Harvey, M. D., R. A. Mussetter and E. J. Wick. 1993. A physical process- biological response model for spawning habitat formation for endangered Colorado squawfish. Rivers. Volume 4, Number 2.

Hildrew, A. G. 1994. Food webs and species interactions. in. The rivers handbook. Hydrological and ecological principles. eds. P. Calow and G. E. Petts Volume 2. Blackwell Scientific Publications. London.

Krueger, C. C. and D. J. Decker. 1993. The process of fisheries management. Chapter 2. in. Kohlor C. C. and W. A. Hubert. eds. Inland fisheries management in North America. American Fisheries Society. Bethesda, Maryland, USA

Minckley, W. L. 1973. Status of the razorback sucker, Xyrauchen Texanus (Abbott), in the lower Colorado River Basin. Southwestern Naturalist 28: 165-187

Papoulias, D. and W.L. Minckley. 1992. Effects of food availability on survival and growth of larval razorback suckers in ponds. Transactions of the American Fisheries Society 121: 340-355.

Ridley. M. and B. S. Low. 1993. Can selfishness save the environment? The Alantic Monthly. 9/93. p 76-84.

Schumm, S. A. and A.C. Gellis. 1989. Sediment yield variations as a function of incised channel evolution in L. M. Brush et al. Taming of the Yellow River: Silt and Floods, 99-109 Kluwer Academic Publishers

Stalnaker, C. B. 1993. Evolution of Instream Flow Habitat Modelling in. The rivers handbook. Hydrological and ecological principles. eds. P. Calow and G. E. Petts Volume 1. Blackwell Scientific Publications. London.

Stanford, J. A. 1993. Instream flows to assist the recovery of Endangered Fishes of the Upper Colorado River Basin: review and synthesis of ecological information, issues, methods and rationale. Final Report. 130-93. to Instream Flow Subcommittee of the Recovery Implementation Program for Endangered Fish Species of the Upper Colorado River Basin. Flathead Lake Biological Station, University of Montana. Polson, Montana.

Tyus, H. M. and C. A. Karp. 1990. Spawning and movements of razorback sucker, (Xyrauchen texanus) in the Green River Basin of Colorado and Utah. Southwestern Naturalist 29:289-299.

Welcomme, R. L. 1979. Fisheries ecology of floodplain rivers. Longman, New York. 315 pp

Wick. E. J., D. L. Stoneburner, and J. A. Hawkins. 1983 Observations on the ecology of the Colorado squawfish (Ptychocheilus lucius) in the Yampa River. Report Number 83-7 Colorado Water Resources Field Support Laboratory. National Park Service, Fort Collins, Colorado. 55pp.